Back-analysis Methods for Optimal Tunnel Design

Sotirios Vardakos

Dissertation submitted to the Faculty of the
Virginia Polytechnic Institute and State University
in partial fulfillment of the requirements for the degree of

Doctor of Philosophy
In
Civil and Environmental Engineering

Marte Gutierrez, Chair
Xia Caichu
Joseph Dove
Matthew Mauldon
Erik Westman

January 24, 2007
Blacksburg, Virginia

Keywords: tunneling, back-analysis, excavation monitoring, optimization

Back-analysis Methods for Optimal Tunnel Design

Sotirios Vardakos

ABSTRACT

A fundamental element of the observational method in geotechnical engineering practice is the utilization of a carefully laid out performance monitoring system which provides rapid insight of critical behavioral trends of the work. Especially in tunnels, this is of paramount importance when the contractual arrangements allow an adaptive tunnel support design during construction such as the NATM approach. Utilization of measurements can reveal important aspects of the ground-support interaction, warning of potential problems, and design optimization and forecasting of future behavior of the underground work.

The term back-analysis involves all the necessary procedures so that a predicted simulation yields results as close as possible to the observed behavior. This research aims in a better understanding of the back-analysis methodologies by examining both simplified approaches of tunnel response prediction but also more complex numerical methods. Today a wealth of monitoring techniques is available for tunnel monitoring. Progress has also been recorded in the area of back-analysis in geotechnical engineering by various researchers. One of the most frequently encountered questions in this reverse engineering type of work is the uniqueness of the final solution. When possible errors are incorporated during data acquisition, the back analysis problem becomes formidable. Up to the present, various researchers have presented back-analysis schemes, often coupled with numerical methods such as the Finite Element Method, and in some cases the more general approach of neural networks has been applied.

The present research focuses on the application of back-analysis techniques that are applicable to various conditions and are directly coupled with a widely available numerical program. Different methods are discussed and examples are given. The strength and importance of global optimization is introduced for geotechnical engineering applications along with the novel implementation of two global optimization algorithms

in geotechnical parameter identification. The techniques developed are applied to the back-analysis of a modern NATM highway tunnel in China and the results are discussed.

Dedications

To my parents and Margarita, for their great support all these years.

Acknowledgements

I would like to express my sincere gratitude to my academic advisor Dr. Marte Gutierrez for his continuous guidance, support and inspiration during my studies at Virginia Tech. I specially would like to thank Dr. Marte Gutierrez for offering me the opportunity to work on exciting projects in the field of geomechanics. I was involved in interesting yet challenging research, and Dr. Marte Gutierrez has always been on my side to provide insight and motivation.

I would also like to extend my deep appreciation to Dr. Joseph Dove, Dr. Matthew Mauldon, and Dr. Erik Westman for all their encouragement, instructive suggestions and ideas that helped me enrich my research during these years.

Finally, I wish to sincerely thank Dr. Xia Caichu from the Department of Geotechnical Engineering at Tongji University, China, for providing data and invaluable support on applying my research methods presented herein, on the case of the Heshang tunnel in China. Dr. Xia Caichu, has provided continuous insight and spent many hours helping me to address various challenges during back-analysis.

The results presented in this paper are part of the AMADEUS (Adaptive real-time geologic Mapping, Analysis and Design of Underground Space) Project funded by the US National Science Foundation under grant number CMS 324889. This support is gratefully acknowledged.

Table of contents

List of Figures

List of Tables

CHAPTER 1. Introduction

The AMADEUS (Adaptive Mapping Analysis and Design of Underground Space) project (2004) sponsored by the National Science Foundation reflects an effort to organize, record and utilize in a timely manner, information which can be obtained directly from the excavated rock mass. Such information is associated with geologic parameters such as rock types and formations, faults and other discontinuity features, condition of discontinuities, statistical presence of joints, rock surface image recording, real-time rock mass classification, deformation and rock stress measurement data. The AMADEUS project involves the synergy of a collection of modern technologies in order to organize this wealth of information and use it in an efficient and useful way to ultimately optimize the design of underground space and become fundamental component of the so called Observational Method as introduced by Peck (1969).

It is obvious that when such an advanced methodology is realized and applied in the field, the engineers and planners of any underground work can improve their designs and lower the cost of the final construction only by initially investing on a reliable array of techniques to safely record and process information in real time. One of the most important components of underground design and construction is the analysis by the use of appropriate analytical, stochastic or numerical methods in an attempt to simulate the behavior and state of the physical problem and ultimately estimate the behavior or state of the surrounding ground. Unfortunately, such attempts are only as good as the values of the input parameters used, the models or the methods assumed. In addition, geological uncertainties that prevail primarily in jointed rock masses, make such efforts difficult. A fundamental component of the Observational Method in tunneling is the use of monitoring data to assess the adequacy of the employed design and the safety margins of the design. These data can be used to calibrate numerical or analytical models so that predicted values of specific magnitudes match the corresponding values of measured data. This process known as parameter identification or back-analysis aims in estimating values of input parameters for numerical or analytical methods that can be used for prediction of rock mass behavior during future construction stages.

This research focuses in the development and applicability of various back-analysis methods for underground excavations. An extensive literature review has been performed on previous work involving parameter-identification problems. Various back-analysis methods and their features are described along with some of the disadvantages.

The present work pioneers in the application of back-analysis methods using widely available numerical modeling software. The main goal is to develop a set of principles, methods and guidelines that can be easily employed by engineers in order to perform back-analysis under given conditions and limitations. The task of parameter identification is not generally easy and the more parameters are involved or the problem becomes more complex, the more the analysis becomes elaborate and complex. This research studies the issues that revolve around the process of parameter identification and attempts to promote methods which have to be reasonable to understand and follow, easy to apply using a programmable numerical code, and easy to maintain. The later perhaps is one of the most desirable features that can be found in the field of operations research algorithms. An algorithm should depend on human interaction as little as possible, yet with out sacrificing reliability or performance. In this study various methods for back-analysis are discussed and examples of applications are also given.

Generally the behavior of underground structures in soft soils or jointed rock masses can be highly non-linear. This non-linearity imposes a great difficulty to most back-analysis procedures, especially when the number of unknowns increases. Very often the parameter identification scheme is influenced by the personal judgment used to obtain initial trial values of the governing parameters to start the back-analysis. This can be a very problematic point and potentially lead the final results to erroneous or unreasonable conclusions. This research has concentrated on development of procedures and guidelines, which do not depend on such a limitation yet they retain the advantage of applying constraints in the governing parameters throughout the whole analysis. The techniques suggested in this research can be adapted to a great range of non-linear geotechnical analysis problems and not only to underground excavations. The research on back-analysis methods is concluded with the application of one of the suggested methods in the case of the Heshang highway tunnel in China. Despite the complex construction

sequence of this tunnel, the availability of monitoring data deemed the project very interesting to examine.

No matter how sophisticated a back-analysis can be, there needs to be a reliable method to collect and process massive geotechnical data especially when dealing with jointed rock mass environments. Such data may provide not only an initial estimate of the encountered conditions in terms of deformability of strength, but also can be used to improve the constraints used in an efficient back-analysis it more efficient. In the context of this research, an outline of the present state on the use of rock mass classification systems for underground space design application will be given while also the need for more reliable newer data acquisition tools will be pointed out. In the present research, we introduce and examine the use of a new electronic tool which aims in making easier and more efficient insitu geologic data acquisition. The tool aims in minimizing paper-based rock mass quality data collection, based on two of the most widely used rock mass classification systems. The tool will have the ability to process the obtained data statistically in order to conclude a general qualitative description for a location, based on independent observations of the governing parameters. Modern technological advances have resulted into useful electronic tools such as the personal digital assistants (PDAs) which are excellent in gathering information which can be easily transported. The description and features of the PDA-based electronic field book for rock mass classification will be given at the end of the present dissertation as a separate appendix.

CHAPTER 2. Research summary

The present research is part of the AMADEUS (Adaptive Mapping Analysis and Design of Underground Space) project, sponsored by the National Science Foundation dealing with Adaptive Mapping Analysis and Design of Underground Space. In modern engineering practices, the Observational Method is a way to optimize the design of a structure by continuously monitoring its behavior during construction. This method offers significant advantages of cost minimization and avoidance of over-design. Also it is a prudent way to identify possible stability problems and modify the construction and safety requirements in a timely manner. There are two main elements fundamental to the Observational Method. The existence of a carefully matched monitoring system for the type of the work, which will provide valuable performance related data and a mechanism to use these data in order to optimize the design itself and apply judgment more safely on the future stages of the construction. The later is ultimately expressed via the process of back-analysis.

This dissertation is organized as follows:

Chapter 3 summarizes the most frequently encountered deformation and stress (or load) monitoring instrumentation and provides information regarding reliability issues and performance properties of each of the different types of monitoring systems. Focus is given on the various sources of error during monitoring and its significance in the final results. Performance properties such as accuracy, sensitivity and repeatability are briefly discussed.

Chapter 4 provides insight on the state-of-the-art of back-analysis methodologies. An extensive literature review is performed and various techniques and applications from previous work are outlined. The types and principles of back-analysis methods are discussed. The chapter focuses in the description of various optimization algorithm classes, which can be used in a parameter identification process. Various algorithms of local and global optimization theory are summarized.

One target of this research is to identify frequently used techniques in tunnel design and relate them to back-analysis methodologies. In chapter 5, traditional methods such as the Convergence-Confinement approach, are fundamentally examined and the limitations are discussed. Such methods are still used today especially in conjunction

with two-dimensional plane strain numerical modeling. This part of the research identifies some of the limitations of different convergence-confinement methods and presents new models in the form of longitudinal convergence formulae that can be used in tunnel modeling. Useful guidelines and examples are given regarding the application of the previous and the newly proposed convergence relations. A method is suggested, where the above principles can be used at a preliminary stage to perform a simplified back-analysis based on instrumentation data.

One of the most popular methods in numerical modeling of tunnels is the use of the two-dimensional plane strain approximation. Despite the modeling shortcomings, it allows for faster analysis time and it can be successfully utilized in predicting the ground-support interaction if some modeling factors are reasonably considered. Chapter 6 focuses on examining the behavior of a popular gradient-based optimization algorithm, in parameter identification problems. The multivariate version of the Newton-Raphson method is employed via the use of a popular commercial geotechnical numerical program. The limitations of equivalent methodologies are discussed along with the requirement of more suitable techniques.

The limitations of local search optimization techniques lead the research into the development and application of alternative methods. Local search algorithms present fundamental theoretical problems in their applicability due to the use of a plane-strain formulation, especially for plasticity problems. In this part of the research two global optimization methods are employed for the first time in back-analysis of tunnel response. These are the Simulated Annealing and the Differential Evolution method and they are described in chapters 7 and 8, respectively.

Both algorithms belong to the class of heuristic search methods and both are based on simulation of natural process. The novelty at the use of these techniques is reflected on the application via a commercially available numerical program of a combinatorial optimization algorithm (Simulated Annealing) in continuous parameter geotechnical problems, especially in modeling tunneling induced displacements and tunnel support loads. The advantages and limitations of this algorithm are described in chapter 7. The algorithm is characterized by easy implementation into any type of programmable geotechnical software, and since it is not gradient or pattern search

direction dependent, it is a strong candidate for highly non-linear constrained back-analysis problems.

This research also appears to be the first to employ a type of genetic algorithm able to deal directly with floating point continuous variables. In the analysis presented in chapter 8, the Differential Evolution strategy proves to be a very powerful optimization algorithm. This analysis is the application of the algorithm in stress analysis-based back-analysis. The performance of this algorithm is compared against the Simulated Annealing and comparative examples and results are given. The limitations of the method and how these could affect the parameter identification are also discussed.

Chapter 9 presents a case study of the Heshang highway tunnel in China. The Differential Evolution algorithm is employed to perform a displacement-based back-analysis of the tunnel based on the available monitoring data. The analysis is performed using the program FLAC. This example also helps to formulate guidelines that should be used when performing a back-analysis procedure using any numerical program.

Chapter 10 summarizes the conclusions of the research on back-analysis for tunnel design. The main features and characteristics of the proposed methods are presented. Guidelines on the use and application of the methodologies are given, some of which also apply to any back-analysis method. The advantages and disadvantages of the presented methods are outlined. The essential role of sound engineering judgment is also discussed.

Modern Personal Digital Assistants (PDAs) have strong potential to facilitate and improve field data acquisition and logging involved in rock mass characterization by the use of rock mass classification systems. A novel approach using an electronic fieldbook to perform insitu rock mass classification is presented in Appendix A. This system can lead to faster data acquisition as it eliminates the need to transmit and convert paper-based data to digital form. In turn, the readily available data can be analyzed faster and information gained from the analysis can be acted upon in a more timely manner.

Finally Appendices B, C and D provide listings of the computer codes, for the implementation, using the FISH language of FLAC, of the different back-analyses studied in this thesis.

CHAPTER 3. Tunnel monitoring systems

Field monitoring is essential in the observational method in tunneling for various reasons. Monitoring provides valuable information especially for back-analysis purposes and feedback from the surrounding ground for the safety of the work, but it also protects legally the work itself as a record of progress and is the primary legal evidence when safety of the tunnel or of nearby structures have been compromised. The type of data and their associated uncertainties influence the decision in different tunneling activities but also the parameter identification processes and results. For this reason an extensive review of modern monitoring equipment and instrumentation was considered necessary and beneficial for the AMADEUS project.

The area of instrumentation monitoring has been examined by various authors including von Rabcewicz (1963), Pacher (1963), Müller and Müller (1970), Londe (1977), John (1977), Dunnincliff (1988), Dutro (1989), Kovari and Amstad (1993) and others. Today a wealth of different systems is available to the engineers of underground construction. Nevertheless, Dunnincliff (1988) points out the importance of an appropriate instrumentation planning program that matches the needs of the performed work.

The questions that need to be answered in such cases is what type of data are required (i.e., deformations, stresses, etc.), the desired accuracy of the measurements, the density distribution and locations of the instruments and the monitoring stations as well as the frequency of the readings. Gioda and Sakurai (1987), Londe (1977), Sakurai (1998) and Sakurai et al. (2003), discuss the importance of measurements in tunnels for back-analysis. Xiang et al. (2003a) discuss the influences of many factors in the optimal layout of measurements. The main conclusions of their research suggest that:

- The measurements should be sensitive to the parameters to be identified,
- Although the system sensitivity is a very important factor, the layout of optimal measurements is not only dependent on it,
- There is no definite relation between the number of measurements and the optimal measurement layout, and
- The logic of preference for monitoring large magnitudes of displacements or strains for back-analysis cannot be established

An outline is given of the most frequently used terms in measurement uncertainties of monitoring equipment. Basic features, characteristics and accuracy issues are briefly discussed for each instrument or method. According to Dunnincliff (1988), uncertainties related to measurement equipment can be described by the following magnitudes: conformance, accuracy, precision, resolution, sensitivity, linearity, hysteresis, noise and error. The last factor is more general and can affect greatly the feedback received from monitoring. Error can be further distinguished into:

- Gross error: due to inexperience, misreading, misrecording, computational errors
- Systematic error: calibration problem, hysteresis, nonlinearity
- Conformance error: improper installation, design problems or limitations
- Environmental error: weather, temperature, vibration, corrosion
- Observational error: variation between observers
- Sampling error: variability in the measured parameters, incorrect sampling method
- Random errors: Noise, friction in components, environmental effects.

In general, measurement methods employed in tunnels should be able to capture the overall behavior of the surrounding ground and not just a few typical sections according to Dutro (1989). Figure 1 shows a typical measuring section of a tunnel. It is often more reliable to measure more sections with decent quality equipment than to have fewer measurement stations with high end measuring components. This is partly the reason why stress measurements in the rock mass or in the liners are not preferred by engineers while deformation measurements are more popular. The simplest rule for monitoring equipment planning is that measurements must be abundant enough but the cost must not be unreasonably high.

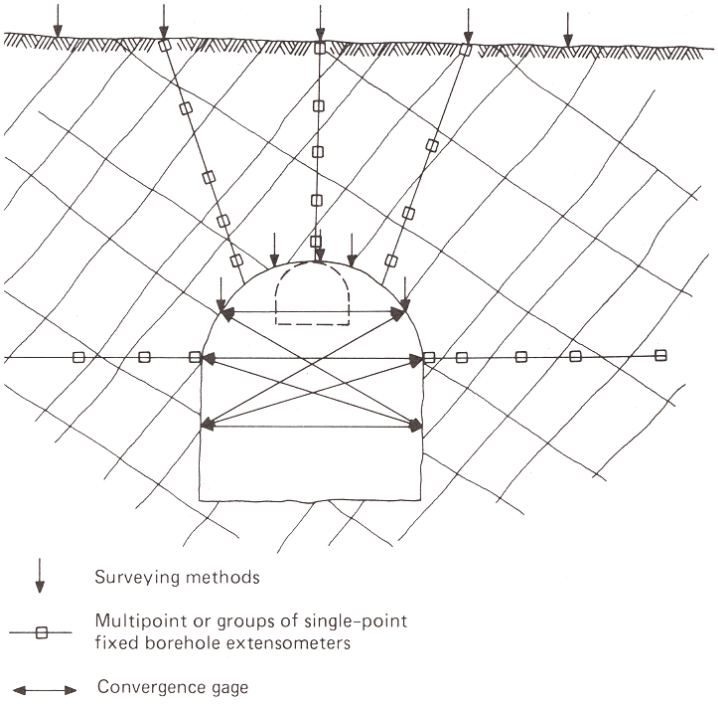

Figure 1: Typical layout of instrumentation in a tunnel (from Dunnincliff, 1988).

Displacement measurements on the tunnel boundary are usually conducted with surveying measurements from a Total Station device, or with a tape extensometer. In the first method, special reflex targets are installed via supporting bolt-studs at the tunnel boundary. The total station device measures by laser beam reflection the coordinates of each point. From the coordinate measurements, independent point deformation or any relative deformation between two points can be made. A series of measurements in time at the same location can reveal the deformation trends of the excavation. The normal magnitude of accuracy for such measurements, depending on the weather conditions in the tunnel can be in the order of 2-4 mm. It is usual that such measurements via surveying are assigned during a project to a special subcontractor who has good experience in such measurements so that maximum accuracies are obtained. Dunnincliff (1988) makes a comprehensive review of the accuracies associated with different surveying methods. Surveying provides absolute deformation measurements when all the analysis is tied to a reference benchmark. Figure 2 shows a typical setup of surveying stations along a tunnel route and Figure 3 presents a typical readout after post-processing of surveying results.

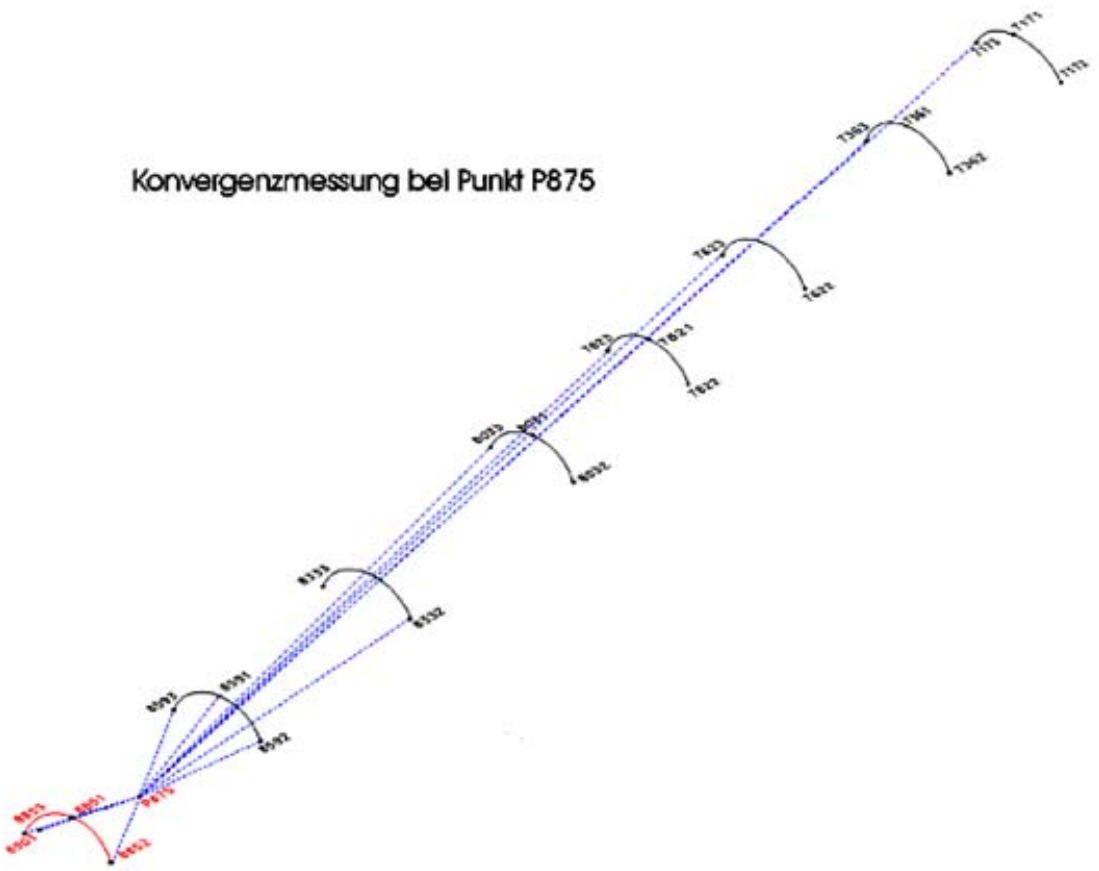

Figure 2: Example of total station-based tunnel monitoring by Hochmair (1998).

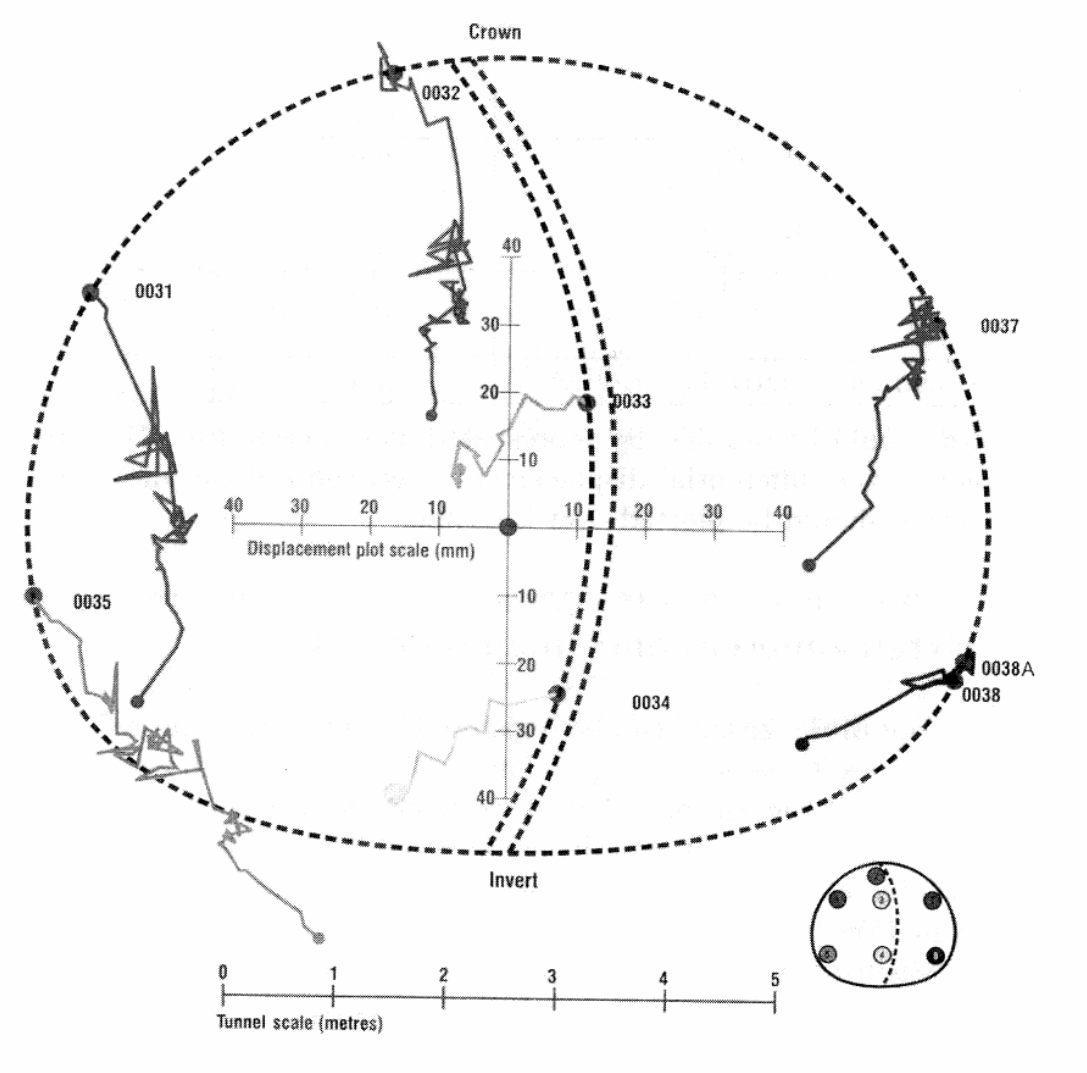

Figure 3: Example of deformation vectors obtained from reflex target measurements around a multi-staged tunneling process. From Kolymbas (2005).

The metal tape extensometer offers typical measuring range of 1-30 m and greater accuracy in the order of 0.1-0.5 mm at the expense of manual measurement between selected points. The sensitivity of modern tape extensometers is in the order of 0.05 mm and repeatability at about 0.1 mm in the best conditions. The metal tape extensometer can only measure convergence (change in distances).

Displacements in the surrounding rock mass are usually made by single or multipoint extensometers. In these devices, the head is fixed at the surface of the ground (mouth of borehole) and up to eight anchor heads can be fixed in various depths. With

this equipment the relative deformation between the head and the individual rod ends can be measured (extension). The multi point borehole extensometer (MPBX) provides relative displacement and not absolute measurements. If the head position is surveyed through time then absolute deformation calculations can be made. Different types of borehole extensometer designs have been presented by various manufacturers. Typical ranges are 50 – 250 mm and precision is around 0.025 mm. The accuracy of modern designs can reach ±0.25% F.S. (full scale) and non linearity is usually less than 0.5% F.S. according to Geokon (2005).

Bolt axial forces can be measured by installed measuring anchors or with a specially designed pressure cell. The measuring anchor allows the measurement of axial force distribution on the anchor body. It is usually a hollow steel anchor in which a compact type of extensometer enclosed. Extensometer measuring wires are pre-installed at specified equal distances inside the rockbolt and their deformation can be related to the rock bolt axial force via its known elastic properties. Measuring anchors have usual lengths of 6.0 m and reading accuracies of 0.01 mm. The anchor cell can only measure one point load and is placed at the head of the anchorage on the rock wall. Both of these devices can measure pressure changes as the anchorage receives load during tunnel advance and results can be used to check the bearing capacity of the installed bolts and any potential problems from bolt overloading.

Shotcrete or concrete stress is measured usually via dedicated flat pressure cells encapsulated in the body of the lining during construction. Such an application is shown in Figure 4. Cells can be accommodated to measure tangential and radial stresses in the shotcrete and are usually installed in pair one perpendicular and one tangential to the tunnel radius. This arrangement is frequently named as NATM cell (Geokon, 2005). These stress cells can measure tangential pressures up to 20 MPa and radial contact stresses up to 5 MPa. They have a resolution of ±0.025 % F.S. and accuracy of ±0.1% F.S. Stresses in steel sets are usually measured by strain gages installed on the body of the steel sets. The information obtained from the gage elements can be highly variable between different sections and is not considered as representative of the overall tunnel behavior by many researchers and engineers.

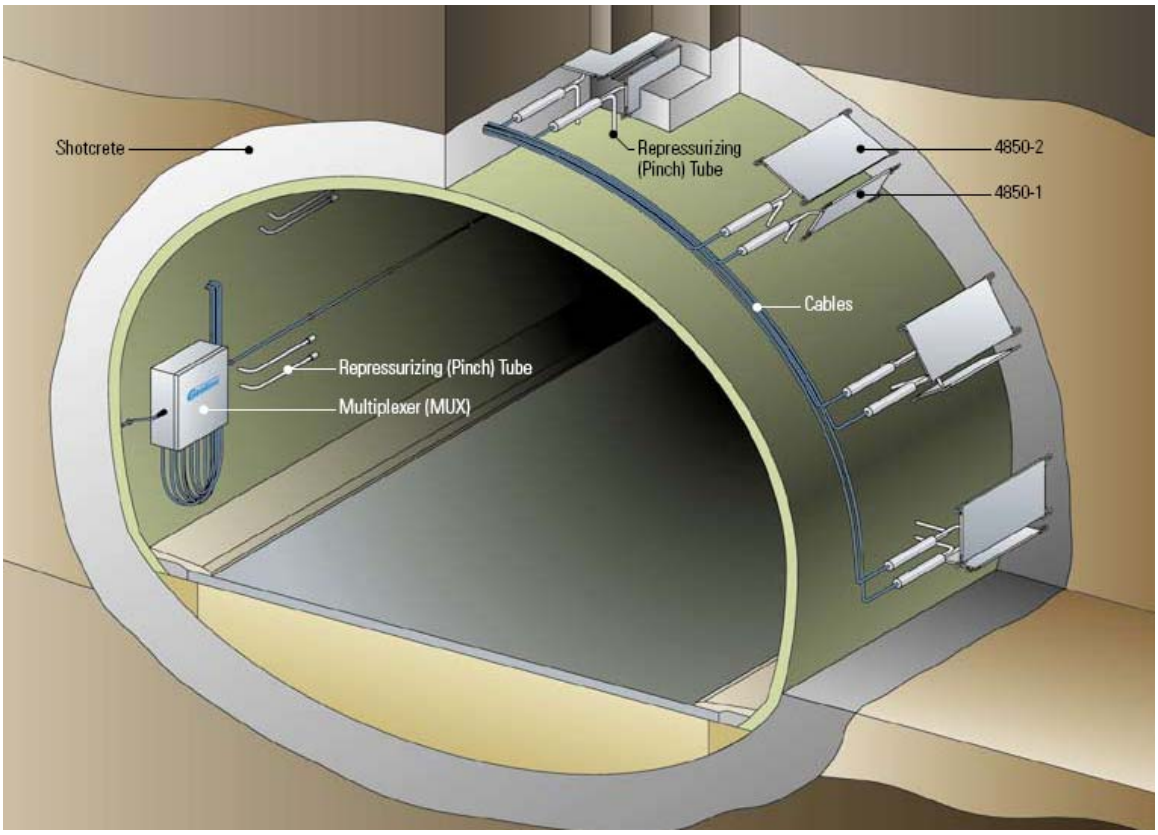

Figure 4: Application of shotcrete stress cells in tunnel monitoring. After Geokon (2006).

CHAPTER 4. State of the art in back-analysis methods

4.1. General principles of back-analysis

The term back-analysis involves a procedure where different parameters and hypotheses of a trial problem, which can be expressed numerically, are varied in order for the results of the analysis to match a predicted performance as much as possible. This procedure is very well tied to the observational method in engineering, promoted as concept in geotechnical engineering by Peck (1969). Generally, the back-analysis involves two separate approaches. In the inverse approach, all the governing equations of a hypothetical numerical model are inverted therefore the known performance becomes an input parameter and the original parameters become the solution of the inverted solution scheme. This approach can only be applied in very few engineering problems under very good control of experiment execution and when a model is simple enough to be invertible. The second approach is more general and adaptable to a series of problems involving multiple unknowns and non linear governing equations and processes. This is known as minimization method, where a dedicated numerical process aims in minimizing the error between predicted and measured performance (e.g., deformations or stresses).

In most geotechnical problems involving underground excavations, stress analyses are great tools in the hands of the designers and engineers. In any of these analyses some steps are essentially common according to Gioda (1985):

1. Some initial knowledge of a subsurface condition exists from geotechnical investigations, the construction documents, etc.
2. A model is assumed to simulate the natural system artificially. This involves usually a numerical method, such as the finite element, the discrete element method etc. A model is also hypothesized for the behavior of elements such as the rock mass, the fractures, etc.
3. Based on laboratory or field tests, initial parameters are chosen to express the strength and elasticity of the involved materials.
4. Assumptions are also made with respect to boundary conditions, initial state of stress etc., and

5. The problem is solved until a stable solution is reached for the governing equations.

Gioda (1985) points out that a distinction of back-analysis methods can also be made considering deterministic and probabilistic approaches. When high precision measurements are available or when the back-analysis model is not highly sensitive to measurement errors, then a deterministic approach can be followed. On the other hand when there can be a quantifiable degree of error in the measuring procedures or when an initial estimate of the descriptive statistics of the governing parameters can be made, then a probabilistic type of back-analysis is more appropriate. Especially for tunneling applications, where complete control of the measuring methods is not possible then weight will be shifted on the application of the probabilistic studies as described later. The later methodology is often described as "Bayesian" or maximum likelihood approaches.

The method which will be used for the AMADEUS project is the direct approach where a separate program routine handles the iterations so that the predictions will ultimately match the measured performance. This involves a minimization process of an error function. An example of an error function is:

$$\varepsilon = \sum_{1}^{m}{}_{i}(u_i - u_{i_m})^2 \tag{1}$$

where u_i is the i_{th} predicted value of performance and u_{im} is the corresponding i_{th} value of measured performance. In its normalized generic version it is given as:

$$\varepsilon = \sum_{1}^{m}\left\{ w_i \cdot \left(\frac{u_i - u_{i_m}}{u_{i\,m}} \right)^2 \right\} \tag{2}$$

In equation (2) w_i is a weight factor that can be applied for each measurement. This can be related with the reliability and quality of the various monitoring data. For example if deformation measurements are considered to be more reliable than lining stress measurements, they can be assigned a weight value higher than that of the lining stress normalized error. Other definitions of functions to be minimized are also possible, but in all cases a program is required to perform the iterations quickly. Obviously, the more the

parameters to be controlled, the longer and more demanding the back-analysis is in terms of computer resources. Equations (1, 2) are generally highly non-linear functions of the unknown parameters and cannot be expressed analytically. A versatile algorithm should therefore be employed to handle the situation.

4.2. Literature review of back-analysis in geotechnical engineering

Cividini et al. (1981) and Cividini et al. (1983) give an insightful review of back-analysis principles, aspects, including also examples of both direct and inversion methods. Their probabilistic analysis shares the concept presented by Eykhoff (1974) in parameter identification. The importance of the error involved in the measurements is taken into account in their analyses. Gioda (1985) presents an example back-analysis, of a geotechnical embankment problem where both the inverse and the direct approach were used. Gioda and Sakurai (1987) also present a survey of back-analysis methods and principles with reference to tunneling problems. Their review and examples involve deterministic and probabilistic approaches. Sakurai and Abe (1981), Sakurai and Takeuchi (1983) present a displacement-based back-analysis methodology that yields the complete initial stress and Young's modulus of the rock mass by assuming the rock as linearly elastic and isotropic. Sakurai and Abe (1981) introduce the concept of maximum shear strain in the estimation of the plastic region around tunnels by using monitoring data for the back analysis. Later Sakurai et al. (1985) introduce the concept of critical strain (maximum shear strain on the elasto-plastic boundary) and use the Mohr-Coulomb criterion for prediction of failure. The concept of "equivalent" elastic modulus is also presented for the overall behavior of jointed rock masses. The concept of critical strain is further refined and its association as a degree of safety and as a hazard indicator is promoted by Sakurai et al. (1985) and Sakurai (1998). In the same work, it is suggested that the term back-analysis should include also a search for a material behavioral model and no model should be taken a priori for such an analysis. In that case, the term "parameter identification" seems more applicable. Sakurai et al. (2003) present a comparison of different back-analysis tools and presents the importance of the assumptions and the type of tool chosen for the back-analysis in the validity and

"correctness" of the back-analysis results. A thorough review of the critical strain concept and its use in back-analysis applications can be found in Sakurai (1993).

Contribution to the probabilistic methods in back-analysis for tunneling has also been provided by Ledesma et al. (1996) and Gens et al. (1996) who describe a minimization procedure along with reliability estimates of the final calculated parameters, coupled with the finite element method. The main elements of the methodology is similar to that of Eykhoff (1974) and Cividini et al. (1981) that make use of a priori information from prior geological investigations. A maximum likelihood approach with extension to Kalman Filtering principles was presented and used by Hoshiya and Yoshida (1996).

Swoboda et al. (1999) suggested the use of the boundary control method to perform back-analysis along with a local search algorithm. This method was later improved and promoted by Xiang et al. (2002) and Xiang et al. (2003b). The numerical results revealed that this is a stable and fast-converging algorithm under certain circumstances. A displacement-based back-analysis method formulated as a combination of a neural network, an evolutionary calculation, and numerical analysis techniques was proposed by Feng et al. (2000). A back-analysis approach named as TBA using three dimensional modeling, has been successfully used by Zhifa et al. (2000). Chi et al. (2001) applied the conjugate gradient method along with a ground volume loss model for back-analysis of a shallow tunnel. Deng and Lee (2001) have used a novel method for displacement-based back analysis using an error back-propagation neural network and a genetic algorithm (GA). An interesting application of back-analysis of insitu stresses based on small flat jack measurements has been performed by de Mello Franco et al. (2002) in the case of a Brazilian rock mine. Lecampion et al. (2002) performed identification of constitutive parameters of an elasto-viscoplastic constitutive law from measurements performed on deep underground cavities (typically tunnels). Their back-analysis was based on local search by using the Levenberg–Marquardt algorithm. Back-analysis based on neural networks has also been presented by Pichler et al. (2003). Their method utilizes an artificial neural network which is trained to approximate the results of FE simulations. A genetic algorithm (GA) uses the trained neural network to provide an estimate of optimal model parameters.

Deng and Nguyen Minh (2003) have presented a back-analysis method based on minimization of error on the virtual work principle. The method showed to be valid for both linear elastic and nonlinear elasto-plastic problems. Feng and An (2004) suggested the integration of an evolutionary neural network and finite element analysis using a genetic algorithm for the problem of a soft rock replacement scheme for a large cavern excavated in alternating hard and soft rock strata. The method of neural networks in back-analysis has also been used by Chua and Goh (2005). In their work, a method termed as Bayesian back-propagation (EBBP) neural network was used via a combination of a genetic algorithm and a gradient descent method to determine the optimal parameters. Finno and Calvello (2005) performed back-analysis of braced excavations using a maximum likelihood type of objective function and local search optimization. Artificial neural networks have also been recently applied by Lee et al. (2006) in back-analysis of shallow tunnels in soft ground. Zhang et al. (2006) have employed a direct search technique and a damping least squares method along with a proprietary three dimensional modeling scheme, to back-calculate geotechnical parameters.

4.3. Optimization classes

Reviews of the generally available optimization algorithm classes can be found in Beveridge and Schechter (1970), Himmelblau (1972), Kuester and Mize (1973), Rao (1996) Venkataraman (2002) and Baldick (2006). Since most of the geotechnical related parameter estimation problems include a highly non-linear function of the involved parameters, some of the most important algorithms suited for non-linear optimization will be briefly mentioned here.

4.4. Local optimization methods

4.4.1. Non linear unconstrained optimization techniques

Based on the use or not of the derivatives of the functions, these optimization algorithms can be further distinguished into two classes: the Direct Search and the Descent Search or Gradient-based methods.

The Direct search methods do not require the computation of any derivatives and as such may be more efficient in some cases at the expense of solution precision. Such examples are:

- Random search method (stochastic-based)
- Grid search method. The search is based on a predetermined grid formed in the multivariate coordinate space
- Univariate search method. The search is done along one coordinate (parameter) and by keeping the other coordinates constant, in a sequential fashion
- Pattern Search methods. The search is based on the information obtained from the previous solution steps which guide the solution towards the direction of the optimum. This class includes the pattern search method of Hooke and Jeeves and the algorithm presented by Powell (1962) and Powell (1964). The later is a more advanced pattern search method and most widely used direct search technique. It can be proven that it is a method of conjugate directions thus it will attempt to minimize a quadratic function in a finite number of steps. The main algorithm is shown in Figure 5.
- Rosenbrock's method of rotating coordinates, which is an extension of the Hooke and Jeeves technique presented by Rosenbrock (1960).
- Simplex method. A type of Simplex analytical algorithm has been primarily developed for linear programming problems. A similarly named method can be used for non-linear problems. The general Simplex version is based on the formulation of a geometric shape of n+1 points in the n-dimensional space. It was initially introduced by Spendley et al. (1962) and later further developed by Nelder and Mead (1965). By sequential processes of comparing the objective function value at the vertices, reflecting, expanding and contracting the simplex, the algorithm approaches a local minimum. It is a very fast and relatively reliable algorithm but for highly non-linear problems the simplex may easily collapse to its centroid and thus fail

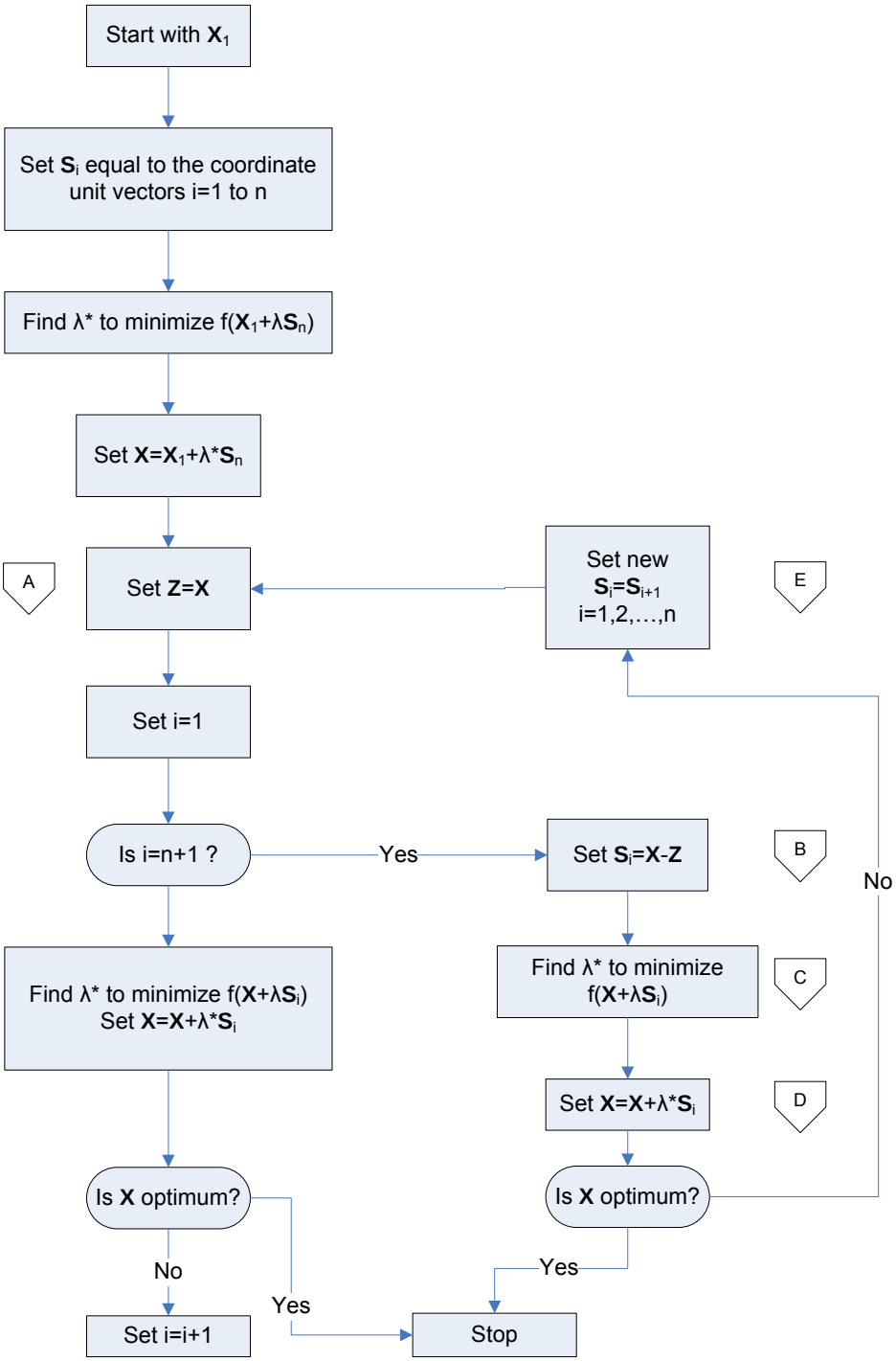

Figure 5: Flowchart for optimization using Powell's method. After Rao (1996).

The Descent search or Gradient-based methods require the computation of the first or even the second order derivatives and as such may be more time consuming. Such examples are:

- Steepest descent. It requires calculation of the n-dimensional gradient of the objective function. Due to the sole exploitation of the gradient, which is a local property of the function, the method is not very successful.
- Conjugate gradient method by Fletcher and Reeves (1964). It has similar characteristics to the method of Powell, and it also uses information from the function gradient. The property of quadratic convergence close to the optimum makes it a fast descent algorithm. Nevertheless it is not as efficient as the Newtonian methods described later.
- The Newton-Raphson method for solving single variable non-linear equations can be extended to approximate solutions of multi-variable equations. The multivariate Newton method assumes that the function can be quadratically approximated by a Taylor series' expansion at any point. As a second order method it utilizes information from the gradient and the Jacobian matrix of the gradients thus the Hessian matrix at each solution step. It is a local search greedy algorithm, and may become difficult to use because of the calculation of so many partial derivatives. More information on the use of this method will be provided in chapter 6. Instead of the Newton method, the Gauss-Newton method using only first order derivatives has shown good results in back-analysis. A modification of the Gauss-Newton method is the Levenberg-Marquardt algorithm. It attempts to combine the features of the steepest descent method when it is away from the optimum and the good convergence of the Newton method when it is close to the optimum.
- Quasi-Newton methods. The computational load of the calculation of the Hessian matrix in the Newton method, as well as the problems arising from the needs for a positive definite Hessian, make the Quasi-Newton methods appealing. They are based on the estimation of the Hessian using

an update scheme, rather than recalculating all the partial derivatives again.

- The Broyden-Fletcher-Goldfarb-Shanno method (BFGS). It is perhaps the most formidable gradient-based method. It is a type of Quasi-Newton and Variable Metric method. It is recognized by quadratic convergence and makes use of prior information from the solution history. It is based on a continuous update of the Hessian matrix rather by using first order derivatives

4.4.2. Non linear constrained optimization techniques

The constrained methods involve linear, non-linear, equality or inequality constraints. Each method is usually able to address a certain type of constraint. Of those methods the most frequently encountered are:

- The Complex (COnstrained siMPLEX) method by Box (1965). This is a very powerful constraint optimization algorithm sharing some of the elements of the Simplex method. It is especially suited for highly non-linear objective functions and under certain circumstances there is a high chance for the method to converge to the global optimum solution. Instead of using n+1 vertices for a geometric shape like a Simplex, the Complex is using a shape of at least n+1 vertices (usually 2n). This creates a polygon able to adapt better in the n-dimensional space and to follow many constraints. In a general sense, the core of this methodology resembles the principles of the mutation and crossover of an array of genes found in the genetic algorithms. In fact for many genetic algorithms the number of trial individuals is in the order of 2n-10n in order to reach a global optimum. The Complex algorithm has been successfully used by Saguy (1982) in global optimization of fermentation processes. It is perhaps the only direct search (non gradient) algorithm which features global optimization strengths. More insight on the implementation of the algorithm can be found in Richardson and Kuester (1973).
- The Generalized Reduced Gradient method (GRG). This is a powerful numerical method able to address non-linear problems with mixed types of constraints. It is

based on the principle of eliminating variables using equality constraints but it may require more intensive programming to be implemented in a code.

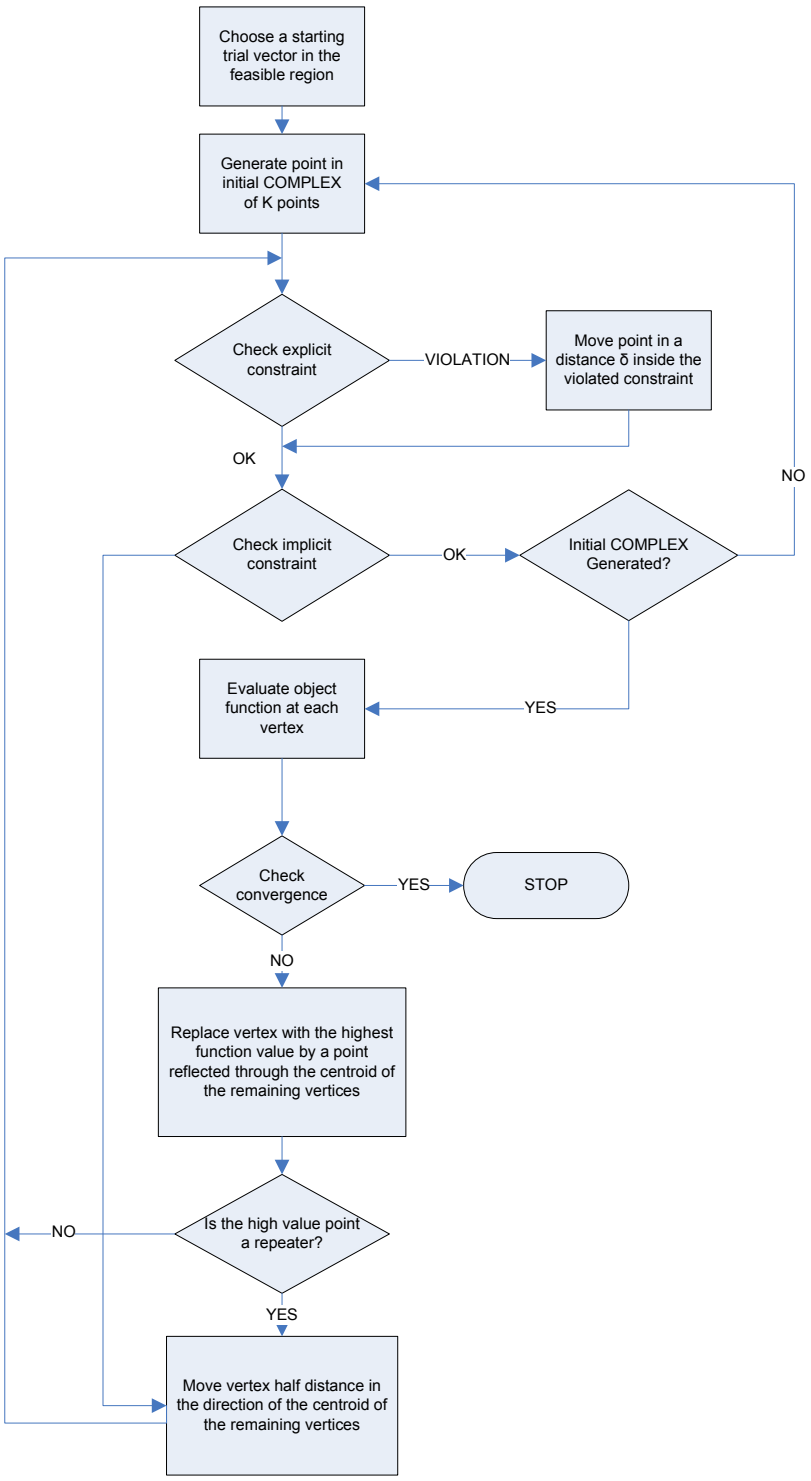

Figure 6: Flochart for the COMPLEX method. After Kuester and Mize (1973).

4.5. Global optimization methods

This is perhaps the most challenging area of Operations Research. The development of techniques to search for a globally optimum solution (if there is one) is highly involving and interesting when efficiency is required. Excellent reviews of global optimization methods can be found in Horst and Pardalos (1994), Pardalos and Romeijn (2002) and Neumaier (2007). Some of these techniques are methods of dynamic programming, branch and bound methods, annealing methods, and genetic algorithms. Of those methods, the last two, which will be further analyzed and presented in the following chapters, are very strong candidates for back-analysis in geotechnical engineering and both are based on simulation of physical processes. Annealing follows principles of metallurgy and thermodynamics while the core of the genetic algorithms is based on the Darwinian theory of survival of the fittest. Their main nature is heuristic thus they do not involve greedy optimization criteria like gradients or pattern search directions. As we shall see, implementation of both of these methods can be advantageous in some geotechnical back-analysis problems especially when "a-priori" information may not be available or when it is unreliable. More insight on the use and application of these methods in back-analysis of geotechnical engineering problems will be provided in chapters 6 and 7.

CHAPTER 5. Simplified parameter identification for circular tunnels using the Convergence-Confinement method

5.1. General

The idea of the ground response curve, or otherwise the "characteristic curve" of the ground mass is considered to originate from Fenner (1938) who also proposed a closed-form solution for the problem of a circular opening in elastoplastic ground. The characteristic curve was later used by Pacher (1963) and was further promoted for empirical tunnel design by various authors such as Brown and Bray (1982), Brown et al. (1983), Panet (1993), Peila and Oreste (1995), Oreste and Peilla (1996), Carranza-Torres and Fairhust (1999), Asef et al. (2000), Carranza-Torres and Fairhust (2000), Alonso et al. (2003), and Oreste (2003). Guidelines for its use have also been suggested by the French Tunneling and Underground Engineering Association (AFTES, 1984) for application in rational tunnel design as described by Panet (2001).

The principles of the method are outlined briefly here. Initially, the ground is assumed to be stressed at an insitu hydrostatic pressure p_o and a tunnel of radius R is excavated. Assuming the radial displacement in the periphery of the opening at a reference section, some inward displacement will be recorded as the tunnel face progresses towards the point of reference. This deformation can be simulated by the action of an equivalent pressure acting internally in the opening which can be expressed as a fraction of the initial in situ p_o stress. This is called the "equivalent support pressure" since it gives the same radial deformation at equilibrium. From the initial pressure p_o the ground is gradually unloaded and for some time it behaves elastically. If the ground reaches its strength, further unloading causes the mass to deform plastically and a failure zone is formed around the opening. If at a certain distance d from the face of the tunnel support is installed, then the support pressure versus support deformation can be plotted on the same coordinate system as the ground characteristic curve plot. The intersection of the rock and support characteristic curves is presumably the point of equilibrium for the ground and support assuming that no secondary effects such as creep or long term strength loss occur in the ground. Perhaps, the most critical point in the above method is estimating how much deformation (or relaxation) has occurred in the rock mass prior to

the installation of the support. The knowledge of this pre-deformation would allow the positioning of the support curve at the right position on the horizontal axis as shown in Figure 7.

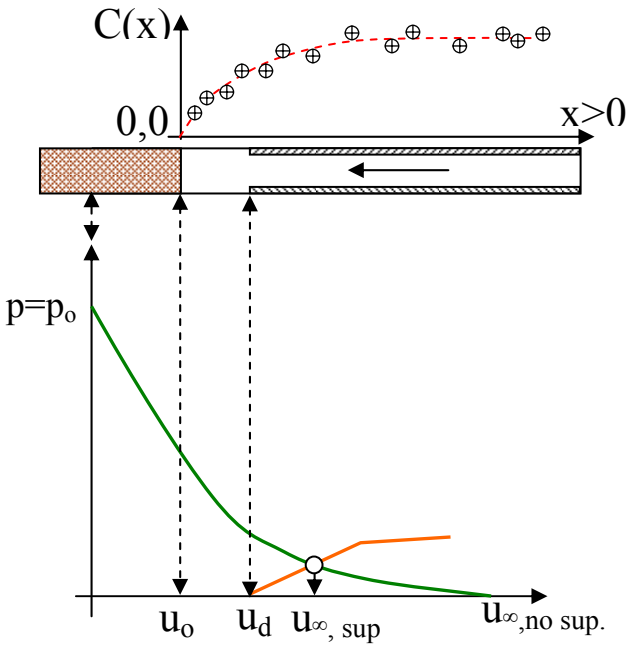

Figure 7: Relation between longitudinal convergence profile and ground-support characteristic curves.

5.2. Back-Analysis using the Convergence-Confinement approach

The convergence-confinement method is a simple yet insightful approach to the problem of ground and support interaction. When it comes to parameter estimation using the convergence confinement method, there are some points that need clarification and or improvement. The data that can be obtained by an appropriate monitoring program are generally deformation measurements and stresses inside the support system. Deformation measurements most often are not absolute but relative, e.g. multipoint extensometers can only measure relative displacements between different anchor points, or tape extensometers measure only relative deformation between two points on the wall of the

tunnel. Measurements by solely using surveying methods cannot incorporate deformations prior to the beginning of the measurements (often starting at the tunnel face). The importance of measurement errors in the use of measurement data for back-analysis has been stressed by Panet (1993), and Cho et al. (2006). Hence back-analysis should be formulated in such a way to use convergence measurements and not absolute deformation measurements which are difficult in most cases to achieve.

In addition, even though support system load monitoring is nowadays more frequent due to advancement of proprietary strain gages and pressure cells equipment (i.e., lining pressure cells), the information which can be obtained from these monitoring systems is susceptible to errors due to uncertainties of the interaction between the ground and the support, the interaction between different support systems and because of variations in the local geology from a monitored section to another. Nevertheless, it is widely acknowledged today that useful qualitative and quantitative information can be obtained by a carefully planned and executed deformation monitoring program. To the present there are two major ways to use the convergence-confinement theory for back-analysis calculations.

5.3. Use of the characteristic curves

Assuming that initial estimates of the ground properties are known, and an estimate of the location of the support curve can also be made, then by knowing two measured quantities such as pressure and deformation (or convergence) at equilibrium, it is possible to back calculate by use of a minimization algorithm the true properties of the ground. This methodology has been presented by Oreste (2005) who proposed back-analyses under various conditions such as: a) when only one magnitude (i.e., pressure) has been measured and two or three uncertain parameters are to be back-calculated, b) when two measurements and two uncertain parameters are iterated, and c) when $\boldsymbol{m}$ measurements are available and $\boldsymbol{n}$ uncertain parameters are iterated. In general, however, it is always prudent to use a higher number of discrete sensors than unknowns for the minimization problem otherwise the solution may not be reasonable from a mathematical perspective. Hence the above back-analysis is more suited when two or perhaps three parameters are unknown, and a reliable support system stress measurement is available.

5.4. Use of Longitudinal Convergence Profiles

Another approach in back-analysis of ground parameters is to use information from convergence measurements as function of the distance from the tunnel face. A typical plot of convergence versus distance from the tunnel face is shown on Figure 7. Back-analyses using a longitudinal convergence profiles, were performed and studied by Gaudin et al. (1981), Panet and Guenot (1982), Guenot et al. (1985), Sulem et al. (1987), and Panet (1993). In this approach, an analytical or computational model linking the ground properties with the developed convergence must be initially assumed. The above researchers used semi-analytical solutions from axisymmetric finite element models to predict the behavior of nearly circular tunnels and with soft support. Strain softening and creep effects were also included in their analyses. Hoek (1999) has also presented an exponential deformation law for total deformation, based on monitoring data from the Minghtan Power Cavern in Taiwan, which can also be found in Carranza-Torres and Fairhust (2000). However, the above solutions do not incorporate the effects of stiff supports in the deformation profiles. In general, all the above models assume a non-supported or lightly supported tunnel (i.e., thin shotcrete layer or light rock bolting).

The above problem of determining the pre-deformation for the convergence-confinement method by incorporating the effects of the support were discussed by Bernaud and Rousset (1992), Nguyen-Minh and Corbetta (1991), Nguyen Minh and Guo (1993) and Bernaud and Rousset (1996). Their approximations provided estimates of the lost convergence before placement of the support, while incorporating the effects of a stiff support. From the above it becomes evident, that the method using longitudinal deformation or convergence profiles (LDPs and LCPs) is promising since many measurement data can be incorporated as input for back analysis with priority on data obtained quickly behind the tunnel front. The use of longitudinal deformation or convergence profiles in combination with the ground characteristic curves is investigated further in this paper.

5.5. Review of existing empirical convergence ratio models

The convergence-confinement method attempts to address the issue of ground-support interaction in a simplified way. This simplicity of course fails to consider the

effects of bending of the structural lining or the effects of interface shear behavior at the support-ground contact. For the purpose of simplified back-analysis, the use of a longitudinal deformation or convergence profile expression is necessary. The equivalent pressure p_i is often expressed as a function of the in situ pressure p_o by the use of the confinement loss factor λ which varies from 0 initially to 1 for a full excavated tunnel and equilibrium conditions:

$$p_i = (1-\lambda)\, p_o \tag{3}$$

In general, the convergence *C(t)* at some time *t* of a tunnel is defined as the change in the distance between two opposing points on the tunnel wall perimeter. Thus:

$$C(t) = D_o - D(t) \tag{4}$$

were D_o is the initial distance and *D(t)* is the distance measured at time *t*.
Obviously there will be a delay for the installation of the monitoring equipment and some convergence can be lost from the monitoring data. Equivalently the convergence can be expressed as (i.e., measured with a tape extensometer):

$$C(x) = 2 \cdot [u(x) - u(o)] \tag{5}$$

where *u(x)* is the radial displacement at some excavated distance *x* considered positive behind of the tunnel face, towards the equilibrated tunnel section and *u(o)* is the radial displacement of the tunnel wall at the location of the monitoring section.

If the measurements commence immediately from the tunnel face after it has been excavated, then the error of back-analysis is minimized, since valuable information of the tunnel behavior can be obtained via frequent measurements close to the face. Most empirical approximations of tunnel convergence are expressed in normalized form as:

$$a(x) = \frac{C(x)}{C(\infty)} = \frac{u(x) - u(o)}{u(\infty) - u(o)} \tag{6}$$

where *C(∞)* is the ultimate convergence of the tunnel at equilibrium conditions.

The empirical expression of the deformation as a function of the distance from the face becomes:

$$u(x) = u(o) + a(x) \cdot [u(\infty) - u(o)] \tag{7}$$

Gaudin et al. (1981), and Panet and Guenot (1982) presented the following estimate of radial convergence $C(x)$ at a distance x from the face of the tunnel for elastic ground:

$$\frac{C(x)}{C(\infty)} = 1 - \exp\left(-\frac{x}{X}\right) \tag{8}$$

where $X \approx 0.84R$

Sakurai (1978) also proposed the calculation of the parameter of the loss factor λ along the relative location of the examined section at distance x from the tunnel face, by the following expression:

$$\lambda(x) = \lambda_o + (1-\lambda_o)\cdot(1-e^{\frac{-x}{X^*}}) \tag{9}$$

where $\lambda_o=\lambda(0)=1/3$ and X^* is a constant

Panet and Guenot (1982) proposed a convergence relation for elastoplastic ground which was validated with various tunnel measurements as well as in general agreement with simplified elastoplastic axisymmetric finite element analyses. The convergence law is given as:

$$\frac{C(x)}{C(\infty)} = 1 - \left(\frac{1}{1+\frac{x}{0.84\cdot R_p}}\right)^2 \tag{10}$$

where R_p is the analytically predicted plastic tunnel radius assuming no support interaction and for the elastic ground case, R_p is replaced by the tunnel radius R. A description of the analytical model can be found in Duncan Fama (1993), and Panet (1995).

Corbetta et al. (1991) suggested the following law assuming similarity with the elastic solution:

$$\frac{C(x)}{C(\infty)} = 1 - \left[\frac{m}{m+\xi(x/R)}\right]^2 \tag{11}$$

where $\xi=u_e(\infty)/u(\infty)$=ratio of the infinite elastic displacement $u_R(\infty)$ to the infinite elastoplastic displacement $u(\infty)$. For a homogenous, isotropic ground the infinite elastic displacement is given as:

$$u_e(\infty)=\frac{p_o}{2G}R \tag{12}$$

m=an empirical factor, G is the shear modulus of the rock mass and ξ is ultimately a function of the stability number defined as:

$$N_s=\frac{2p_o}{\sigma_{c\,mass}} \tag{13}$$

p_o is the average ground stress, $\sigma_{c\ mass}$ is the average unconfined compressive strength of the ground.

For the case of linearly elastic ground behavior, AFTES recommendations suggest the following relation to calculate the confinement loss factor:

$$\lambda_d=1-0.75\cdot\left[\frac{0.75\cdot R}{0.75\cdot R+d}\right]^2 \tag{14}$$

The above relation predicts a loss factor of λ_d=1-0.75=0.25 for d=0 (exactly at the tunnel front) which means that some 25% of final deformation is likely to occur at the tunnel face. If $N_s\leq1$ the rock mass remains in the elastic state. For an elastic- perfectly plastic ground, the final radial displacement is calculated from the relation:

$$u_{final}=u_\infty=\frac{1}{\xi}\frac{p_oR}{2G} \tag{15}$$

where G is the shear modulus of the mass. As a result the following equations are obtained:

$$a(d)=1-\left[\frac{0.75\cdot R}{0.75\cdot R+\xi d}\right]^2 \tag{16}$$

The expression by Hoek (1999) is an exponential deformation relation for total deformation, based on monitoring data from the Minghtan Power Cavern in Taiwan, which can also be found in Chern et al. (1998). The relation is as follows:

$$\frac{u_R(x)}{u_R(\infty)} = \left[1 + \exp\left(\frac{-x/R}{1.1}\right)\right]^{-1.7} \tag{17}$$

For the case of supported tunnels a simplifying assumption is that of an elastic-perfectly plastic support of known geometric and behavioral properties. The load-deformation curve can be obtained and superimposed on the support pressure-deformation plot of the rock mass. However especially for stiff supports, the actual installation of the support changes the characteristics of the convergence profiles and thus makes the estimation of the origin of the support curve in the load-deformation plot more difficult. This issue was addressed initially by Nguyen-Minh and Corbetta (1991), and Bernaud and Rousset (1992) who proposed what is known as implicit methods and which are described later. The method by Bernaud and Rousset (1992) was incorporated in the simplified back-analysis presented in this paper. The details of the above method are given by Bernaud and Rousset (1996) and only the main elements will be described here. The method makes a modification of the original equation (10) by Panet and Guenot (1982) to incorporate the effects of the support. The new relation becomes:

$$\frac{C(x)}{C(\infty)} = 1 - \left(\frac{1}{1 + \frac{\alpha^* \cdot x'}{0.84}}\right)^2 \tag{18}$$

where $x' = x/R$, $a^* \approx 1.82\sqrt{RS} + 0.035\phi$, and RS is the relative stiffness of the lining to the surrounding ground: $RS=K_{sn}/E_m$. As a general approximation Bernaud and Rousset (1996) also suggested the following estimate for the radial deformation at the face:

$$\frac{u(o)}{u(\infty)} = 0.413 - 0.0627 \cdot Ns, \qquad for \;\; 1 < Ns \leq 5 \tag{19}$$

5.6. New convergence ratio models

5.6.1. General procedure

An extensive parametric analysis was performed to determine the effects of the stiffness of the support and the unsupported span length d of the tunnel, on the longitudinal deformation profiles. The deformation profiles are a useful tool to estimate the required pre-relaxation for a 2D (plane strain) numerical analysis and are very often used in the tunneling practice for preliminary purposes or to verify support design. The commercially available program FLAC 2D by the Itasca Consulting Group (2005) was used in an axisymmetric mode to perform this task.

The ultimate goal is to check the validity of the convergence estimates by the previous methods and to suggest any modifications if necessary. FLAC is a robust finite difference based code which allows for large strain calculations while it retains fairly good numerical stability. The axisymmetry mode essentially yields the same results as if a three-dimensional analysis code was to be used for a circular opening under hydrostatic conditions. With a small modification, the models can also incorporate a support member by using continuum elements of higher stiffness i.e. to simulate concrete or shotcrete application on the tunnel wall. The Mohr-Coulomb constitutive model was used to simulate the elasto-plastic behavior of the rock mass, since it has the most wide use so far in the literature and previous research. An example finite difference grid is shown in Figure 8.

The following assumptions were made in the analysis. The tunnel is circular with a radius R=5.0, excavated in isotropically stressed ground with p_o=5.0 MPa (about 200 m overburden). The rock mass average elastic modulus is E=5 GPa and the Poisson's ratio is constant at ν=0.25. Dilatancy effects are not taken into account in the preliminary stage. The tunnel is excavated at a constant rate of d/R normalized advancement and when support is implemented in the models, the support is also installed at a constant rate and it is finalized at d/R before the tunnel face. The support elements use a linearly elastic model.

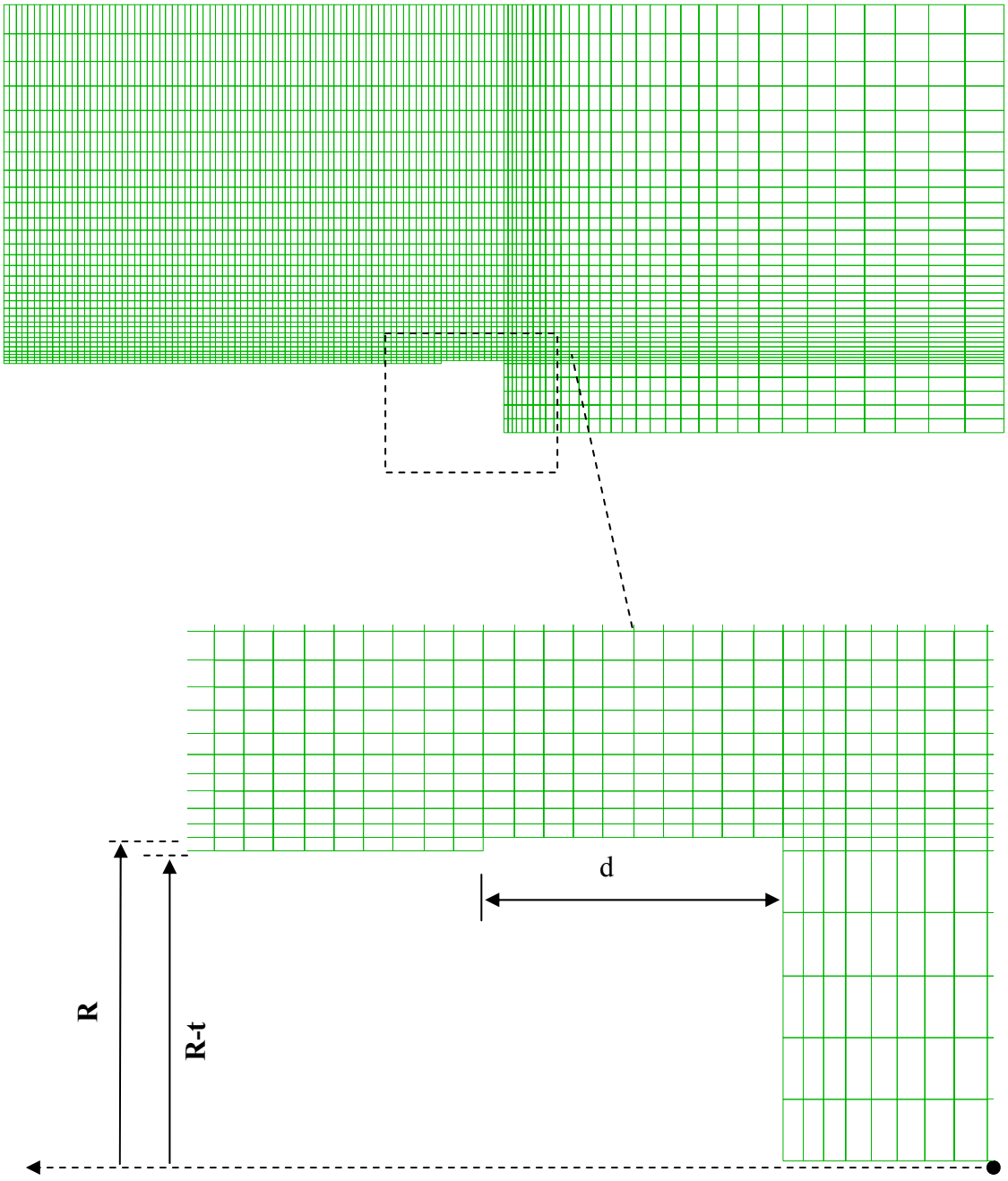

Figure 8: Axisymmetric tunnel model in FLAC.

Different cases were studied. These included supported and unsupported tunnels in elastic or elastic-perfectly plastic ground. For the plasticity cases a comprehensive set of 80 pairs of the shear strength parameters c and ϕ were first calculated, corresponding to stability numbers N_s= 2, 3, 4, and 5. Therefore, there are 20 parameter pairs for each stability number. N_s=1 designates the limit state for elastic behavior, while N_s>1 designates theoretically a plastic state for circular openings with no support at full deconfinement. The relative stiffness and the unsupported span were also varied to study the change in behavior. A routine was written in FLAC's proprietary FISH programming language to assist in the parametric iterations. Longitudinal deformation profile (LDP) data were automatically taken directly from the FLAC output converted to convergence data expressed as $C(x)/C(\infty)$ and batch-processed thru non-linear regression in the program Matlab in order to maintain precision and avoid corruption of data.

5.6.2. Results of numerical analyses

Unsupported tunnels

After all FLAC results were processed, it was found in agreement to the existing literature models that an exponential law can be used with good accuracy to predict tunnel convergence. However, this was realized for all cases of unsupported or supported ground, in elastic or elastoplastic conditions. This general convergence model can be expressed as:

$$\frac{C(x)}{C(\infty)} = 1 - \left(\frac{1}{1 + \frac{x/R}{\beta_1}} \right)^{\beta_2} \leq 1.0 \qquad (20)$$

This relation was found to agree the best with the data. Other relations were also tried by the regression procedure but with less success. The above expression agrees generally with most convergence approximations today. However it is more adaptive due to the existence of two parameters, β_1 and β_2. These two parameters essentially control the geometry of the convergence rate versus the distance from the face. So the task was to investigate how these parameters change with the materials properties.

For the unsupported tunnel in elastic ground equation (10) by Panet and Guenot (1982) was verified in most cases with minor variations in the values of $\beta_1 \approx 0.85\text{-}1.1$ and $\beta_2 \approx 2.0$. For the unsupported tunnel in plastic ground the results showed good fit when β_1 and β_2 are given by the following expressions:

$$\beta_1 = 7.46 - \frac{6.84}{1+\left(\frac{R_p/R}{3}\right)^{3.27}} \quad , \quad \beta_2 = 2 \tag{21}$$

where R_p the analytically predicted plastic radius. At low values of normalized plastic radius $R_p/R<1.3$, results from (21) are in good agreement with the original approximation by Panet and Guenot which predicted that $\beta_1=0.84<(R_p/R)$. For higher values of plastic radius a better prediction is obtained by equation (21).

With respect to the convergence at the tunnel face it is widely accepted that a percentage of 20-30% is lost at the face. This value is important in back-analysis based on convergence data since it has to be deducted from the predicted deformations in order to estimate convergence values along the tunnel length. Multiple non-linear regression on the data showed that the proposed relation (22) gives a good fit. In most cases the ratio was in the range 15-25%.

$$\frac{u(o)}{u(\infty)} = p_1\left(\frac{R_p}{R}\right)^{p_2} \tag{22}$$

where: $p_1 = 0.2N_s^{\,0.223}$, $p_2 = -0.0076N_s^{\,3} + 0.105N_s^{\,2} - 0.488N_s + 0.196$

The above relation gives a useful approximation that incorporates reasonably the variation of the tunnel face convergence, depending on the stress-strength conditions. This approximation can be used for back-analysis of unsupported or lightly supported tunnels by use of longitudinal convergence profiles.

Of the frequently used approximations, the Hoek-Chern normalized curve has a more mild profile and which is constant and irrespective of the plastic conditions. This is due to the fact that the convergence rate according to (17) is:

$$\frac{C(x)}{C(\infty)} \approx \frac{\left[u(x)/u(\infty)\right]^{Chern-Hoek} - 0.3}{0.7} \tag{23}$$

This curve generally predicts slower convergence close to the face than any other curve. The Panet and Guenot, the Nguyen-Minh and Corbetta (1991) approximation and the approximation suggested previously yield essentially the similar results for low normalized plastic radii as shown in Figure 9 a-e. Assuming the same convergence at the tunnel face for consistency, the curves by Panet and Guenot (1982), Nguyen-Minh and Corbetta (1991) and the approximations given by relations (20) and (21) show quick convergence under mild or heavy stress conditions and are fairly close to each other.

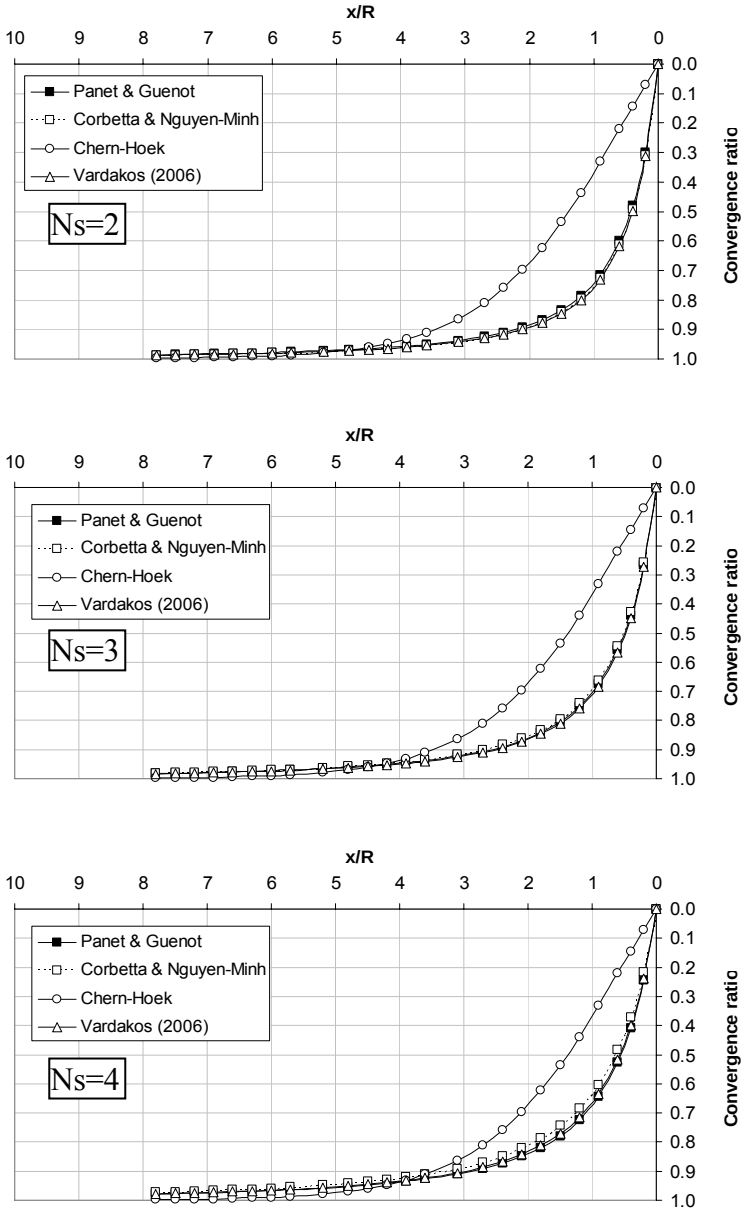

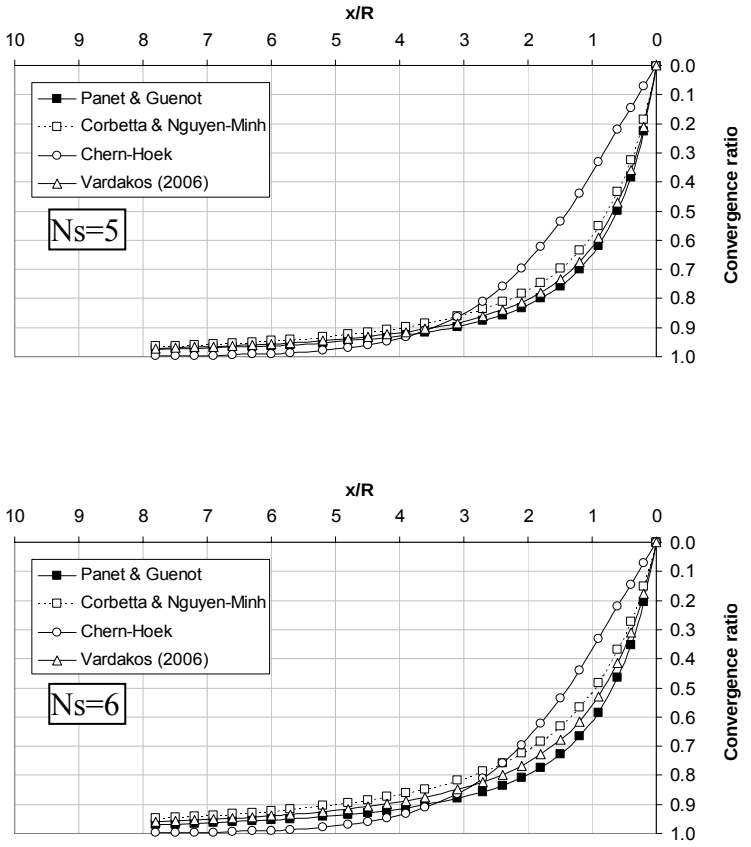

Figure 9: Convergence ratio plots for different models and stability numbers

Supported tunnels

In reality when a support system is installed the behavior of the ground characteristic curve will change. This is better understood if we theorize the new reinforced or supported rock mass, as a new material with a new stiffer response to unloading. Homogenization methods to estimate the overall characteristic curve are described by Peila and Oreste (1995), and Kolymbas (2005). Otherwise the effects of the support stiffness and the unsupported span must be incorporated in a reasonable basis. From a theoretical standpoint, the ultimate goal is to propose a convergence law of the form:

$$\frac{C(x)}{C(\infty)} = f\left(\mathbf{p},\ \frac{d}{R},\ RS\right) \tag{24}$$

where **p** is the parameter vector, *d/R* is the unsupported normalized distance and *RS* is the relative stiffness of the support liner to the ground. An extensive series of parametric

studies were performed by Vardakos and Gutierrez (2006) on supported tunnels using FLAC both assuming linear elastic and elasto-plastic ground. The relations for β_1, β_2 have been revised during this research to incorporate compatibility with a wider range of problems based on more parametric analyses. The following cases were examined: d/R= 0.4, 0.8, 1.0, 1.6, 2.0 and the lining Young's modulus= 10, 15, 20, 25 and 30 GPa.

For the case of elastic ground, due to the existence of two governing parameters, the relative stiffness RS and the unsupported normalized span d/R, the best fit was obtained when both the β_1 and β_2 parameters change according to the following set of empirical equations:

$$\beta_1 = p_1 RS^{-p_2} \tag{25}$$

$$p_1 = 0.375\left(\frac{d}{R}\right)^{-0.053}$$

$$p_2 = 0.107\left(\frac{d}{R}\right)^{-0.224}$$

$$\beta_2 = p_3 RS^{-p4} \tag{26}$$

$$p_3 = 1.56\left(\frac{d}{R}\right)^{-0.021}$$

$$p_4 = 0.0065\left(\frac{d}{R}\right)^{-1.588}$$

By combining the above approximations and by simultaneous use of the ground reaction curves one can obtain an estimate of the convergence along the length of a supported tunnel in elastic ground. The solution should approximate the behaviour of the circular tunnel as long as the relative stiffness RS as expressed above, is in the range RS=0.08-0.3. The Poisson's ratio does not affect the solution much and should not be a concern.

For the case of supported tunneling in elastoplastic ground, post processing of the results showed agreement with the convergence model of equation (20). The variables β_1 and β_2 showed a clear tendency to simultaneously increase with the numerically predicted by FLAC plastic radius R_p for each case, as they also marginally increase with stability

number N_s. Alternatively the model by Bernaud and Rousset will be used along with some modifications for back-analysis purposes. Post processing of FLAC results also showed a wide ratio and that in most cases the deformation ratio at the tunnel face is in the range 22-35%. The approximation given by equation (19) does not consider explicitly the effects of support stiffness or the unsupported distance. Useful information was gained from the FLAC predictions in order to improve on this estimate. Unlike the case of the unsupported tunnel in plastic ground, where the percentage of deformation at the tunnel face shows a power relation with the plastic radius, in this case a nearly linear relationship exists. Through the parametric analyses it was found that the following set of equations can be used to estimate the radial displacement ratio

$$\frac{u(o)}{u(\infty)} = p_1\left(\frac{R_p}{R}\right) + p_2 \tag{27}$$

where p_1 and p_2 depend on the relative stiffness of the lining and the ground and the unsupported normalized distance d/R, and the normalized maximum plastic radius of the unsupported tunnel R_p/R. Based on regression analysis, the approximations for p_1 and p_2 can be expressed as follows:

$$p_1 = \frac{p_3 RS}{p_4 + RS} \tag{28}$$

$$p_2 = 0.083\left[e^{0.233(d/R)}\right] Ns^{0.552e^{0.188(d/R)}} \tag{29}$$

$$p_3 = 0.072\left[e^{1.182(d/R)}\right] N_s^{-0.076e^{3.06(d/R)}} \tag{30}$$

$$p_4 = 0.028e^{\left[-1.026(d/R)+0.357 N_s e^{0.9(d/R)}\right]} \tag{31}$$

Hence, by using a closed-form solution for the ground behavior, an empirical expression for the convergence rate along the tunnel length and a non linear optimization algorithm a simple back-analysis can provide a first degree of approximation to a problem.

5.7. Probabilistic back-analysis method

For simplified back-analysis purposes there are two main elements required to perform the calculations. First the computational model which will perform the calculations and second a powerful optimization algorithm that handles the iterative procedure. The computational model in this case must be able to incorporate the effects of the support in tunnels and should not only handle unsupported tunnels. A closed-form solution using Mohr-Coulomb or Hoek-Brown plasticity models (and a flow rule) may provide the ground characteristic curve for the unsupported tunnel. Advanced solutions exist today that can incorporate strain softening constitutive models but for simplicity will not be discussed here.

The method employed in the computational model incorporates uncertainty by using an initial estimate based on field or laboratory characterization of various properties and the corresponding variances of the parameters. It also uses uncertainty in the measured values of performance via measurement error or correlation between measurements. The basic structure of the method can be outlined here and results from preliminary applications in back-analysis are given. It is important to note that this method should be used when the number of measurements exceeds the number of unknowns. A review of the "Bayesian" back-analysis principles are given by Cividini et al. (1981), and Gioda (1985).

We can assume that $\mathbf{u}_{meas}$ represents a vector of convergence measurements which are influenced by errors described by the vector $\Delta\mathbf{u}_{meas}$. It is possible to assume that the expected value (mean) of the error vector is not significant, thus:

$$E\left|\Delta\mathbf{u}_{meas}\right| = 0$$

The covariance matrix of the errors is then:

$$\mathbf{C}_{u_{meas}} = E\left|\Delta\mathbf{u}_{meas} \cdot \Delta\mathbf{u}_{meas}{}^{T}\right| \tag{32}$$

If all the measurements are statistically independent then $\mathbf{C}_{\text{u meas.}}$ is a diagonal matrix. Similarly to the Bayesian theory, the "a priori" data assumed in this analysis are the expected values of the unknown parameters, and their variances. Thus $\mathbf{p}_o = E\left|\mathbf{p}\right|$ where $\mathbf{p}$ is the parameter vector.

$$\mathbf{C}_{p_o} = E\left|[\mathbf{p} - \mathbf{p}_o] \cdot [\mathbf{p} - \mathbf{p}_o]^T\right| \tag{33}$$

If the entries of the $\boldsymbol{p_o}$ vector are correlated then $\mathbf{C}_{p_o}$ is a non diagonal matrix. For instance there may be a correlation between strength parameters c, ϕ and depth (or equivalently stress magnitude). The average elastic modulus of the rock mass may also be depth (or stress) dependent.

The error function that is to be minimized is:

$$\varepsilon = [\mathbf{u}_{meas} - \mathbf{u}(\mathbf{p})]^T \cdot \mathbf{C}_{u_{meas}}{}^{-1} \cdot [\mathbf{u}_{meas} - \mathbf{u}(\mathbf{p})] + [\mathbf{p}_o - \mathbf{p}]^T \cdot \mathbf{C}_{p_o}{}^{-1} \cdot [\mathbf{p}_o - \mathbf{p}] \tag{34}$$

This error function is composed of two parts. The first term represents the difference between the measured and the predicted performance quantities and the second the difference between the assumed and current trial parameter vector. In both terms the differences are weighted by the inverted covariance matrices whose elements reduce in value with increasing uncertainty. The above equations can be used in conjunction to the Convergence-Confinement method and a convergence rate approximation in a probabilistic-based back-analysis program by using the Microsoft Excel software and the Solver® utility. The later is a powerful non-linear optimization program based on an extension of the Generalized Reduced Gradient algorithm and can be used to minimize the error function given in equation (34).

5.8. Simplified back-analysis by using convergence models

5.8.1. Case of a supported tunnel in elastic ground

In this case the model presented in (20, 25, 26) is used as an approximation of the convergence rate along the tunnel length. The tunnel has radius R=5.0 m and is supported by 20 cm of shotcrete liner. The shotcrete is assumed to have an average Young's modulus of 25 GPa and it is installed at d=4m (d/R=0.8). By closed-form solutions the normal stiffness of the liner is K_{sn}=1100 MPa (RS=0.275). We also hypothesize that convergence measurements are available at 25 points behind the face of the tunnel. For this reason convergence data were obtained by a FLAC simulation assuming the "true optimum" properties show in Table 1. These were used as input for the back-analysis. A

variable error of 2.0 to 3.0 mm was used for the convergence measurements. Table 1 also shows the "a priori" information assumed in the analysis.

For any set of initial parameters the characteristic curve of the ground is given by:

$$u_g = (p_o - p_i)\frac{R}{2G} \tag{35}$$

The support curve is described by:

$$p_s = p_i = K_{sn}\frac{(u_g - u(d))}{R} \tag{36}$$

$$u(d) = \left[1 - \left(\frac{1}{1 + \frac{d/R}{\beta_1}}\right)^{\beta_2}\right] \cdot [u_{eq} - u(o)] + u(o) \tag{37}$$

$u(o) \approx 0.25 * u_{eq}$

The convergence profile, depends on the values of the above parameters, thus the back-analysis will also lead to the solution of the above system, with respect to the equilibrium conditions. For simplicity we assume that the governing parameters are uncorrelated and data from multiple measurements have variations in their errors (i.e. extensometer and surveying measurements). The convergence dependent error function (34) can be easily programmed in Excel. By using the mean values as the initial trial vector, the Excel Solver tool can be utilized to seek the minimum of the error function. The execution of the program gives the solution presented in Table 1, which are fairly close to the actual parameters that were used in FLAC initially.

The optimal solution procedure described above yields a local optimum only. Other lower minima may still exist if the iterations start from a different trial vector. If a second trial is performed and the the iterations start from the "a priori" information: po=7.0±0.5 MPa, Em,o=5000±400 MPa and νo=0.25±0.01, using the same input convergence data, we obtain an optimal vector (Table 1) which is again very close again to the initially used properties in FLAC. The results of this example are shown in Figure 10 and Figure 11.

Table 1: True optimum, initial trial and solution vectors of simplified back-analysis problem

Analysis # / Parameter	True optimum	Trial 1		Trial 2	
		Initial	Final	Initial	Final
E_m (MPa)	4000	4500±200	4262	5000±400	4000
p_o (MPa)	8.0	7.5±0.5	8.29	7.0±0.5	7.83
v	0.25	0.25±0.02	0.258	0.25±0.01	0.252
$u(d)$ (m)			0.01		0.01

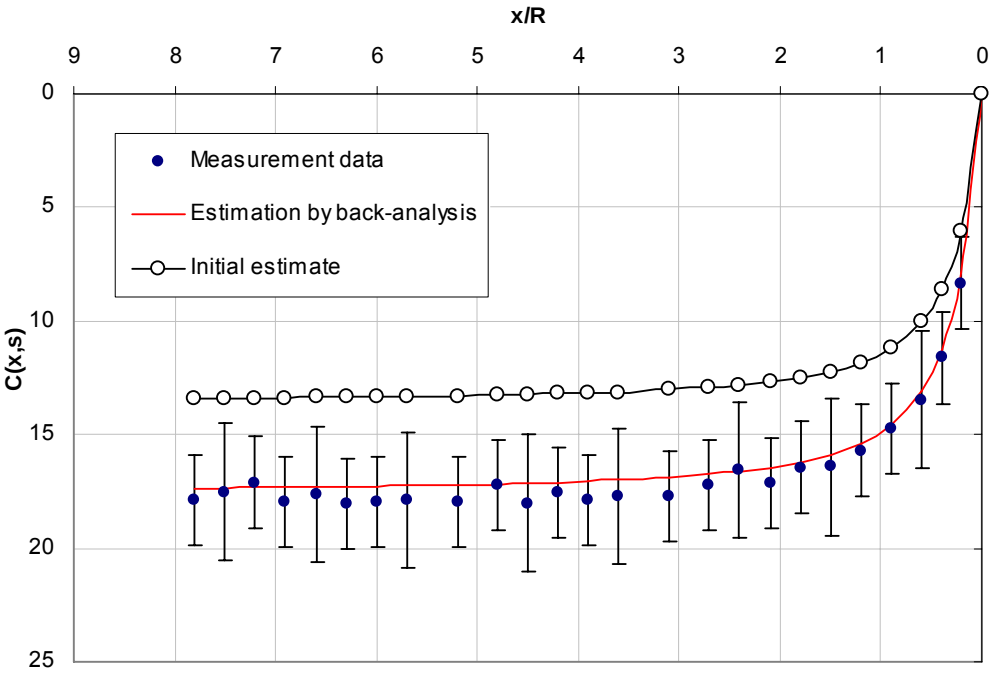

Figure 10: Original and final convergence estimates for tunnel in elastic ground case.

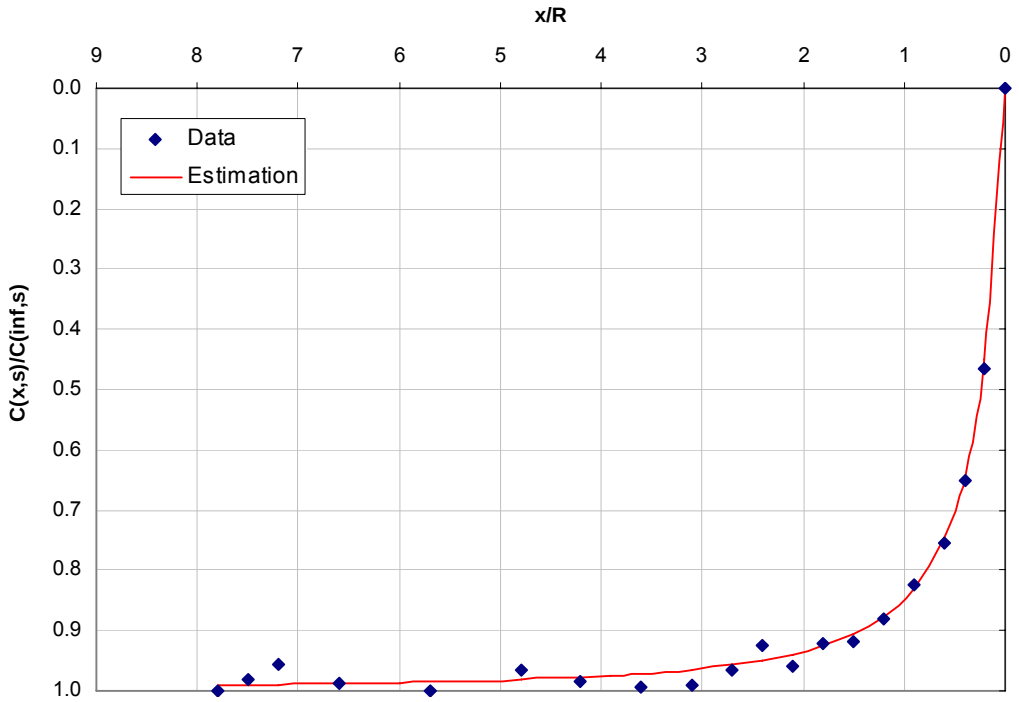

Figure 11: Monitored and predicted by back-analysis convergence ratio estimate.

5.8.2. Case of a supported tunnel in elasto-plastic ground

In this case the model proposed by Bernaud and Rousset (1996) is used to approximate the convergence rate along the tunnel. Convergence data from an axisymmetric FLAC model were used as input for the back-analysis. The data used to generate convergence data from FLAC are summarized in Table 2. Relation (26) was used to estimate the ratio of the radial deformation at the tunnel face. Due to the non-linearity of (26) it is more efficient to enter the $u(o)$ as a search parameter for the optimization by superimposing the equity constraints of (18) and (27).

Convergence data were selected at 25 points behind the face of the tunnel and a variable error of 2-4 mm was applied to the data to simulate uncertainty. Again the use of Excel Solver is advantageous in order to solve the non-linear system of equations during back-analysis. In this case the unknowns are the vector $\boldsymbol{p}$ and the pre-deformation $u(d)$ at the point of support installation. The set up of the system of equations for equilibrium is composed of the characteristic curve (closed-form solution), the support curve and the error function to be minimized. The initial information used for the back-analysis

consisted of the property values shown in Table 2. The same table shows the converged solution.

Table 2: True optimum, initial and final vectors, during simplified back-analysis by use of the elasto-plastic tunnel convergence model.

Analysis # / Parameter	True optimum	Trial 1	
		Initial	Final
E_m (MPa)	3000	2500±700	2500
v	0.25	0.25±0.01	0.25
p_o (MPa)	7.0	7.5±0.5	6.2
c (MPa)	1.0	0.8±0.1	0.8
ϕ (°)	25	20±4	23.4
ψ (°)	0.0	0.0	0.0
$u(d)$ (m)			0.019

This solution is generally close to the $\mathbf{p}^*$ vector and the value of $u(d)$=0.02 m predicted by the FLAC model, but it is unsatisfactory due to the difference in the estimate of the far field stress. Furthermore, other minima may still exist and they need to be searched.

An alternative approach is to investigate stochastically the existence of other local minima in the region of the mean property values. For this reason, a Monte-Carlo type of simulation was performed using built in functions in Excel. Random trial parameter vectors are generated from the initial "a priori" information assuming normally distributed always values. A Visual Basic code was written for this purpose. For each of these trial vectors the back-analysis is repeated and the optimal vectors are recorded along with their respective value of the error function. For this type of problem it was observed that around 50 generations would yield enough information for the governing parameters. For each back-analysis cycle the minimization process requires approximately 15-35 iterations to converge depending on the starting vector. From the simulations, it is possible to choose a number of candidates of optimal vectors. These, can later be used for a more elaborate back-analysis procedure in order to minimize the

computational time. Table 3 presents a series of 40 back-analysis cycles. In some cases there was no feasible solution in the process and an error occurred (but without stopping the process). From the optimal solutions, six vectors with the lowest error achieved, were chosen for comparison. Figure 12 presents the objective function (error) values for the back-analysis trials. From we can note the variation and scatter in the optimal values for parameters p_o, ϕ, E and $u(d)$. The lowest achieved error value (trial 6) corresponds to property estimates that are very close to the theoretical solution:

p_o=7.12 MPa, ϕ=24.3°, c=0.95 MPa, ψ=0.1°, E=2912 MPa, v=0.25.

The closeness of results can also be attributed to the fact that a good approximation for the percentage of radial displacement at the face was used which naturally restricts the optimal solution. Figure 13 presents the measurement data with their associated noise and the six lowest error fitted curves, corresponding to different optimal solution vectors.

Table 3: Back-analysis solutions based on convergence data only, and by Monte-Carlo procedure.

trial	p_o	ϕ	c	ψ	E	v	*Error*	*u(d)*
1	5.71	19.12	0.70	0.10	2300.66	0.278	41.980	0.015
2	5.82	16.98	0.82	0.10	2450.70	0.250	34.428	0.018
3	2.60	11.97	1.30	0.09	1086.55	0.310	#N/A	0.020
4	8.79	30.34	1.32	0.13	4310.26	0.276	2471.087	0.014
5	7.29	26.53	0.89	0.10	3146.32	0.250	21.319	0.017
6	**7.12**	**24.33**	**0.96**	**0.10**	**2912.22**	**0.250**	**20.583**	**0.018**
7	5.25	16.76	1.06	0.10	1935.01	0.249	48.740	0.020
8	5.62	19.00	0.99	0.11	2330.63	0.257	41.374	0.021
9	6.66	23.38	0.91	0.11	3094.81	0.271	33.405	0.021
10	3.92	0.00	2.10	0.18	1864.28	0.268	#N/A	0.021
11	8.04	24.32	1.02	0.11	3256.11	0.261	1457.104	0.014
12	1.19	11.47	1.05	0.17	1009.64	0.262	#N/A	0.019
13	7.18	17.40	0.67	0.09	2045.54	0.244	382.863	0.013
14	7.19	24.14	0.86	0.11	3216.57	0.257	22.388	0.022
15	7.16	24.03	1.01	0.10	3672.75	0.252	25.962	0.022
16	6.03	22.19	0.85	0.12	2901.64	0.248	38.813	0.021
17	6.28	24.15	1.07	0.10	2488.64	0.250	26.220	0.021
18	3.24	17.28	0.84	0.12	2033.89	0.277	#N/A	0.021
19	7.57	20.57	0.83	0.10	2599.92	0.251	846.007	0.014
20	7.11	18.77	1.28	0.10	2255.35	0.257	134.281	0.021
21	6.03	21.26	0.88	0.13	2677.09	0.261	86.418	0.023
22	6.06	20.16	1.18	0.10	2353.22	0.235	58.511	0.023
23	3.99	18.21	1.02	0.04	2191.18	0.262	#N/A	0.023
24	7.65	21.16	0.86	0.10	2703.46	0.253	1014.895	0.015
25	2.82	14.49	1.10	0.15	1536.32	0.269	#N/A	0.021
26	7.75	21.97	0.90	0.10	2843.90	0.255	1105.500	0.015
27	3.02	16.68	0.76	0.20	1930.58	0.267	#N/A	0.021
28	7.77	22.13	0.91	0.11	2871.96	0.255	1079.798	0.014
29	5.40	16.18	0.91	0.10	2618.08	0.250	43.216	0.020
30	7.38	25.56	0.83	0.10	3501.81	0.250	22.863	0.020
31	5.92	14.97	1.17	0.11	2750.15	0.261	44.283	0.021
32	7.21	19.20	1.27	0.10	2347.35	0.252	129.669	0.021
33	3.98	18.12	1.01	0.04	2176.48	0.270	#N/A	0.023
34	7.60	20.77	0.84	0.10	2634.81	0.252	971.191	0.016
35	3.94	17.46	1.01	0.10	2058.78	0.267	#N/A	0.022
36	6.77	14.17	0.51	0.09	1479.57	0.235	143.152	0.015
37	6.54	22.37	1.10	0.10	1780.24	0.242	76.549	0.026
38	7.53	22.10	1.70	0.08	2856.30	0.147	#N/A	0.028
39	7.93	23.40	0.97	0.11	3095.20	0.259	1676.825	0.019
40	7.16	19.36	1.50	0.10	2376.91	0.251	163.854	0.023

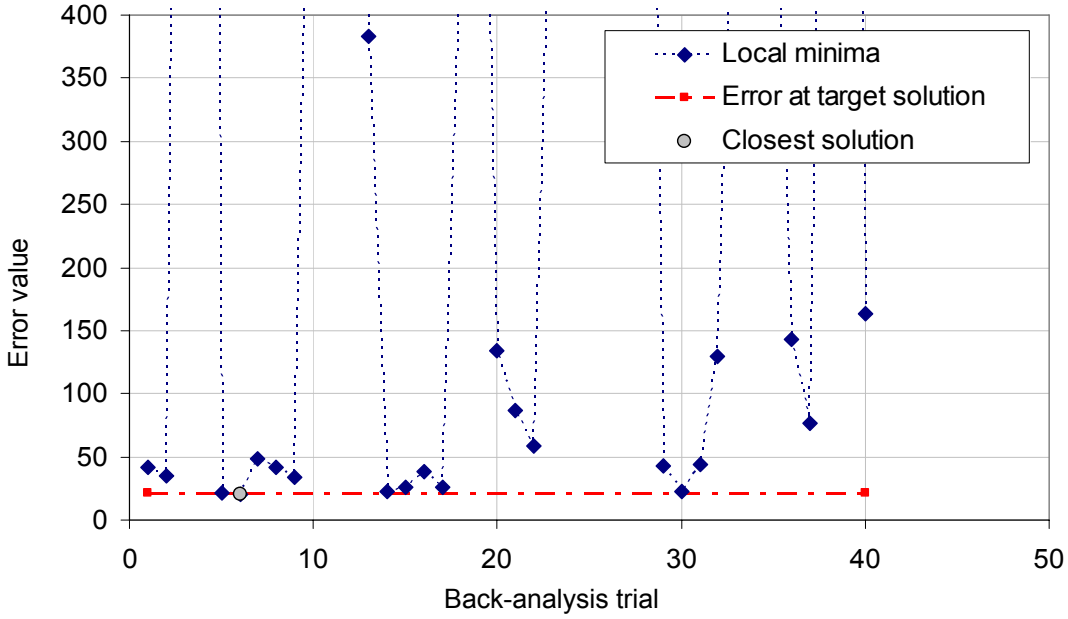

Figure 12: Error estimate from 40 Monte-Carlo back-analysis cycles using convergence data only.

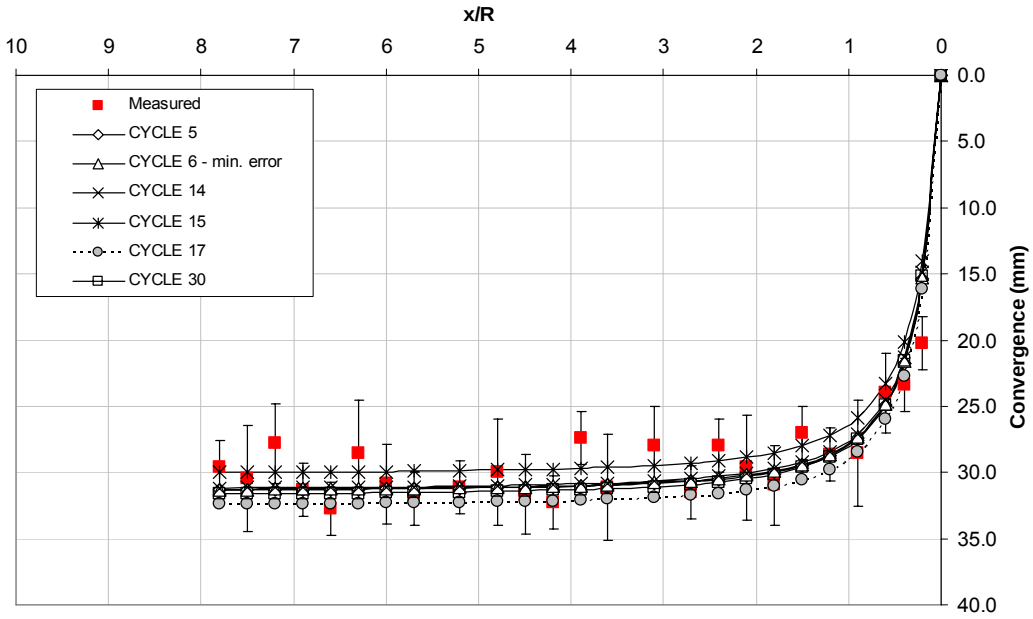

Figure 13: Convergence estimates by Monte-Carlo based back-analyses

It becomes apparent from the above, that the use of the Convergence-Confinement method along with an empirical relation of convergence rate and the use of convergence data can be used efficiently in a multi-parametric back-analysis. The methodology, however, is sensitive to the estimation of the ratio of radial deformation at the tunnel face to the ultimate equilibrium deformation. With an imprecise estimate function it is difficult to achieve a unique solution. The same conclusion can be extended to a back-analysis using a plane strain two dimensional model. During such an analysis one would need to use an approximation for the pre-relaxation, and most often convergence, instead of deformation measurements (e.g., from extensometers or surveying methods).

It is also possible to extend the method by incorporating stress measurements. Stress measurements are generally more difficult to perform and are most susceptible to error, due to the variation of ground properties, support system or monitoring equipment installation issues, ground-support interaction mechanisms, etc. It is interesting though to examine the back-analysis procedure from a fundamental standpoint by incorporating lining stress measurements. The same back-analysis procedure and model as the above were used in this case. From the FLAC model that was used to create artificial monitoring data for the back-analysis, the average stress at the lining-rock mass interface was calculated at $p(eq)_{FLAC} = p_i \approx 0.7\,MPa$ and a typical measurement error of 0.07 MPa was assumed. This measurement was incorporated in the objective error function (at each trial step of the process an equilibrium support pressure is calculated by the system of non-linear Convergence-Confinement equations). The results from 40 Monte-Carlo back-analysis cycles are shown in Table 4 and Figure 14. Again there is scatter in the local optima but considering the non linearity of the problem and the imposed constraints few solutions are actually acceptable. The solution from cycle 35 gives the minimum error:

p_o*=7.25 MPa, ϕ*=28.3°, c*=0.84 MPa, ψ*=0.1°, E*=3054 MPa, ν*=0.25, $p(eq)$*=0.67 MPa.

This result is very close to the theoretical optimal solution corresponding to the initially used FLAC input properties. The characteristic curves of the ground and the support corresponding to the optimal solution are shown in Figure 15. The difference in

the solutions obtained by using convergence data only and by combining convergence and stress data, is very small since a good approximation was already assumed in the analyses. The stress measurement should be incorporated in the back-analysis whenever unreliable deformation measurements exist or when an unreliable estimate (i.e., an arbitrary choice of 25 or 30% deformation ratio) is used to access the radial displacement at the face. Depending on the reliability of this estimate, fitting a convergence profile approximation curve to convergence data only does not warrant the uniqueness of the solution even by using a probabilistic approach which can scan over a wide range of values.

Table 4: Back-analysis solutions for the supported, circular tunnel in plastic ground model.

trial	p_o	ϕ	c	ψ	E	v	$p(eq)$	$Error$	$u(d)$
1	3.37	15.84	0.88	0.09	1776.73	0.257	#N/A	#N/A	0.027
2	7.59	20.72	0.82	0.10	2626.25	0.252	1.53	899.48	0.018
3	3.03	17.70	0.58	0.09	2102.92	0.277	#N/A	#N/A	0.024
4	7.38	19.04	0.78	0.10	2331.94	0.248	1.86	811.80	0.017
5	1.19	12.57	0.58	0.09	1211.52	0.270	#N/A	#N/A	0.024
6	7.97	23.72	0.89	0.10	3151.35	0.259	1.27	1047.23	0.016
7	5.24	19.52	0.79	0.10	2446.36	0.274	0.59	59.03	0.021
8	2.40	17.56	0.43	0.10	2058.92	0.274	#N/A	#N/A	0.021
9	8.55	28.44	1.01	0.10	3976.43	0.271	0.91	1364.57	0.015
10	6.90	28.79	0.86	0.10	2738.99	0.250	0.71	21.78	0.018
11	6.56	31.65	0.91	0.10	2226.01	0.249	0.64	27.21	0.019
12	7.96	23.71	0.90	0.10	3149.60	0.257	1.06	130.73	0.020
13	1.94	14.89	0.55	0.09	1604.26	0.281	#N/A	#N/A	0.022
14	7.28	18.24	0.76	0.10	2192.73	0.246	2.05	791.42	0.015
15	7.83	22.68	0.87	0.10	2968.41	0.257	1.06	152.50	0.023
16	7.62	22.32	1.14	0.10	2901.94	0.250	0.69	122.76	0.025
17	0.77	16.20	0.31	0.09	1856.27	0.227	#N/A	#N/A	0.025
18	7.25	17.98	0.75	0.10	2145.90	0.245	2.00	788.43	0.017
19	7.74	21.91	0.85	0.10	2834.74	0.255	1.09	236.41	0.025
20	6.19	11.24	1.32	0.08	955.16	0.073	1.96	1946.57	0.026
21	7.66	22.93	1.68	0.11	3002.16	0.205	#N/A	#N/A	0.032
22	8.42	27.38	0.98	0.10	3791.00	0.268	0.53	1795.73	0.022
23	2.46	18.70	0.54	0.10	2284.10	0.288	#N/A	#N/A	0.024
24	8.22	25.80	0.94	0.10	3514.96	0.264	1.07	1216.76	0.016
25	7.16	22.18	1.06	0.10	3507.42	0.245	0.58	35.35	0.020
26	1.56	12.39	0.58	0.09	1171.44	0.298	#N/A	#N/A	0.020
27	8.24	25.94	0.95	0.10	3539.32	0.265	1.23	1096.48	0.014
28	1.43	13.81	0.45	0.10	1408.65	0.295	#N/A	#N/A	0.018
29	8.51	28.04	1.00	0.10	3907.44	0.270	1.13	1179.30	0.012
30	6.95	24.40	0.81	0.10	3255.20	0.259	0.88	30.32	0.017
31	5.35	28.28	0.86	0.10	1563.48	0.249	0.829701	40.46	0.018
32	1.69	17.30	0.31	0.10	2014.58	0.274	#N/A	#N/A	0.020
33	8.57	28.59	1.01	0.10	4003.80	0.271	0.977452	1313.40	0.014
34	6.46	28.22	0.85	0.10	2379.14	0.249	0.801058	25.32	0.017
35	**7.25**	**28.37**	**0.84**	**0.10**	**3054.58**	**0.250**	**0.674713**	**21.50**	**0.019**
36	6.36	22.45	0.84	0.10	2915.57	0.268	0.706226	30.94	0.020
37	5.98	21.82	0.83	0.10	2814.47	0.249	0.61623	30.52	0.020
38	4.12	4.75	1.36	0.10	3153.57	0.288	#N/A	#N/A	0.021
39	7.48	19.83	0.80	0.10	2470.42	0.250	1.892154	803.64	0.014
40	5.50	21.56	0.79	0.10	2465.70	0.250	0.571786	37.84	0.021

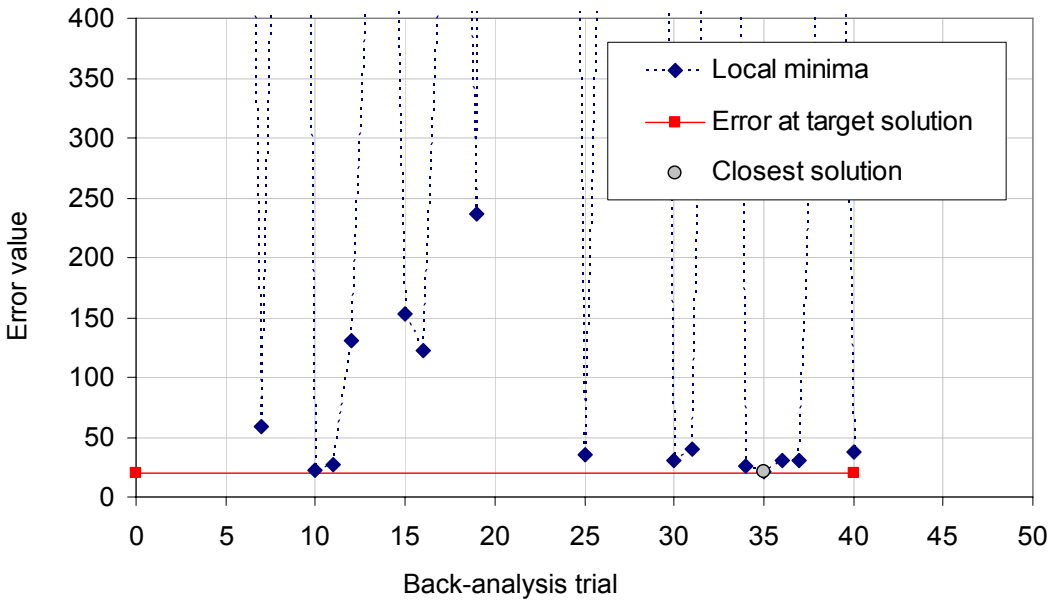

Figure 14: Error estimate from 40 Monte-Carlo back-analysis cycles using convergence and support system stress data.

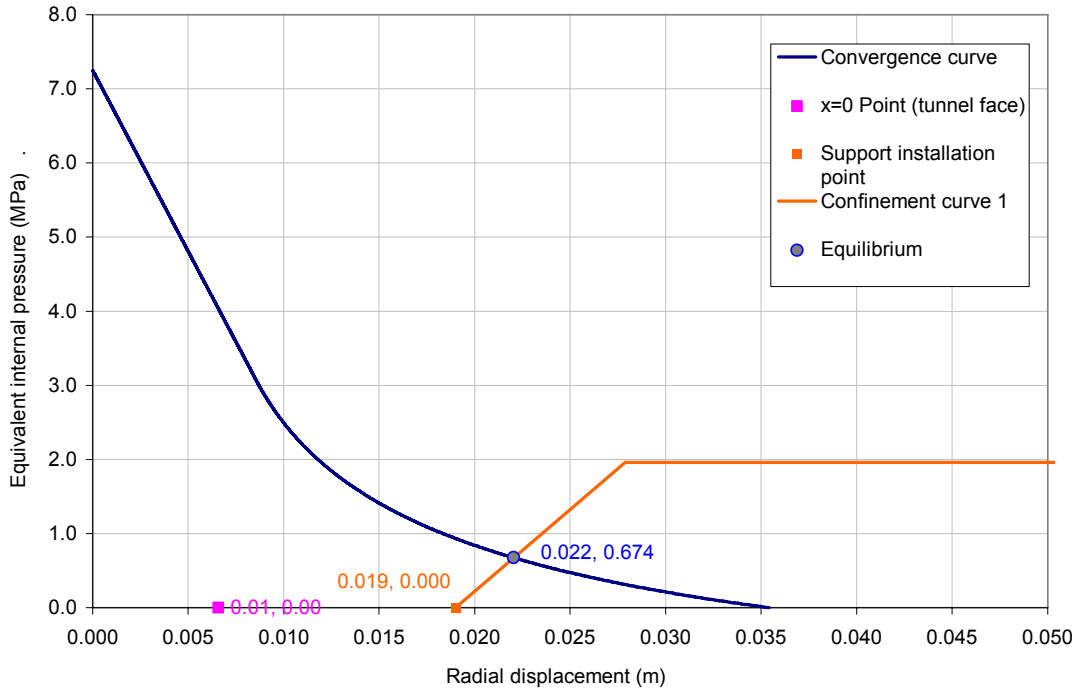

Figure 15: Characteristic curve after probabilistic-based back-analysis

5.9. Conclusions

From the above analysis is becomes obvious, that a simplified, probabilistic-based back-analysis for circular tunnels can be accomplished using a combination of closed form solutions and an empirical convergence rate approximation. Especially in the elasto-plastic ground case, the optimization system is generally sensitive to small value changes of far field stress p_o, strength properties and Young's modulus. The assumption of an empirical approximation for the convergence development also influences the solution. Experience from multiple parametric analyses using axisymmetry models has shown that variations in the convergence profiles cannot easily be quantified. Equation (20) was shown to be valid for the majority of the examined cases, and further study is performed to investigate the variation of parameters β_1 and β_2 with the ground and support conditions. Today, in many cases, the previously mentioned convergence-profiles are used to make an assessment of pre-convergence before the tunnel is supported, or to fit such curves in convergence data for an first estimate of ground properties.

When using the objective function (33), the traditional assumption is made that the first trial (in absence of other information) is the mean value vector of the governing parameters. This paper shows that this assumption can be misleading for a back-analysis procedure in the absence of a reliable way to incorporate the ground relaxation at the face, or in the absence of support stress measurement data. In this case it is recommended to combine the approach incorporating the uncertainties in the rock mass and the data quality through the use of a "Bayesian" type of approach given in equation (34) in combination with a heuristic type of simulation of the starting trial values during the simplified back-analysis. The descriptive statistics of the governing parameters are kept constant and always reflect the engineering judgment of the modeler. The choice of starting vector proves significant to overlook. From the analyses it was also evident that the assumption of radial displacement ratio at the tunnel face can influence the back-analysis solution, therefore it is recommended to check the change in the solution vector by varying the initial estimate of the ratio of radial deformation at the face. Two approximations have been presented in this paper in order to estimate this ratio under elasto-plastic conditions of unsupported and supported circular tunnels.

The software Excel incorporating the Generalized Reduced Gradient algorithm proves is a powerful and convenient optimization tool for quick back-analysis of circular tunnels. Hence a better appreciation of starting parameters for a more time consuming numerical-based back-analysis is possible.

CHAPTER 6. Parameter identification using a local optimization method

6.1. General

A gradient based local optimization method is used to perform back-analysis of tunneling induced deformations. The method is based on the multivariate version of the Newton-Raphson algorithm. This algorithm, due to its quadratic convergence properties, is considered to be fairly fast. As such, it can be proved that it establishes the minimum of a quadratic function in one iteration. Jeon and Yang (2004) have used this method in back-analysis of two geotechnical parameters. Other possible local optimizer candidates to be used in geotechnical problems would be the Broyden- Fletcher-Goldfarb-Shanno (BFGS) method and the Complex method described in section section 4.4 from the classes of gradient and non-gradient optimization techniques respectively. The main points and issues when using a gradient technique can be summarized as follows:

- The gradient of a function f, ∇f, establishes the direction of steepest ascent. Hence the negative of the gradient represents the direction of steepest descent
- The evaluation of the gradient is based on the evaluation of partial derivatives. There may be cases where the objective function being minimized is differentiable but the derivative calculation is impractical
- The gradient may not be defined at all points especially close to constraint boundaries of the function or in other abrupt points
- Even if all the above problems are solved, the final solution will be influenced by the initial trial values and the solution will be closest to the original trial. This of course holds true for any local search method. The global optimum may not be attained easily

Nevertheless, from a fundamental point of view it is interesting to study how such an algorithm can be used to perform a simple yet frequently encountered problem of tunneling related back-analysis. The problem of a deep circular tunnel will be used in the application of the algorithm.

6.2. The Newton-Raphson algorithm

The function $f(\mathbf{X})$ can be expanded using the Taylor series including its quadratic terms as:

$$f(\mathbf{X}) = f(\mathbf{X}_i) + \nabla f_i^T (\mathbf{X} - \mathbf{X}_i) + \frac{1}{2}(\mathbf{X} - \mathbf{X}_i)^T [J_i](\mathbf{X} - \mathbf{X}_i) \tag{38}$$

where $[J_i]$ is the Hessian, matrix of the second order partial derivatives.:

$$[J_i] = \begin{bmatrix} \frac{\partial^2 f}{dx_1^2} & \frac{\partial^2 f}{dx_1 dx_2} & \frac{\partial^2 f}{dx_1 dx_3} & \dots \\ \frac{\partial^2 f}{dx_2 dx_1} & \frac{\partial^2 f}{dx_2^2} & \frac{\partial^2 f}{dx_2 dx_3} & \dots \\ \dots & & & \\ \frac{\partial^2 f}{dx_1 dx_n} & \dots & & \frac{\partial^2 f}{dx_n^2} \end{bmatrix}$$

For the minimum, the Kuhn-Tucker conditions specify:

$$\frac{\partial f(\mathbf{X})}{\partial x_j} = 0, \qquad j = 1, 2, \dots, n \tag{39}$$

From equations (38) and (39) we have:

$$\nabla f = \nabla f_i + [J_i](\mathbf{X} - \mathbf{X}_i) = 0 \tag{40}$$

If the Hessian matrix is not singular the solution of equation (40) gives:

$$\mathbf{X}_{i+1} = \mathbf{X}_i - [J_i]^{-1} \nabla f_i \tag{41}$$

For non-quadratic non-linear functions, equation (41) may have difficulty in approaching the minimum. It may converge to a relative maximum or diverge or reach a saddle point. A modification of the Newton-Raphson method is the following:

$$\mathbf{X}_{i+1} = \mathbf{X}_i - \lambda_i^* [J_i]^{-1} \nabla f_i \tag{42}$$

where λ_i^* is the optimal step size along the direction $-[J_i]^{-1} \nabla f_i$. The optimum value of step size λ can be found by using one of the one-dimensional optimization techniques such as the Golden Section method. For this step the objective function must be unimodal

in a short range of λ to find the optimal λ^*. The Golden Section method requires the input of a range in which to seek the optimal value of λ and a maximum number of iterations. This hybrid method was implemented in the commercially available, finite difference-based numerical code FLAC 2D ver. 5.0.

The required finite difference approximations can be obtained from the following finite difference formulae for functions of two or more variables.

$$\frac{\partial f}{\partial x_1} = \frac{f(x_1 + h_1, x_2) - f(x_1 - h_1, x_2)}{2h_1} \tag{43}$$

$$\frac{\partial f}{\partial x_2} = \frac{f(x_1, x_2 + h_2) - f(x_1, x_2 - h_2)}{2h_2} \tag{44}$$

$$\frac{\partial^2 f}{\partial x_1^{\,2}} = \frac{f(x_1 + h_1, x_2) - 2f(x_1, x_2) + f(x_1 - h_1, x_2)}{h_1^{\,2}} \tag{45}$$

$$\frac{\partial^2 f}{\partial x_2^{\,2}} = \frac{f(x_1, x_2 + h_2) - 2f(x_1, x_2) + f(x_1, x_2 - h_2)}{h_2^{\,2}} \tag{46}$$

$$\frac{\partial^2 f}{\partial x_1 \partial x_2} = \frac{f(x_1 + h_1, x_2 + h_2) - f(x_1 + h_1, x_2 - h_2) - f(x_1 - h_1, x_2 + h_2) + f(x_1 - h_1, x_2 - h_2)}{4h_1 h_2} \tag{47}$$

These approximations are used to assembly the *n*-dimensional gradient of the function and the *n* x *n* Hessian matrix. As we will see, a critical step in this process is the choice of the step size for each of the governing parameters. For the assembly of the Hessian matrix it is assumed that the mixed derivatives of the objective function are continuous functions. Therefore, according to Schwartz's theorem, the order of differentiation does not matter. This is generally true for the smooth type of "least squares" type of objective function (equation 2) used herein (assuming infinitesimal function behavior).

6.3. Back-analysis using the Newton-Raphson method

Very often the back-analysis of tunneling-induced displacements is based on the assumption of linear-elastic behavior of the rock mass. Even though this may be misleading for excavations were a plastic zone occurs around them, it is still an interesting problem and quite true for supported tunnels were the ground failure is kept to a minimum. A set of two problems was examined in this case. In the first case the case of an unsupported tunnel under isotropic stress conditions, was examined. In the first case, two parameters were searched during the back-analysis, the elastic modulus E and the far field isotropic stress p_o. In the second case an unsupported tunnel is being excavated in elastic ground under anisotropic stress conditions. In the later case, the unknowns are the elastic modulus E, the Poisson's ration v, the vertical and horizontal stresses σ_y and σ_x (or equivalently the vertical stress and the K_o ratio). Both of these cases where chosen as reference problem for the back-analysis, since they are distinguished by uniqueness of their respective solutions and the existence of a closed-form solution makes cross comparison easy. The commercial software FLAC 2D ver. 5.0 was used in the analysis. The tunneling problem and the back-analysis algorithm were implemented by using the proprietary FISH programming language of FLAC. Initially the problem was solved using a known set of elastic, and stress level parameters. A plane strain condition was assumed for this case. A more elaborate discussion on the choice of plane strain versus a full three dimensional analysis will be further discussed in chapter 7. Figure 16 shows the quarter tunnel model designed in FLAC. The tunnel has radius R=5.0 m and the model extends 50 m.

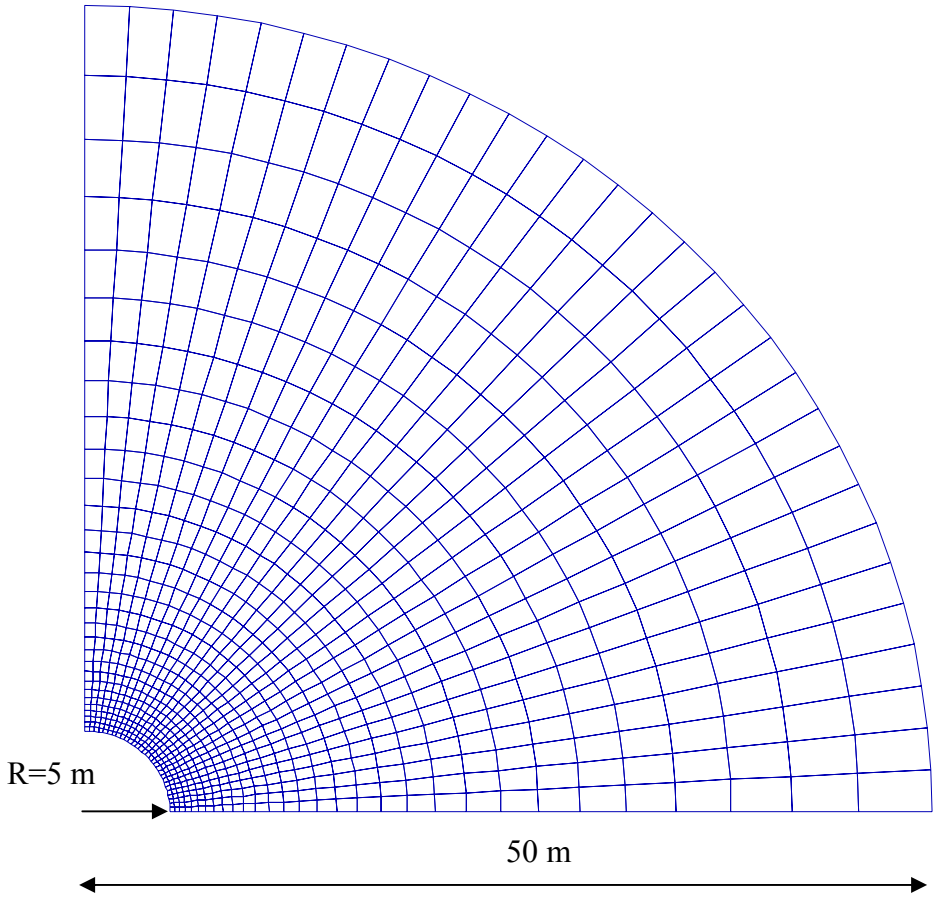

Figure 16: Circular tunnel numerical model in FLAC (x10 m.)

6.3.1. Case of a circular tunnel in elastic ground – two-variable problem

In this case an initial tunnel model was solved using the properties shown in Table 5. The radial displacements at three gridpoints with R_1=R=5.0, R_2=5.9 and R_3=8.7 m were obtained from the analysis and used as input for the back-analysis. The objective function of equation (2) with weighting factors w_i=1 for all points was used. In this case the one-dimensional step size calculation was omitted, thus the step size λ was constant and equal to 1. Three different initial trial vectors were assumed. The convergence criterion used, was an accepted total parametric convergence of 10^{-4}. The total parametric convergence is taken as:

$$\tilde{c}_{tot} = \sum_{i=1}^{n} \frac{p_{i+1} - p_i}{p_i} \tag{48}$$

where p_i and p_{i+1} are values of the parameters at iteration i and $i+1$ respectively.

Table 5: Input properties and back-analysis results for the twin parameter problem

Parameter	True optimum	FDD step size	Trial 1		Trial 2		Trial 3	
			Initial	Final	Initial	Final	Initial	Final
E (MPa)	3000	60	2500	3002	4000	3000	4500	3006
p_o	7.0	0.05	7.5	7.0	8.0	7.0	6.0	7.0

The results presented in Table 5 show extremely smooth behavior and repeatability of results. This is primarily due to the simplicity of the problem, having only one optimum in the search space. The quadratic nature of the method becomes evident from the fast convergence. Representative results from trial 3 are shown in Figure 17. The method essentially reaches the correct and converged solution at cycle 7. The convergence criterion is satisfied at cycle 12 and the analysis is stopped. The FISH program for the ordinary Newton-Raphson method is available by contacting the author.

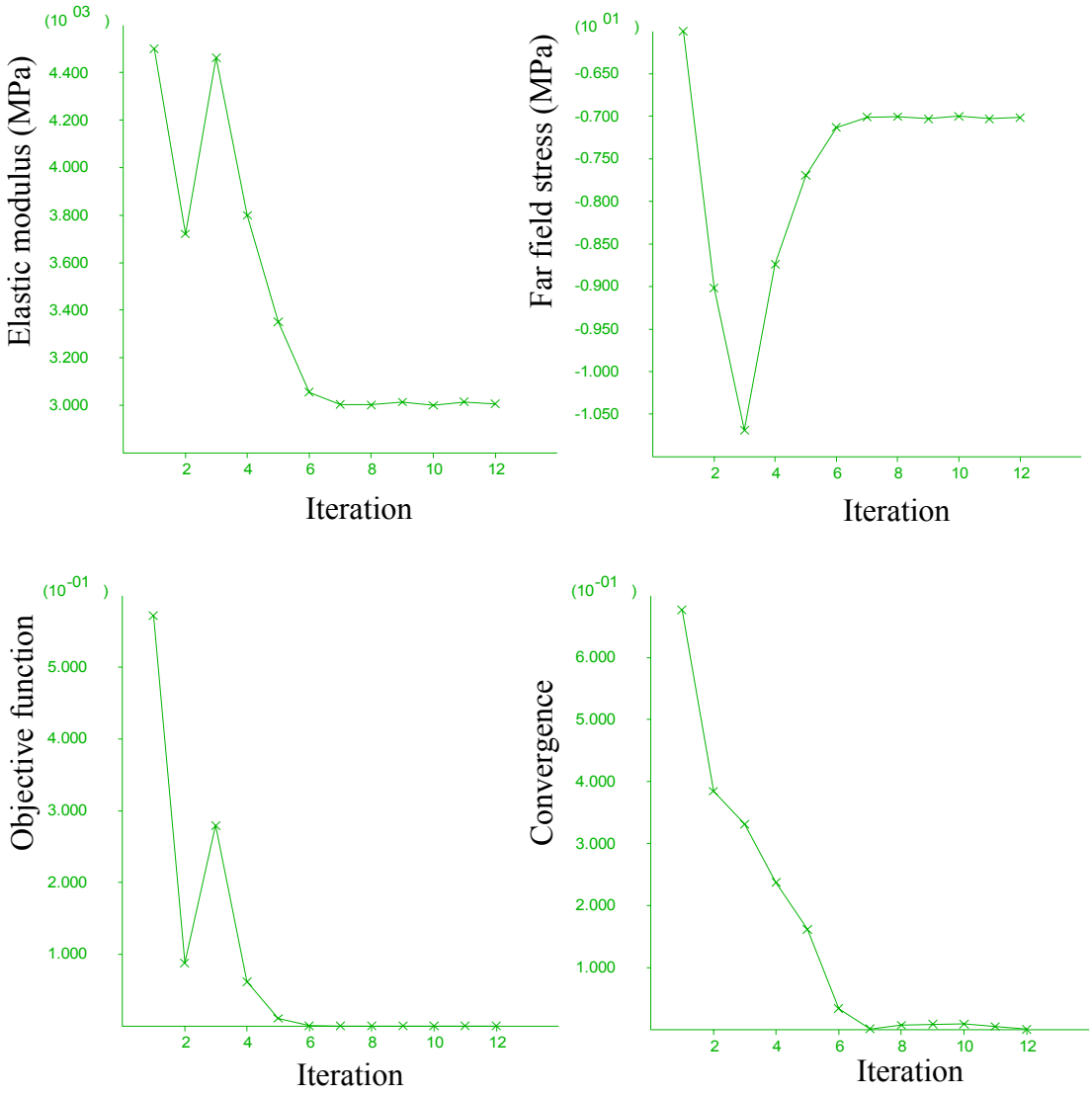

Figure 17: Results from back-analysis using the Newton-Raphson method in FLAC.

6.3.2. Case of a circular tunnel in elastic ground – four-parameter problem

In this case, the hybrid methodology of the Newton-Raphson and the Golden Section were employed for the back-analysis of four parameters. Initially the problem was attempted to be solved with the ordinary Newton-Raphson method, but as the earlier discussion identified, the method becomes unstable. The scanning range for the Golden Section was taken to be [-1.2, 1.2] and the number of Golden Section iterations was set to 22. Measurements were taken along two sets of three gridpoints with R_1=R=5.0, R_2=5.9 and R_3=8.7 m, three on the centerline above the crown and three on the springline of the tunnel. The deviatoric stress as well as the Poisson's ratio will be easier to identify using these points, due to the sensitivity of the measurements at these locations. Table 6 presents the results of the analyses. Once again, the adequate performance of the algorithm was evident. Both trials results in the same and exact solution. The solution is practically obtained in 7 cycles and it converges at the specified convergence after 17 cycles. The results are shown in Figure 18 and the FISH program containing the hybrid algorithm can be obtained by contacting the author.

Table 6: Input properties and back-analysis results for the four parameter problem

Parameter	True optimum	FDD step size	Trial 1		Trial 2	
			Initial	Final	Initial	Final
E (MPa)	4500	200	5500	4527	6000	4524
v	0.25	0.018	0.26	0.252	0.25	0.252
p_y (MPa)	7.0	0.3	7.5	7.01	8.0	7.0
p_x (MPa)	4	0.3	4.5	4.0	4.7	4.0

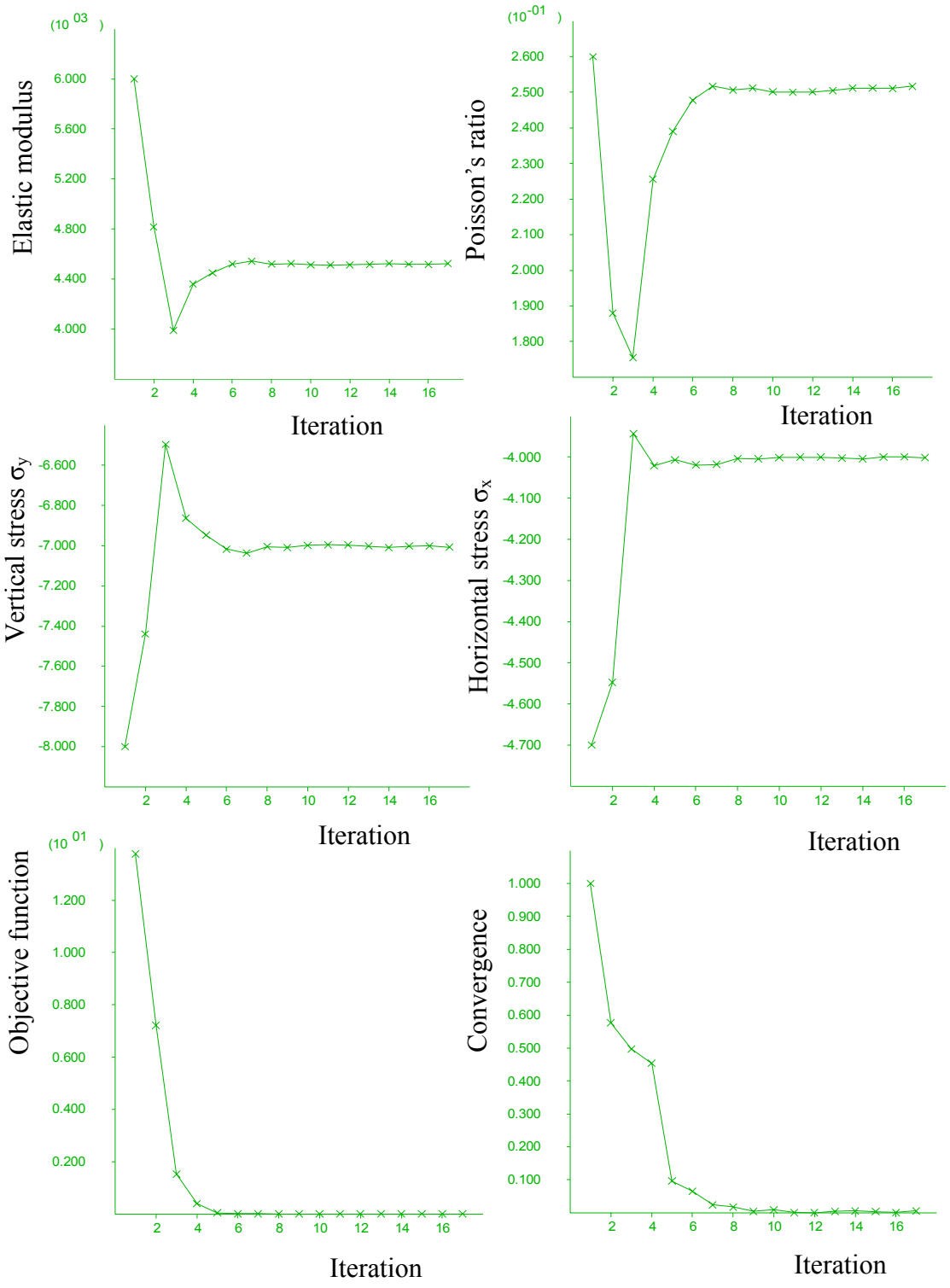

Figure 18: Results from back-analysis of four paramters using the Newton-Raphson method in FLAC.

6.4. Conclusions

The gradient based methods are formidable algorithms, but present some shortcomings. The involvement of gradients makes the process difficult when using numerical analysis for each function evaluation such as the finite element method. When the number of unknowns is low (i.e., two or three parameters) the back-analysis could be dealt with easily. However, when the number of unknowns increases then the process becomes not only computationally expensive but sometimes impossible. In the case of the Newton-Raphson algorithm, the first and second order derivatives need to be calculated so that the Hessian matrix (diagonal matrix of the second partial derivatives) is assembled at each temporary solution vector. A finite difference-based derivative sub-routine needs to be executed in order to perform this calculation. For each function term involved in the finite differences, a dedicated numerical analysis needs to be performed. Even when all this is programmed the required step sizes h_i for the finite difference derivatives should be calibrated. Too short or too large of a step may yield erroneous derivatives. A general rule of thumb would be to keep the ratio of the step size over the average expected parameter value constant for all parameters.

Furthermore in most of the direct and gradient based algorithms, a one-dimensional step calculation must be performed along a pre-calculated direction of optimization in order to optimize the solution at that stage (monotonous decrease of the objective function is the characteristic response of such algorithms). This involves a sub-routine such as the Golden Section method to estimate the required step size λ. This process requires more iterations so that a reasonable and efficient step size is found. The process may become quite time consuming.

Another difficulty is the implementation of constraints. A penalty function procedure by assigning a large error value upon violation of a constraint, could provide the constraints, but could easily make the objective function non-differentiable. The above methodology was attempted for the more realistic case of a supported circular tunnel in elastic and in elasto-plastic ground. In this model it was realistically assumed that the support is installed after a 50% relaxation of the tunnel and the measurements from multipoint extensometers commence at that time. This monitoring time lag is very often the case in the actual construction and a proper back-analysis approach should be

able to deal with this as well. When the relative measurements are used for the back-analysis, i.e., extensometer measurements or underground surveying methods then the objective function becomes highly non-linear and the possible number of local extrema multiply. Thus, there can easily be a variety of parameter vectors that minimize the function. This is one of the reasons why displacement monitoring should commence not only as soon as possible after the excavation but also it should be performed by various methods to increase the potential and the reliability of a back-analysis. The application of the hybrid Newton-Raphson method for a supported tunnel, using any type of relative measurement or even with the assistance of incorporating lining stress measurements, showed poor results. Tests with four and six parameter problems revealed that the gradient-based approach is not a reliable tool when the problem becomes complicated.

The issues that often come up revolve mainly around the gradient calculations. The first order derivatives are relatively straightforward to estimate. However the estimation of the Hessian matrix can the most daunting task. The choice has to be made for a good estimate of finite difference derivative step sizes. Even in the simplest case of two variables, the step size should be chosen so that the incremental change in the governing parameter has an impact in the model behavior and thus in the objective function. A small step size can be undetected by the analysis, thus instead of a good estimate of the derivative the method creates "noise" instead. A large step size h_i, on the other hand can make the analysis oscillate without being able to stabilize in a proper search direction. This in conjunction with a non-linear objective function which has multiple local optima, makes the back-analysis a difficult task. The core of Newton-Raphson method is generally based on the ability to calculate or at least estimate the gradients and the Hessian matrix reliably. Thus it is influenced greatly by computational precision. Step sizes must be increased as the number of unknowns increases to overcome precision tolerance and subsequent data noise in finite difference derivative evaluations. The nature of the objective function used, is such that many local optima theoretically exist, and these are densely located close to each other, especially when plastic parameters are involved (many nearby sets of strength, stress or elastic parameters can minimize the function). When such conditions exist the Hessian matrix may be impossible to estimate practically. Even if it was possible, then the final answer would

inevitably suffer from the “a-priori” assumption of the first trial, since the Newton is very good at finding local optima close to the initial trial.

Therefore alternative methods should be developed that can adapt and deal with the non-linear behavior of the ground and also with the highly non-linear objective function that will be minimized. As it was shown in chapter 5, even the use of a very robust local search algorithm (Generalized Reduced Gradient) can give misleading back-analysis results and a more thorough investigation may be required. The conclusions of chapter 5, revealed the requirement for a more global search strategy. In fact the hybrid Monte-Carlo and local search approach is the oldest global search strategy in optimization. It features the notion that many trials are made, and of those trials the ones yielding the worst results are discarded in favor of the “strong” and more probable solutions. This simple yet powerful logic of the theory of global optimization will be presented in the next chapters. Two of the most pronounced representatives from the area of global optimization are employed in a novel fashion by using the programming capabilities of the commercial software FLAC.

CHAPTER 7. Back-analysis of tunnel response using the Simulated Annealing method

7.1. General

An alternative methodology to deal with this complexity and sensitivity of the various methods can be found in the recent evolution in the areas of the genetic algorithms, the neural networks, but also in the heuristic nature of algorithms such as the Simulated Annealing (SA) introduced by Kirkpatrick et al. (1983). The last method belongs to a general class of combinatorial optimization techniques and it has gained attention for the solution of large scale discrete or even continuous optimization problems where highly irregular objective functions with multiple local optima may exist. The SA algorithm has been used by Long (1993) and by Mauldon et al. (1993) in modeling of hydraulic fracture conductivity. It was also applied by Scherbaum et al. (1994) in parameter identification of earthquake induced ground motion modeling. The following section describes the features of the SA algorithm used in the proposed back-analysis.

7.2. Description of simulated annealing

The SA algorithm shares its name from the metallurgical process of metals such as steel. A gradual and sufficiently slow cooling procedure from the heated phase, leads to a final material with theoretically perfect crystalline structure with the minimum number of imperfections and internal dislocations. This corresponds to the state of low internal energy. On the contrary when a quick cooling schedule is followed, then the final product attains more imperfections and higher energy state. During cooling, nature follows inevitably its own optimization path for the given circumstances. This is what the annealing algorithm tries to simulate. The theoretical basis of the SA algorithm is that when the cooling schedule is sufficiently slow, the higher is the probability of converging to the global optimal solution, assuming that there is one in the mathematical sense. This is particularly useful in cases of nonlinear objective functions of geotechnical back-analysis problems where multiple minima may exist. A true downhill algorithm will attempt to approximate the closest feasible solution. Here lies the strength of the SA algorithm. It is not a “greedy” algorithm since its structure allows for uphill movements as well. This is especially beneficial to nonlinear elasto-plastic geotechnical problems. In the case that an elasto-plastic model is assumed and the actual behavior is purely elastic,

then back-analysis of the involved plasticity parameters may never converge to an optimal solution. The use of a heuristic approach, as implemented here, bypasses the problem. The algorithm is allowed to scan the behavior of the numerical system under various conditions, purely elastic or elasto-plastic. Even if the back-analysis is started from the global optimal vector, the annealing will proceed and not get stuck at that point. As it will be seen later, even if the annealing process leads to a non global but optimal point, significant information can be gained from the behavior of the objective function during the annealing. Simulated annealing has been initially used in discrete optimization problems, such as the traveling salesman problem, or on the optimization of circuit board design. Later on its use was extended to applications in continuous optimization. An extensive review on the method and its behavior can be found in Otten and Ginneken (1989).

The SA algorithm as was described earlier posses an interesting thermodynamic analogy. When sufficient time is available for cooling, the higher is the probability of attaining a minimum energy state at the end. Or otherwise if the solution of a numerical system is controlled in such a way, that the system "scans" at progressively less feasible vector solutions, then there is good chance to converge to a global optimum. The process is related with the Boltzmann probability distribution:

$$P(E) \propto \exp\left(\frac{-E}{kT}\right) \tag{49}$$

Thermodynamically equation (49) expresses that if a system has equilibrium at each temperature T, its energy is probabilistically distributed among various possible energy levels E. In the above equation, k is the natural Boltzman constant relating temperature to energy. This is significant for the SA algorithm. Even if the system has reached a low temperature, thus it more restricted in its possible energy states, it still has a small chance to escape from a locally optimum energy state in attempt to find a better globally optimum, by taking an essentially uphill movement with corresponding temporary increase in the energy (or the value of the objective function).

Let's assume that the generic objective function is:

$f(\mathbf{X})$ and $\mathbf{X}$ is the n-dimensional solution vector (50)

We are seeking the $Min[f(\mathbf{X})]$ subject to the following constraints:

$$\mathbf{\Omega}: x_i^{\,l} \le x_i \le x_i^{\,u},\ i=1,\ldots,n \tag{51}$$

The solution starts from an initial trial (or prior geotechnical assumption) $\mathbf{X}_1$. An initial starting temperature T_o also needs to be assumed. A dedicated cooling schedule is required to perform the SA. This cooling schedule function determines how the temperature is decreased from an initial value T_o during the annealing. This is an important stage and various cooling schedules can be tried. An example annealing schedule often encountered in the literature is to use an exponential cooling:

$$T_k = T_o \cdot CR^k \tag{52}$$

where, T_k is the temperature at each cooling stage k, and CR is a cooling rate (CR<1). As the number of cooling stages increases the temperature close to to theoretical optimal procedure should approximate zero. The cooling schedule will be composed of a large number of cooling stages NT and temperature is kept constant during each stage.

The temperature is initially set to T_o and the objective function is calculated and stored at the initial trial point. At each temperature stage T_i, the system is let to try a large number NI of different, sequentially and randomly generated combinations (or permutations) of solution vectors around the present trial. Hence:

$$\mathbf{X}_{i+1} = \mathbf{X}_i + (\Delta\mathbf{X}) \tag{53}$$

The vector change $\Delta\mathbf{X}$ must yield a new vector relatively close to the previous point and not too far. The constraints can also be implemented at this step. If a new perturbation does not satisfy relation (51) then the random generation is repeated until a valid trial vector is found.

The new vector is used as input in the numerical analysis and a new objective function value $f(\mathbf{X}_{i+1})$ is found. The new trial is accepted if it leads to a decrease of the objective function value:

$$\Delta f = f(\mathbf{X}_{i+1}) - f(\mathbf{X}_i) \le 0$$

On the other hand, if $\Delta f > 0$, then the criterion by Metropolis et al. (1953), is used to control the acceptance or not of the present trial. The probability of the objective value change is calculated and compared to a random number $r \in [0,1]$. Thus, by omitting the Boltzmann's constant *k* from (49):

$$P(\Delta f) = \exp\left(\frac{-\Delta f}{T}\right) \tag{54}$$

If this probability is greater than a randomly generated number r, the new solution is accepted and becomes the starting solution for the next iteration. Otherwise, if the probability is less than *r*, the new solution is rejected and the present solution remains the same from the previous step. The algorithm flow chart is presented in Figure 19.

The random generation $\Delta\mathbf{X}$ of perturbations around a present solution vector also needs some consideration. Press et al. (1999) discusses the importance and efficiency of various methods of calculating the $\Delta\mathbf{X}$ vector. The present implementation involves a simple scheme which was found to be efficient for this type of problem. Let's assume that the parameter *i* has a present solution value of x_i, and constraints $x_i^{\,l} \le x_i \le x_i^{\,u}$. Similar constraints are involved for all other parameters. A new perturbed value may be found by:

$$x_i^{\,new} = x_i + 2 \cdot \Delta s_i \cdot (rnd_i - 0.5) \tag{55}$$

where, $x_i^{\,new}$ is the new value by perturbation, Δs_i is the specific parameter perturbation step size, and rnd_i is a random number between 0 and 1, for the i^{th} parameter. Therefore, there is a uniformly distributed probability of choosing any new parameter value in the $[x_i - \Delta s_i, x_i + \Delta s_i]$ range, as long as it satisfies the constraints, as shown in Figure 20. The choice of the step size Δs_i, which is different for each parameter, depends on many factors and may also be problem specific. A good general rule, which was followed in the present analysis, was to choose Δs_i in such a way that the values of the ratio $\Delta s_i / (x_i^{\,u} - x_i^{\,l})$ are comparable between all parameters. The step sizes Δs_i, need to be relatively small in order to yield a new parameter value close to the previous one, but large enough so that the whole feasible solution vector space is scanned during the

annealing process. If the step size becomes too short then there can be gaps in the possible reconfigurations (perturbations) in the trial parameter sets. If the step sizes are too large, then the solution could easily wander all over the space. It is a good tactic to calibrate the annealing properties in combination with the step sizes, so that the trial vectors present a gradual transition from point to point. This requires some experimentation with the algorithm.

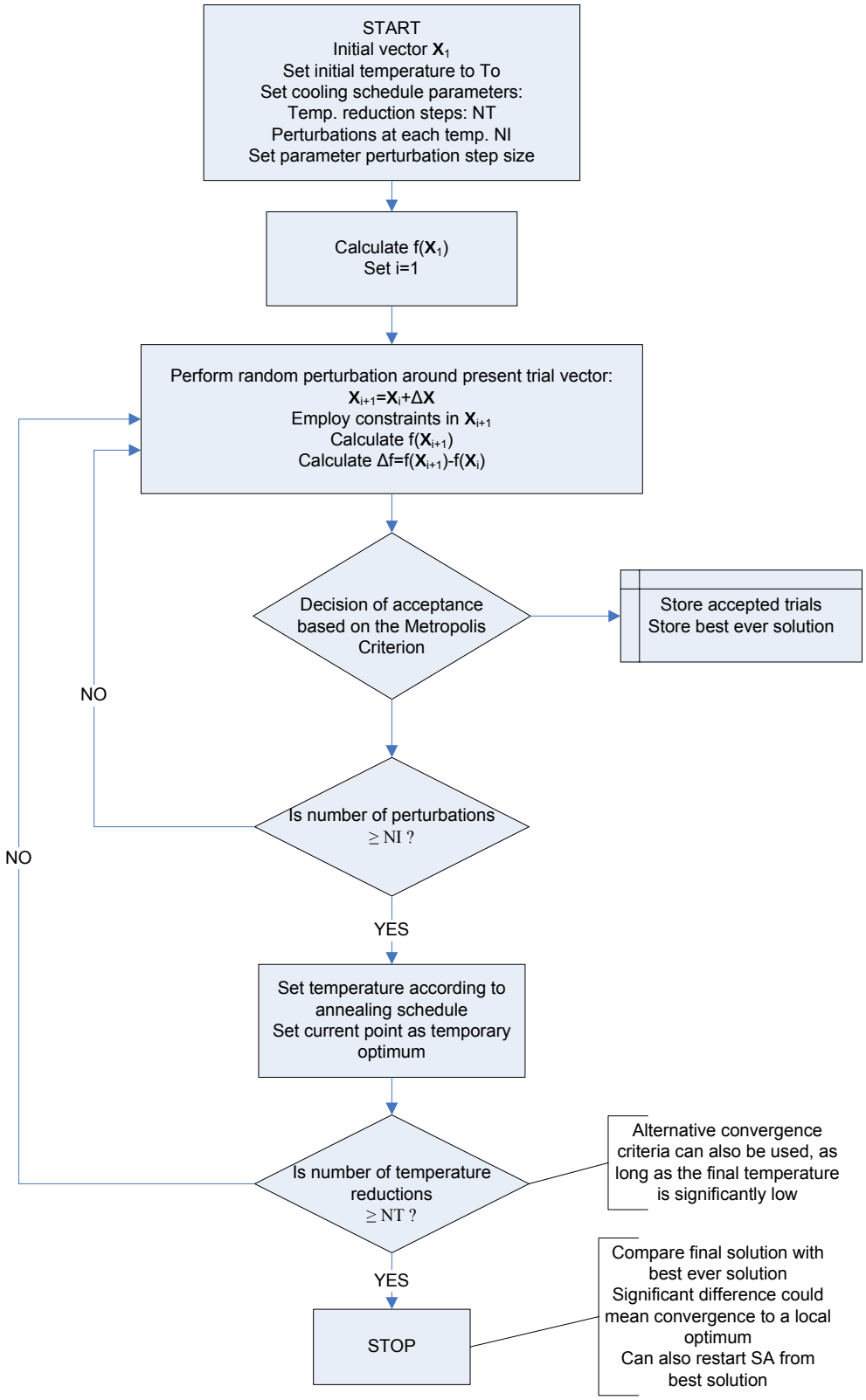

Figure 19: Flow chart of Simulated Annealing algorithm implemented in FLAC

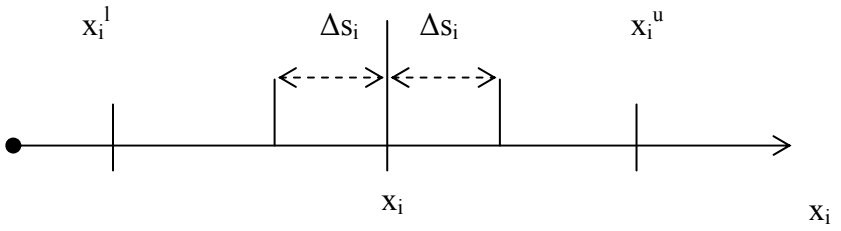

Figure 20: Implementation of constraints and perturbation sampling range during the annealing process

An approach which can also increase the algorithm's efficiency is to reduce the step size for some or all of the parameters, after a prescribed number of temperature reductions. This can potentially lead to better and more precise solution, by allowing narrower sampling, after the algorithm has approached the general area of the global optimum. This approach was implemented in the present algorithm by reducing the step size at 70% of the cooling. Corana et al. (1987) have applied the SA algorithm to continuous variable function minimization and identify the difficulties associated with this implementation. They suggest a modification using a stochastic sampling scheme so that the average number of successful (accepted reconfigurations) is approximately half of the total number of trials. Their implementation was tested against the Simplex method of Nelder and Mead (1965) and against a type of Adaptive Random Search, using highly non-linear functions of multiple local optima. Their results showed the superiority of this algorithm over others when it comes to estimation of minima. A similar modification scheme has been suggested by Venkataraman (2002) to boost the performance and efficiency of the original algorithm. Another implementation that could be followed in order to minimize the computational time is to modify the problem from a continuous optimization to a discrete one. By assuming an accepted solution precision, each parameter search space can be discretized into a finite number of prospective trials. For example during back-analysis, for each parameter, the feasible search range can become a discontinuous series where each trial is increased from its previous value by an amount:

$$(p_{max}\text{-}p_{min})/N_i \tag{56}$$

where p_{min}, p_{max} are the constraints and N_i the desired finite number of possible values of each parameter. Such an implementation deviates significantly from the general continuous optimization scheme, but by reducing the theoretically high precision demand of the continuous minimization problem, a more efficient and fast solution progress could be attained. The above method may not necessarily yield the true global optimum which, as a vector, may not be represented by any combination of the discrete parameter values, but a solution very close to it can be obtained, especially when the feasible solution search range is not particularly extended. Thus by simplifying the problem to a discrete form the solution time can be greatly reduced, at the expense of solution precision.

7.3. Back-analysis of a circular tunnel in elastoplastic ground using a closed-form solution and SA

In this case the theoretical closed form solution of the problem of a circular hole in an infinite Mohr-Coulomb medium is used for verification of back-analysis using the Simulated Annealing algorithm. The FISH programming language was used to perform the closed-form calculations. The finite difference grid model presented in Figure 16 was used to store the analysis results by using the provisional extra grid variable commands of FLAC. The closed-form solution uses only the model's grid geometry for the calculations and for storage purposes only. It is also an efficient way to program the algorithm in the same language that can be used later for full numerical analysis-based parameter identification. The tunnel was assumed to be unsupported for simplicity, but a support system can be also included by using the approximations presented in chapter 5. The ground is assumed to be elastic-perfectly plastic and there are six parameters to be identified. The Elastic modulus E, the Poisson's ratio v, the far field stress p_o, the cohesion c, the friction angle of the ground ϕ and the dilation angle ψ. The total deformations at six grid points and the tangential stress close to the tunnel were used as monitoring data for the back-analysis. The six grid points were located in such a way that they penetrate in the average expected plastic zone around the tunnel opening, given the range and relation of strength and stress parameters used. The cooling schedule chosen is expressed by equation (52). The back-analysis was executed three times to investigate the repeatability of the results. The initial assumptions along with the converged solution as

well as the values of the true optimum are shown in Table 7. The table shows all the parameters used for each of the analyses, along with the configuration of the annealing schedule. The constraints of all the parameters along with the step size for each parameter are also shown. From the results it is shown that generally there is a good agreement between the converged-solution and the theoretical global optimum. Trial 2 has converged to a nearby local optimum since both the elastic modulus and the far field stress are lower than the globally optimum parameters. It is remarkable though that the predictions of the strength and dilatancy parameters are all very close. Trials 2 and 3 were started from the same initial trial vector which does not matter since the algorithm is heuristic based and independent on the initial trial point. The evolution of the objective function values is shown in Figure 21.

Table 7: Back-analysis results of circular tunnel problem in Mohr-Coulomb ground.

Analysis / # Parameter	True optimum	1		2		3	
		Initial	Final	Initial	Final	Initial	Final
E (MPa)	8000	7000	8365	6000	7380	6000	8436
v	0.25	0.26	0.26	0.23	0.28	0.23	0.26
p_o (MPa)	7.0	8.0	7.2	8.0	6.1	8.0	7.1
c (MPa)	0.8	1.2	0.93	1.0	0.6	1.0	0.64
ϕ (°)	30	28	27.6	32	31.3	32	33.3
ψ (°)	2.0	0.8	1.9	1	2.4	1	1.99
To		1.4		1.4		1.4	
NT		200		200		200	
NI/NI[NT>70]		150/300		150/300		150/300	
CR		0.95		0.95		0.95	
E min–max Δs_E		6000-9000 400		6000-9000 400		6000-9000 400	
v min–max Δs_v		0.23-0.3 0.01		0.23-0.3 0.01		0.23-0.3 0.01	
p_o min–max Δp_o		6.0-9.0 0.4		6.0-9.0 0.4		6.0-9.0 0.4	
c min–max Δs_c		0.3-1.5 0.15		0.3-1.5 0.15		0.3-1.5 0.15	
ϕ min–max Δs_c		25-35 1		25-35 1		25-35 1	
ψ min–max Δs_ψ		0.1-3.0 0.4		0.1-3.0 0.4		0.1-3.0 0.4	

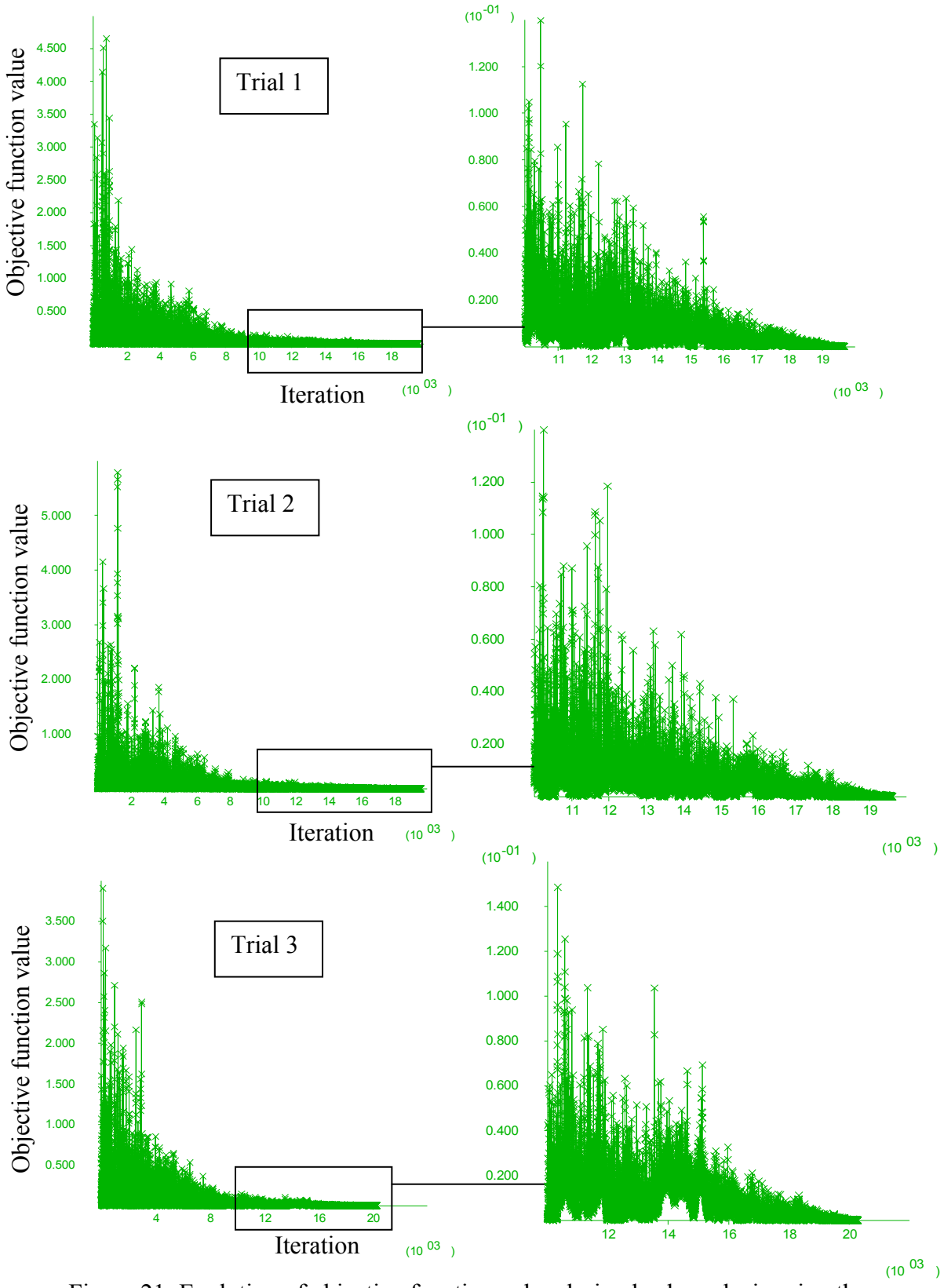

Figure 21: Evolution of objective function value during back-analysis using the Simulated Annealing algorithm.

7.4. Case of a deep circular tunnel in elastoplastic ground

7.4.1. Problem description

The SA method was used for the back-analysis of a circular tunnel in elastoplastic ground. The target was to use a frequently encountered case of the circular tunnel in plastic ground and perform the back-analysis under plane strain conditions. The use of a widely available numerical code is also advantageous. The plane strain numerical approximation is still today perhaps the most often encountered and used analysis tool. The main advantage is the execution speed, which leads to timely solutions for a wide range of geotechnical scenarios of a particular problem. Conversely, a plane strain approach, requires the approximation of the three-dimensional tunneling effect, that occurs ahead of the excavation face, using an approximation such as the approximation relationships presented in chapter 5. Clearly, by using a three-dimensional code all these elements are bypassed at the expense of computing time.

The choice of the numerical code (plane strain vs. three-dimensional) can also influence the amount and type of monitoring data that can be used for a back-analysis. Deformation and lining stress measurements often take place in deep rock tunnels. It is also rare that a complete history of deformation measurements is available, unless instrumentation in the form of multi point borehole extensometers has commenced ahead of the main tunnel heading, from a pilot tunnel or from the ground surface. Deformation measurements are therefore, almost always relative. An amount of displacement has already occurred by the time the monitoring starts, and it is not always easy to assess. This is a true fact and plays equal role in back-analysis using any of the above methods. The above conditions formulate a highly non-linear objective function which is difficult to address. In the tunnel case examined here, the plane-strain models were used for quick solution times. The same algorithm can be applied to a three-dimensional model.

It was assumed that the tunnel is excavated under anisotropic stress conditions, in an isotropic ground characterized by a Mohr-Coulomb failure criterion. Initially the problem was solved using a known set of elastic, plastic and stress level parameters. The parameter values used are shown in Table 8. The same model as the one used for the back-analysis using the Newton-Raphson method was employed.

Other additional parameters such as the insitu shear stress τ_{xy}, or the dilation angle $\psi°$, may also be implemented easily in the algorithm. The three-dimensional tunneling effect is simulated by the Convergence-Confinement approach. The tunnel periphery is let to relax at 50% of its initial insitu stress, and then support is installed. This amount of relaxation is taken arbitrarily for this example and practically corresponds to support installed at some small distance from the tunnel face. Support composed of a one-pass, 20 cm thick shotcrete liner, is installed and then the tunnel is let numerically to relax fully, until ground-support equilibrium is achieved.

Relative displacements and lining loads were used as input for the back-analysis. To simulate closer a real case, the hypothesis is made that monitoring does not commence before the tunnel is excavated, but commences at the installation of the support liner. These conditions, in conjunction with the plane strain approximation, result in a very irregular objective function with multiple local optima. These factors are the most frequently encountered in construction monitoring and in the post processing of results. Instrumentation is composed of three multipoint borehole extensometers, one at the wall, one at 45° angle from the horizontal, and one at the crown. The locations of the instrumentation are shown in Figure 22. The length of the extensometers was taken so that they penetrate through a potential plastic zone, estimated using average strength parameters. The axial loads developed in the shotcrete, were also monitored at the same three points as the heads of the extensometer locations.

Since the analysis is plane strain, the objective function of the back-analysis can be better "shaped" by employing measurements susceptible to changes of the parameters of interest. All measurements were assumed to have the same weight factor w_i=1. The use of relative displacements only (in two dimensional analyses) can potentially lead to multiple local extrema of the objective function, thus making back-analysis difficult. The inclusion of lining loads allows the function to become more sensitive in changes of ground strength parameters and ground elastic modulus and can save time during the back-analysis process. The tunneling problem and the back-analysis algorithm were implemented by using the proprietary FISH programming language by Itasca. The next paragraph presents the results of a series of back-analysis and the performance of the used algorithm.

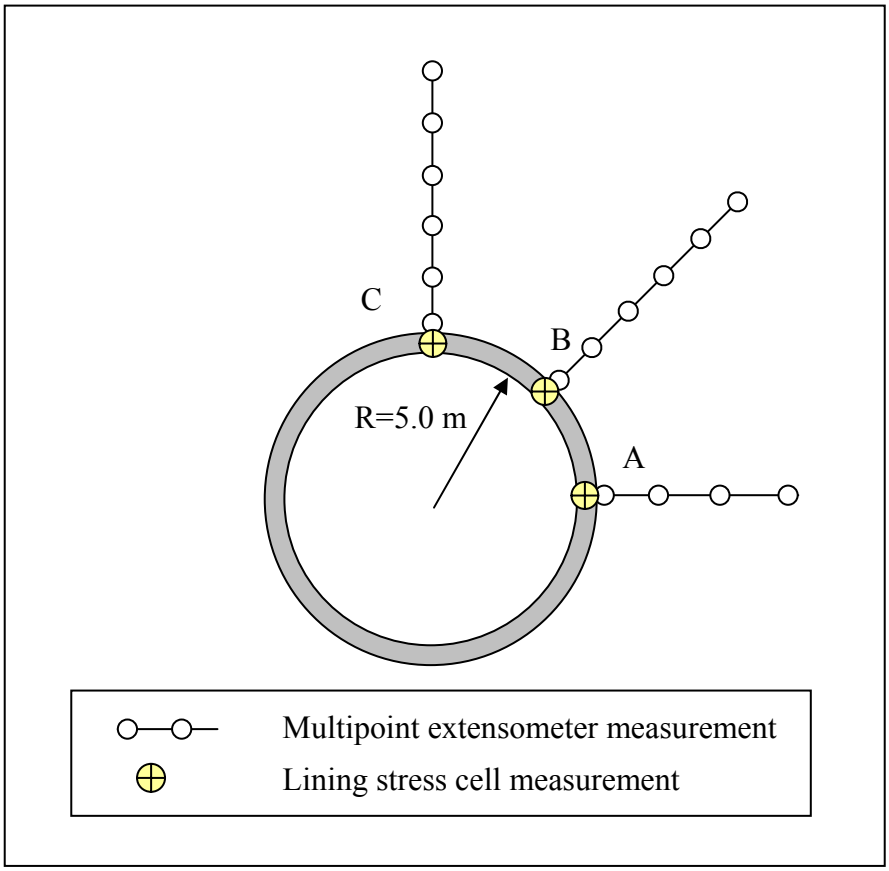

Figure 22: Monitoring locations and instruments around the circular tunnel

7.4.2. Algorithm performance and results

A series of back-analyses were performed using various starting points, in order to study the behavior of the algorithm. The results from six analyses will be presented here and discussed. Table 8 presents the initial trial vectors, along with the annealing properties tried for each analysis. The exponential cooling schedules used are shown in Figure 23. At NT=70, corresponding to approximately 95% of the cooling, the step size for the elastic modulus, Poisson's ratio, σ_y and σ_x, was reduced to approximately half of the original value. Other methods of gradually reducing the step sizes ΔS_i may also be implemented. The annealing schedule was followed to a 99.5% cooling percentage, at which the analysis was assumed to have converged.

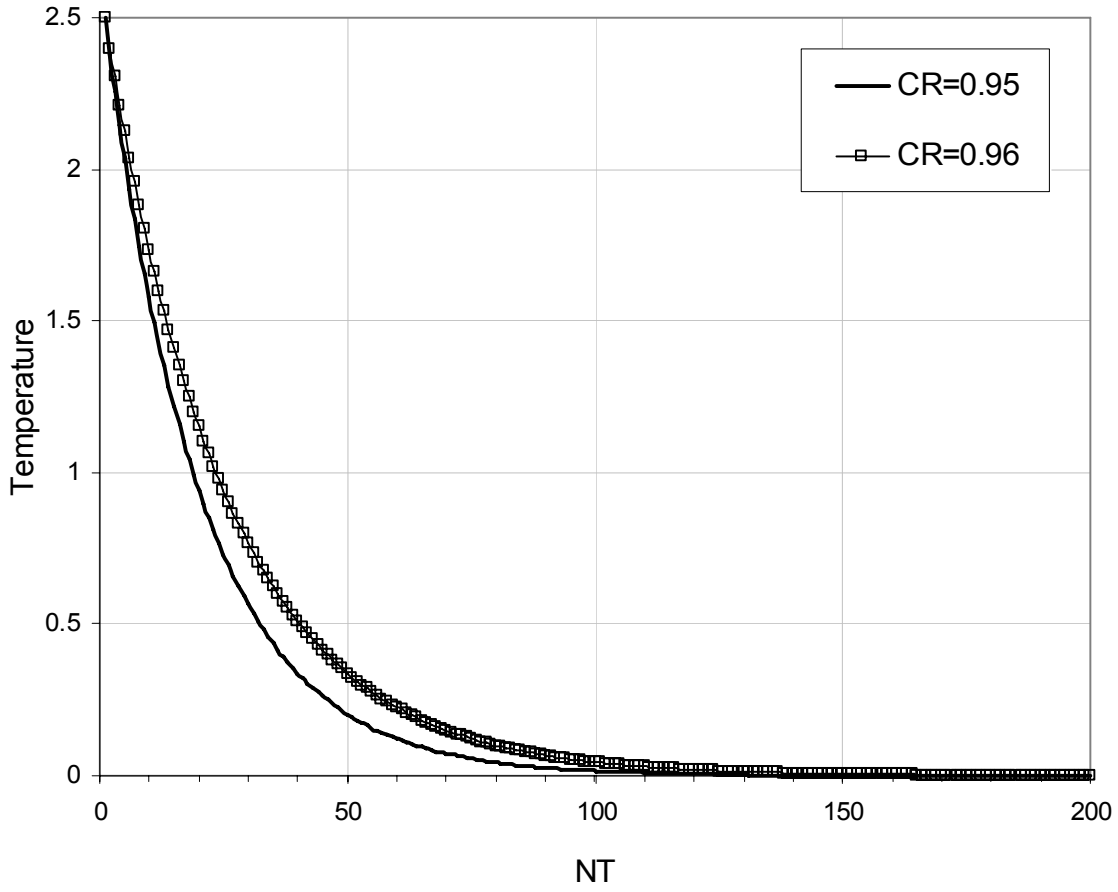

Figure 23: Exponential cooling schedules used for the Simulated Annealing back-analysis

The results of the analysis are summarized in Table 9. The final solution and the best solution found are shown for each of the trials. The results show that there is generally a good agreement with the theoretically accurate solution of Table 8, especially for cases 1, 3, 5 and 6. In cases 2 and 4 the best ever solution is closer to the actual optimum. The best solution of case 4 is the closest to the global solution vector. It is apparent that in some cases the solution was influenced by the presence of nearby local optima and attempted to converge there.

Table 8: Initial trial properties and SA parameters used in back-analysis

Analysis # / Parameter	True optimum	1	2	3	4	5	6
E (GPa)	6.0	5.2	7.0	5.7	5.3	5.3	6.5
v	0.25	0.23	0.27	0.24	0.26	0.26	0.24
σ_y (MPa)	14	12	13	13.5	12.8	12.8	13.2
σ_x (MPa)	6	5	7	6	5.3	5.3	5.7
c (MPa)	0.8	0.5	0.9	1.2	1.3	1.3	1
φ (°)	30	26	27	32	28	28	26
To		2.5	2.5	2.5	2.5	2.5	2.5
NT		95	95	110	110	110	110
NI/NI$^{[NT>70]}$		150/180	150/180	150/250	150/250	150/270	150/270
CR		0.95	0.95	0.96	0.96	0.96	0.96
E min–max Δs_E		5.0–7.5 300	5.0–7.5 300	5.0–7.5 300	5.0–7.5 300	5.0–7.5 300	5.0–7.5 300
v min–max Δs_v		0.22–0.3 0.01	0.22–0.33 0.01	0.22–0.33 0.01	0.23–0.33 0.01	0.23–0.33 0.01	0.23–0.33 0.01
σ_y min–max Δs_y		12–15 0.6	12–15 0.6	12–15 0.5	12–15 0.6	12–15 0.6	12–15 0.6
σ_x min–max Δs_x		5–8 0.5	5–8 0.5	5–8 0.4	5–8 0.5	5–8 0.5	5–8 0.5
c min–max Δs_c		0.3–1.5 0.15	0.3–1.5 0.15	0.3–1.5 0.15	0.3–1.5 0.15	0.3–1.5 0.15	0.3–1.5 0.15
ϕ min–max Δs_φ		25–33 1	25–33 1	25–33 1	25–33 1	25–33 1	25–33 1

Table 9: Back-analysis results for deep tunnel problem using SA

Analysis # Param.	1		2		3		4		5		6	
	final	best	final	best	final	best	final	best	final	best	final	best
E (GPa)	5.8	5.5	6.2	5.7	6.0	5.9	5.2	6.0	5.9	7.1	5.7	5.2
v	0.25	0.25	0.26	0.25	0.26	0.25	0.24	0.25	0.26	0.25	0.25	0.25
σ_y (MPa)	14.1	13.4	13.2	13.4	14.4	13.7	13.1	14.0	14.9	14.7	14.4	13.4
σ_x (MPa)	6.3	5.8	5.5	5.7	6.1	5.8	5.6	6.0	6.3	6.2	6.4	6
c (MPa)	0.81	0.79	0.75	0.77	0.76	0.77	0.97	0.75	0.73	0.75	0.83	0.86
ϕ (°)	30.3	29.7	29.2	30.0	31	30.1	27.3	30.5	31.8	30.4	30.6	29.4

The result outcome can be better understood, in relation to the order of magnitude of the objective function value at the optimum. The exact solution essentially yields a very low value of the function having an order of magnitude 10^{-9}. This level of precision may be difficult to be attained by the SA algorithm and FLAC by using large step sizes. The existence of multiple local optima can be expected since the objective function makes use of relative displacements and some useful information has been lost due to the delay in the monitoring instrument installation. That information, which is predominantly composed from elastic strains developed during the first stages of the tunnel relaxation, could have been useful for the back-analysis by shaping the numerical problem to a well defined one. The algorithm may find some local optima, which are not too far away from the theoretical solution. A small perturbation of the globally optimum parameter vector may lead the function to attain small but higher order values comparable to those of other local optima. This issue becomes apparent from the solution record. The SA method attempts to search the feasible solution domain and any local minima should be captured and identified in the history of stored successes.

From all analyses it was evidenced that the solution would eventually show preference to two or three local solution clusters amongst which one corresponds to the correct one. The most pronounced local minima areas attract the algorithmic process, and can be identified from the solution history. This is advantageous over the traditional algorithms that drive the analysis towards the closest optimal solution. The parameters most unstable to the back-analysis are shown to be the average elastic modulus E of the ground and the vertical insitu stress σ_y. Despite the nonlinear nature of the problem, the plastic parameters are always back-analyzed with fair success and precision, even though the constraints are fairly wide. This is a considerable advantage of the algorithm. During the analysis the method attempted to minimize the objective function even at low temperatures, where the algorithm evolves into a downhill optimization process. It is important to have a high number of perturbations at low temperatures, so that the solution is better tracked.

Figure 24 presents the expected plastic zone, the vertical displacements and lining axial loads at the globally optimum solution. For comparison, the results of the back-analysis are shown in Figure 25-30. Figure 31 shows the characteristic uphill movements

of the Simulated Annealing during the optimization progress. The algorithm converges to the area of the global minimum towards the end.

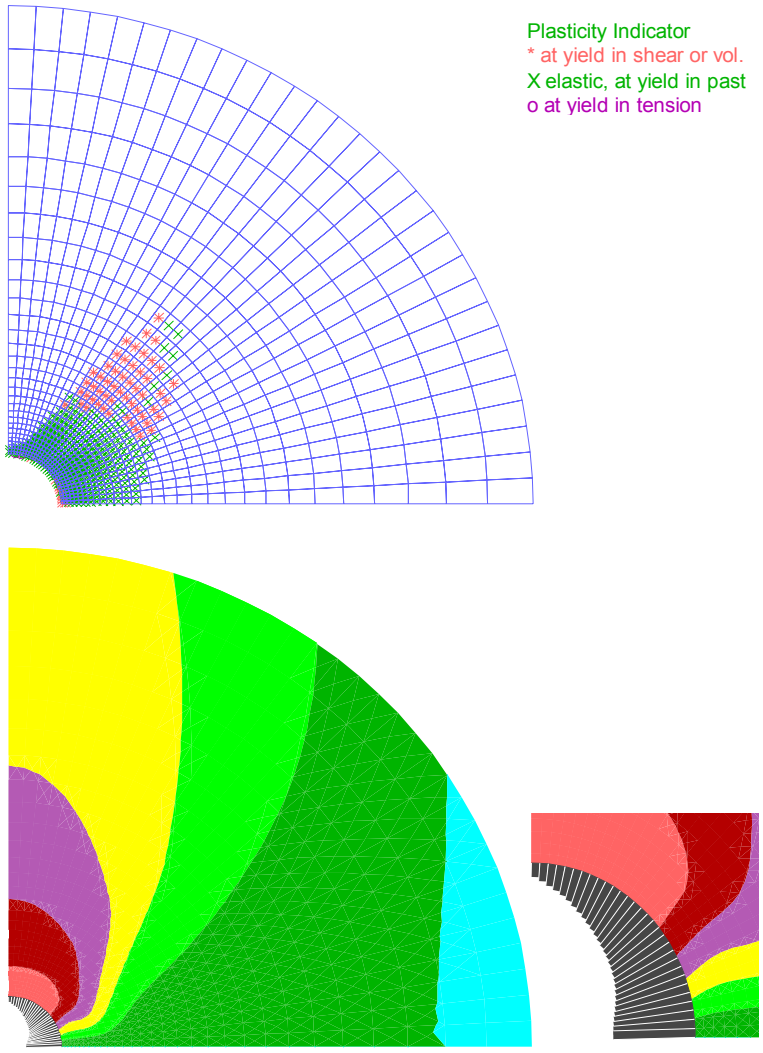

Figure 24: Results from global optimum point . a) Plastic zone around the tunnel, b) Vertical displacements and lining axial load distribution (MN).

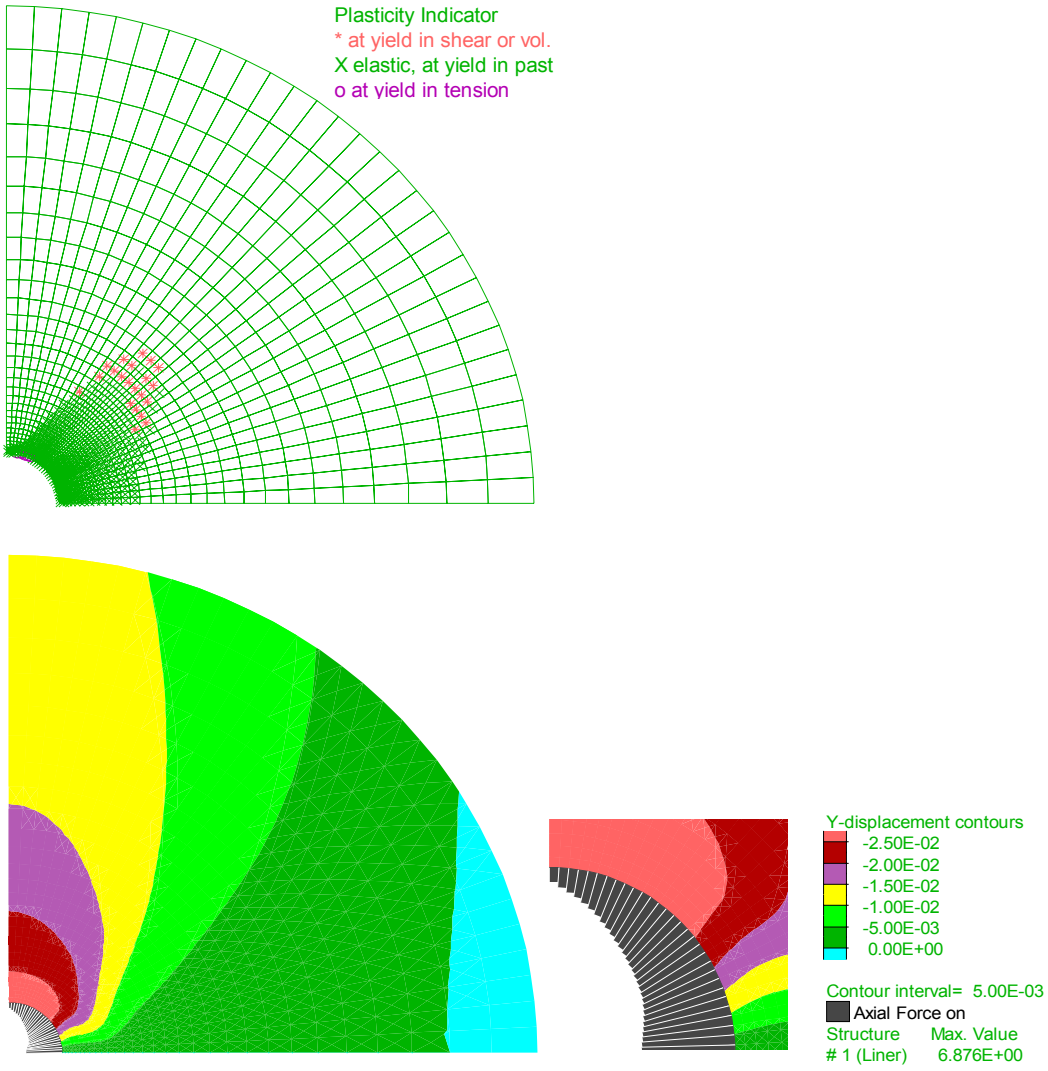

Figure 25: Back-analysis results from trial #1.

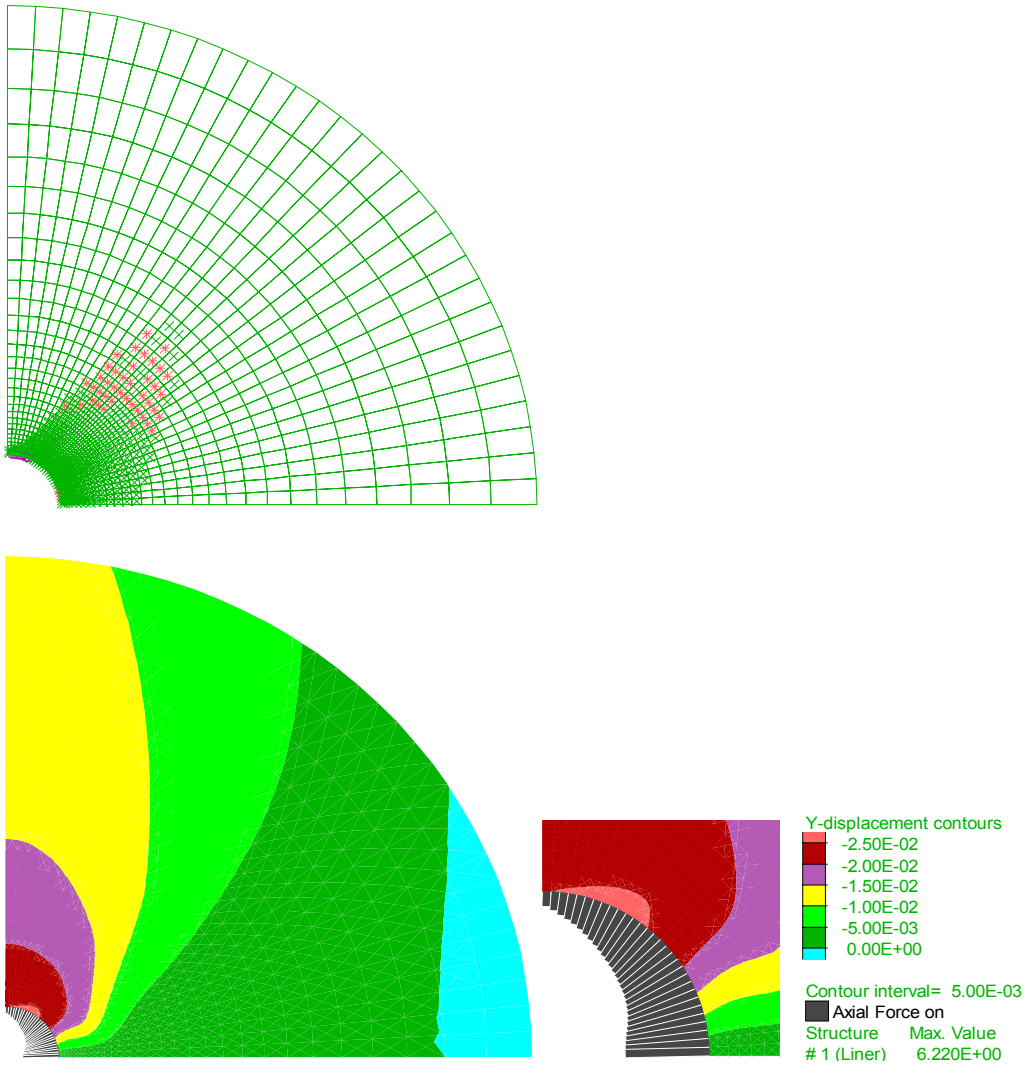

Figure 26: Back-analysis results from trial #2.

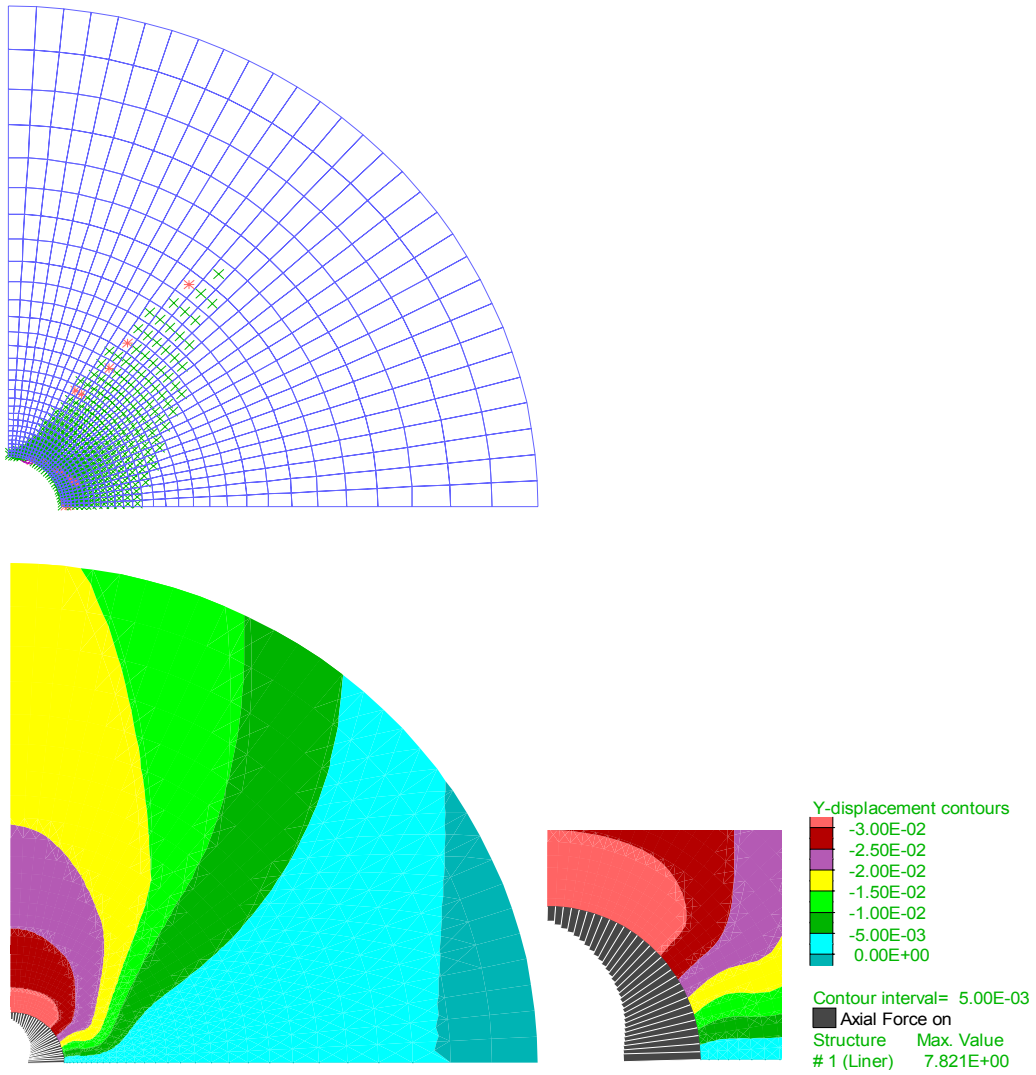

Figure 27: Back-analysis results from trial #3.

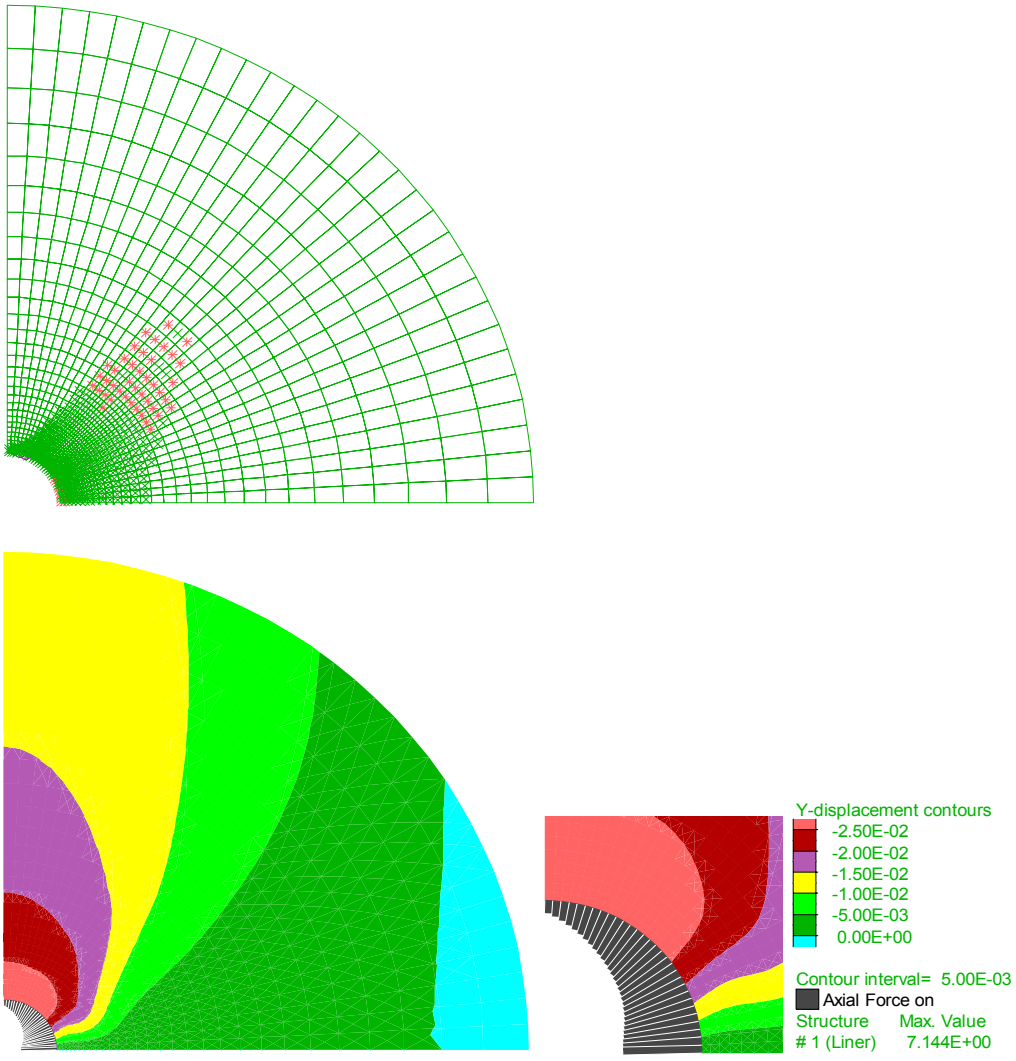

Figure 28: Back-analysis results from trial #4.

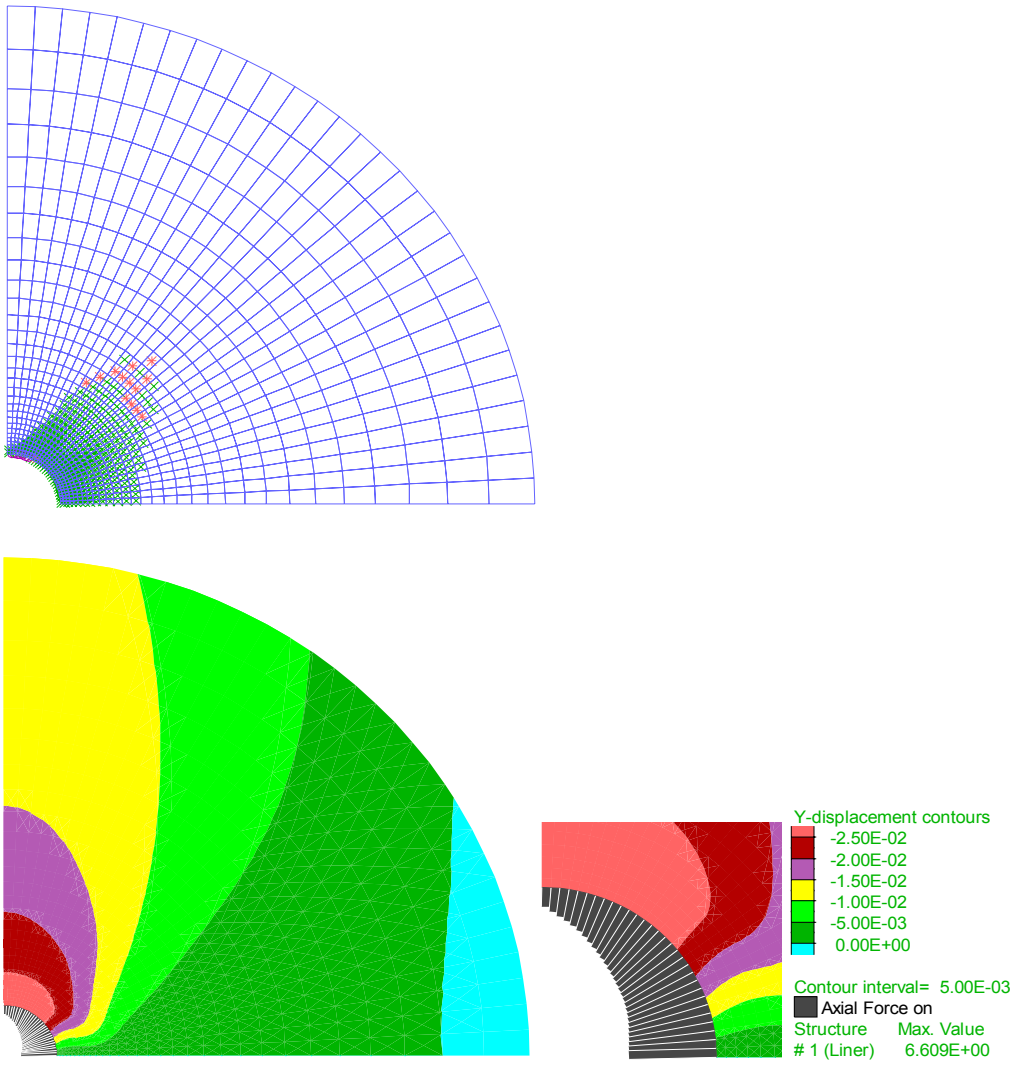

Figure 29: Back-analysis results from trial #5.

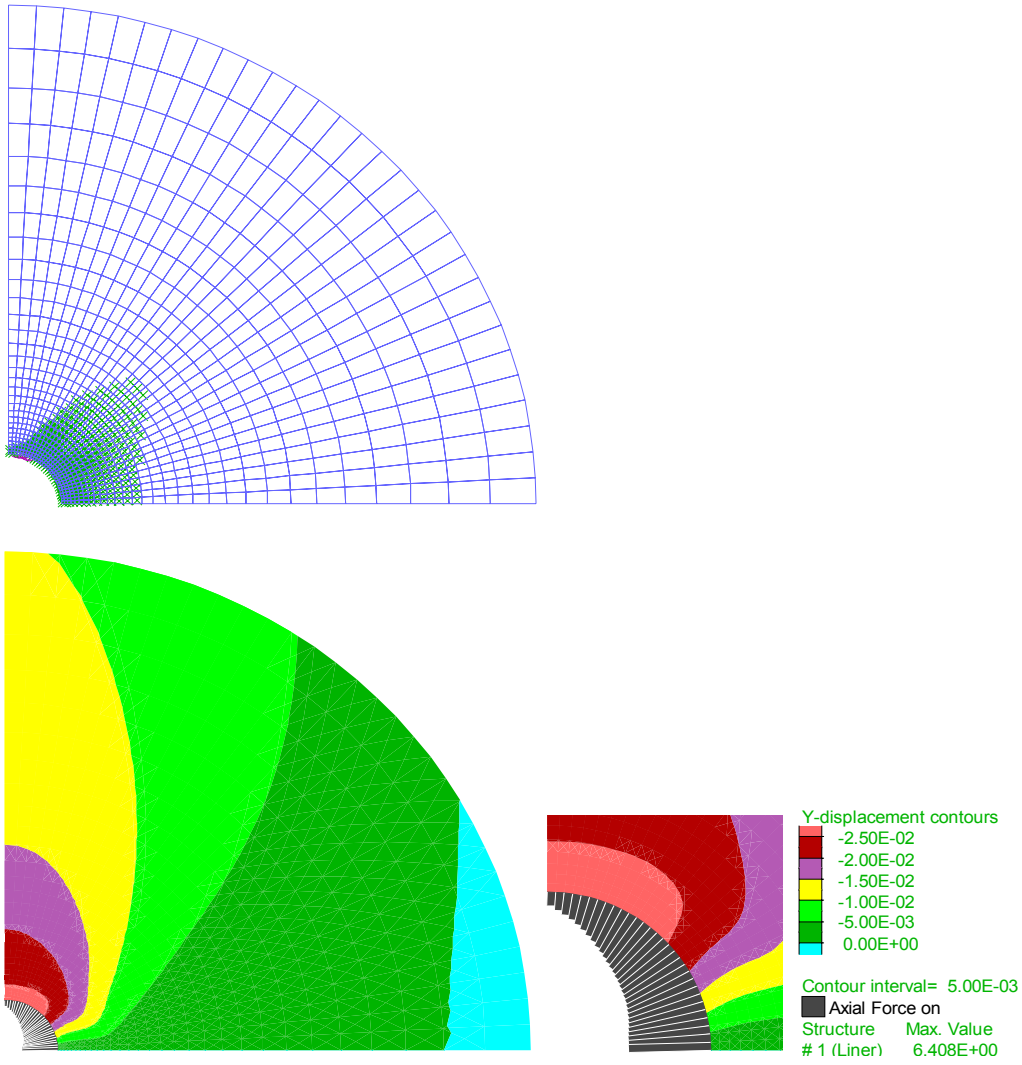

Figure 30: Back-analysis results from trial #6.

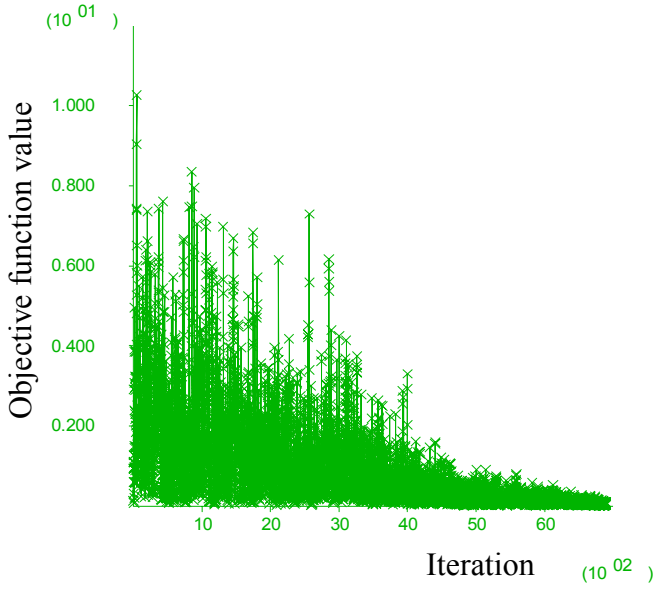

Figure 31: Plot of the objective function values during the execution of the back-analysis for trial #6. The frequent uphill movements are characteristic of the Simulated Annealing algorithm.

In order to study the importance of the relative displacement measurements, as they were used in the previous examples, back-analysis was performed on several models assuming plastic ground conditions and no support. This is also a difficult task to perform, since there are no lining stress measurements. In these cases it was assumed however that measurements at the same nodal points (as the extensometer locations) commenced before the ground is excavated. Such a condition occurs frequently at shallow urban excavations. The results which are summarized in Table 10 showed good behavior of the algorithm used. Representative results of the later back-analysis are shown in Figure 32. The optimization progress is shown in the objective function plot of Figure 33. Mostly sure, the proposed methodology is promising and may be applied easily in commercially available software. The most significant features of the method are its heuristic nature and its ability to take uphill movements during the optimization. Problems regarding back-analysis of elasto-plastic parameters can be addressed in this way. The representative algorithm programmed in the FISH programming language is available by the author.

Table 10: Back-analysis results of unsupported circular tunnel in plastic ground using SA and FLAC.

Analysis # / Parameter	True optimum	1
E (GPa)	6.0	5.5
v	0.25	0.25
σ_y (MPa)	12	12.2
σ_x (MPa)	6	5.9
c (MPa)	1	0.97
ϕ (°)	30	30.2
T_o	2.5	
NT	90	
NI/NI$^{[NT>70]}$	150/200	
CR	0.95	
E min–max Δs_E	4500-8000 300	
v min–max Δs_v	0.22-0.3 0.01	
σ_y min–max Δs_y	10-14 0.5	
σ_x min–max Δs_x	5-8 0.4	
c min–max Δs_c	0.3-1.5 0.15	
ϕ min–max Δs_φ	25-33 1	

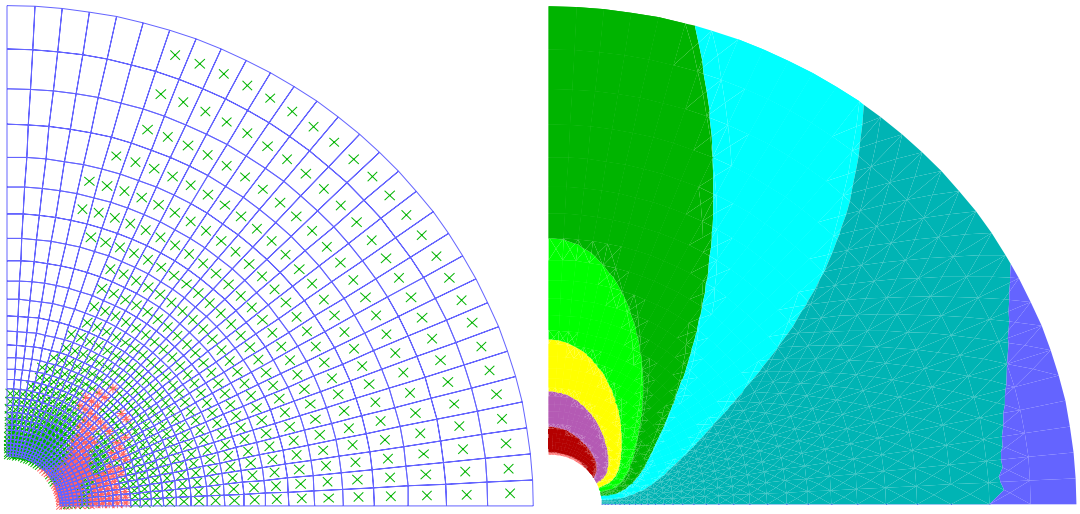

Figure 32: Back-analysis results from unsupported tunnel model in plastic ground.

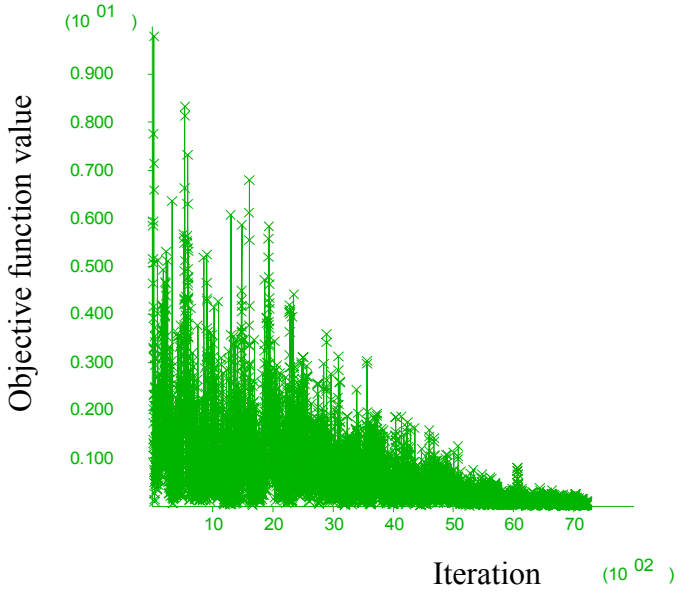

Figure 33: Evolution of objective function during the progress of Simulated Annealing in unsupported tunnel model.

7.5. Case of a shallow circular tunnel in plastic ground

7.5.1. Problem description

Based on the previous analyses it is evident that the Simulated Annealing is a very formidable algorithm for optimization of highly non-linear problems, and can cope adequately in cases where multiple local optima may exist. Clearly the performance of this algorithm is superior to previously examined techniques in establishing the global or a solution very close to the global one if such one exists. The ability to incorporate constraints and any number of parameters easily makes it ideal for geotechnical parameter identification problems. The importance of a powerful optimization technique was also stressed out, especially when relative displacements are used for monitoring the excavation and for the back-analysis as well. In this section, the same algorithm is employed to perform a back-analysis of a shallow excavation. This problem arises when tunneling in urban environments, where ground surface deformations should be kept to a minimum. Even though it is a more challenging problem from a construction stability standpoint, it may offer a wealth of useful monitoring data. In such cases monitoring most often starts before the excavation, via ground inclinometers, multipoint extensometers installed from the ground surface, or with surface surveying. Shallow excavations through soft soils often suffer from ground or otherwise volume loss. Thus the settlement observed at the surface is mainly due to two reasons. One is due to the elastic or inelastic strains that develop from the gradual tunnel excavation. The short overburden often does not allow the advantageous formation of an arching effect (existing in deep tunnels) thus these problems are more prone to instability. On the other hand when this instability is increased, tunnel closure may be counteracted by over-excavating ground material leading to volume loss and further deformations on the surface. Other phenomena such as consolidation or even secondary deformation of soft clays can also exist. Timely monitoring is thus very important and should be done not only for parameter identification purposes but also for modeling technique and assumption verification.

In this case the problem of a supported shallow tunnel in plastic ground is examined. The monitoring is assumed to commence at a pre-construction stage, thus the

majority of significant strains in the ground should be captured by the equipment. For this example only the tunnel relaxation before installation of the support is modeled.

Figure 34 shows the constructed finite difference grid in FLAC. Due to symmetry only half the geometry is modeled.

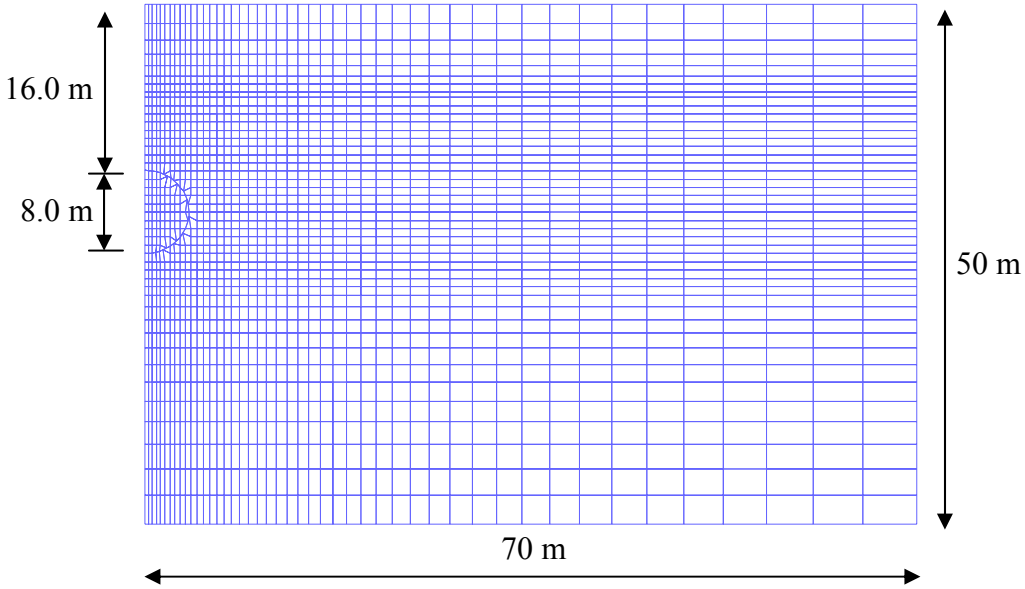

Figure 34: Shallow tunnel model in FLAC.

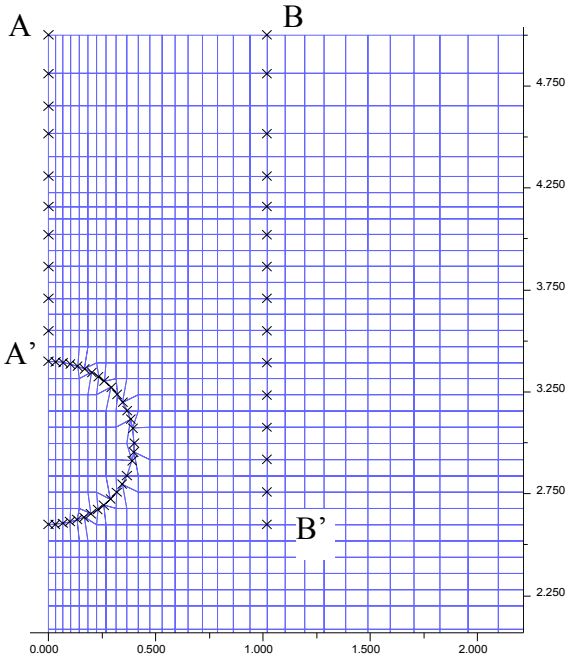

Figure 35: Deformation monitoring points

Figure 35 shows the locations of the selected deformation monitoring gridpoints. During back-analysis it was assumed that the overburden displacements are monitored relatively, using a multipoint extensometer. Therefore all displacements along AA' were subtracted from the displacements of the surface point A. It was also assumed that horizontal movements were monitored close to the tunnel by an inclinometer BB'.

7.5.2. Algorithm performance and results

In this fundamental example, four parameters would be estimated by back-analysis. The ground elastic modulus E, the K_o ratio, the cohesion c and friction angle ϕ of the ground. The initial parameters used to create the monitoring data in FLAC are shown in Table 11 along with the results of the back-analysis. The stresses were initialized using a constant unit weight γ=23 kN/m^3 but by altering the K_o ratio at each iteration.

Table 11: Back-analysis results for shallow tunnel problem using SA.

Analysis # / Parameter	True optimum	final	best
E (kPa)	30000	29450	29260
Ko	0.5	0.48	0.5
c (kPa)	8	3.7	5.96
ϕ (°)	25	27.5	25.2
T_o	2.5		
NT	80		
NI/NI$^{[NT>70]}$	150/200		
CR	0.96		
E min–max Δs_E	20000-45000 1700		
K_o min–max Δs_{Ko}	0.3-0.6 0.02		
c min–max Δs_c	2-20 1.2		
ϕ min–max Δs_ϕ	20-35 1		

From the results it is obvious that the method is successful in establishing a solution very close to the theoretical global optimum. Figure 36 presents the progression of the parameter identification during the annealing progress. The non smooth behavior with the parameters perturbating constantly is characteristic of the algorithm used. The solution vector is attracted to the region of the global minimum towards the end of the cooling schedule as evidenced also by the objective function value from Figure 37.

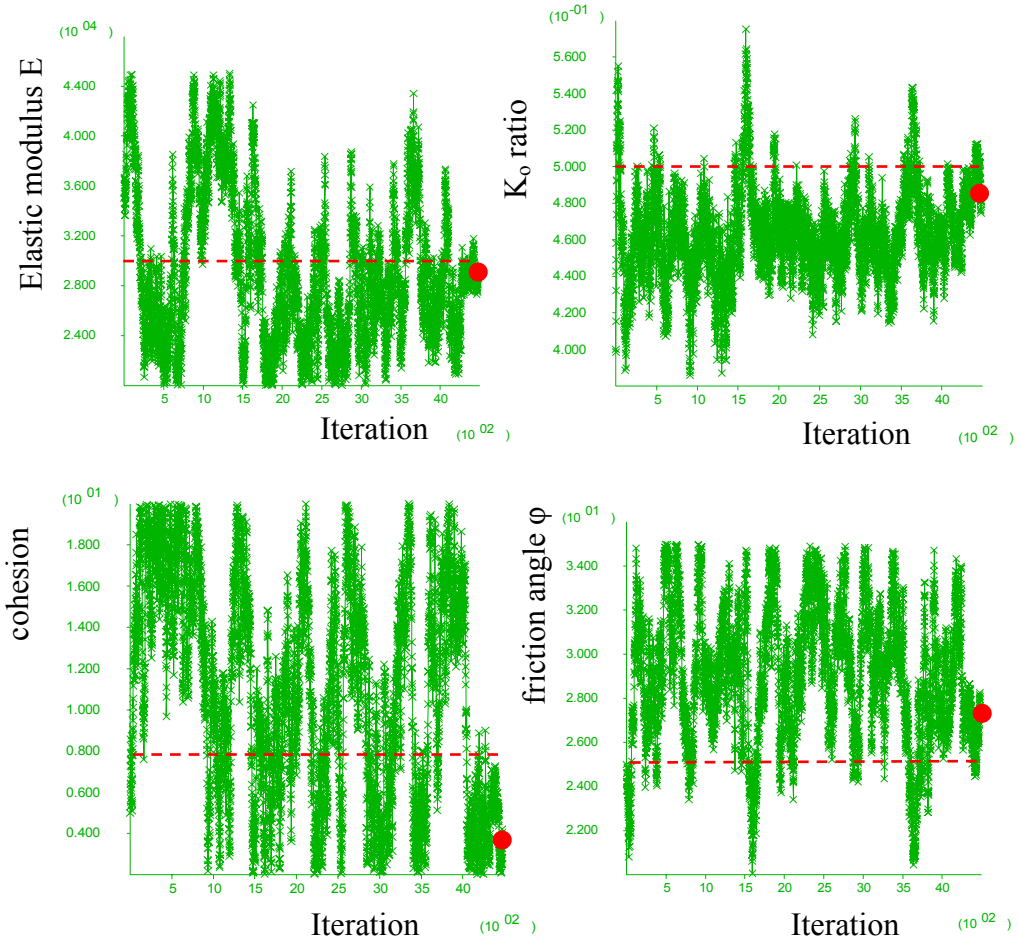

Figure 36: Progression of parameter identification problem using the SA algorithm in FLAC. The theoretical global optimum is shown in dotted line, while the final solution is shown in circles.

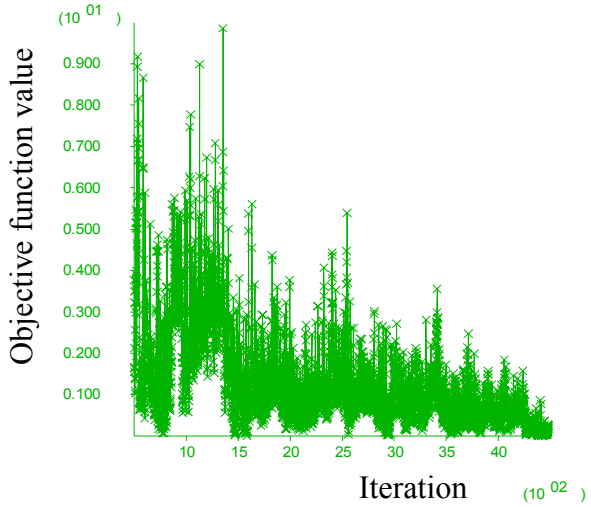

Figure 37: Objective function value during back-analysis of shallow tunnel problem.

7.6. Conclusions

In the present paper a new methodology of performing back-analysis for underground excavations, or other geotechnical problems is introduced. The method is based on the use of the Simulated Annealing algorithm, and shows good performance under ill defined non-linear problems. The algorithm attempts to simulate the annealing process of metals from the hot semi-solid phase to a complete cooled solid phase. This numerical process performed in analogy to the thermodynamic principles characterizing the cooling of steel. At high temperatures the natural system is allowed to perturb its formation in order to decrease its energy. Equivalently the numerical system is allowed to test different solutions, thus parameter combinations, so that it minimizes the objective function. The ability to take uphill movements during the heuristic process is advantageous for non-linear problems, having multiple minima. When sufficient cooling time and sufficient re-arrangements of the system are performed, then the method has a high probability of finding the global optimum solution, assuming that there is one.

The suggested method is very promising for wide range of problems, but its application is problem specific. The algorithm can be modified and altered to better suit certain problems. The most important parameters in the analysis are the initial temperature, the cooling schedule and the time allocated for possible re-arrangements at each temperature. A discussion of the choice of the importance and efficiency characteristics of cooling schedules is given by Hajek (1988). The search step size for

each parameter also influences the convergence end efficiency of the code. A possible way is to program a gradual reduction of the search step sizes of the involved parameters, along with the annealing schedule. It is recommended to calibrate the SA model parameters before applying the method efficiently in back-analysis. The method also offers practically no user intervention during the execution of the algorithm and constraints can be easily employed. It may also be practical to restart the SA process from the “best ever” solution found either at a pre-described number of temperature reductions or even at the end of the original annealing process. Generally the method should be calibrated in such a way that the algorithm retains its efficiency at narrow valleys of the objective function. The solution search should progressively become more restricted as the temperature decreases.

CHAPTER 8. Back-analysis of tunnel response using the Differential Evolution method

8.1. General

The analysis presented so far has been aimed to reveal some of the problems of parameter identification and possible ways to overcome these. It has been observed that the performance of local search methodologies is not efficient for geotechnical problems, where the objective function possesses multiple local optima and when the problems are ill-defined due to lack of appropriate type and quantity of monitoring data. A novel way has been presented, where back-analysis is performed using the Simulated Annealing algorithm. The application of the standard algorithm by Kirkpatrick et al. (1983) has shown that it has a good potential for use in non-linear geotechnical problems. The downside of the method is that it generally requires a slow annealing schedule with ample "time" for perturbations at each temperature so that the probability of finding the global optimum increases. This may be computationally inefficient if a faster solution is required. On the other hand the method allows for complete tracking of the solution progress and its use of memoryless and heuristic nature offers the potential identification of various local optima with strong regions of attraction of the solution. Further advancements in the implementation of the algorithm in addition to the high performance of modern computing machines, allow for its use in continuous variable optimization problems.

An alternative optimization scheme is the use of another method that also attempts to simulate natural processes. The use of Genetic Algorithms (GA) is a very attractive candidate in a parameter identification scheme. Simpson and Priest (1993) provide a discussion on the use of GAs in geotechnical applications. Feng et al. (2000), and Feng and An (2004) have employed GAs in back-analysis of geotechnical problems. Wang et al. (2004) have also used GAs in identification of dynamic rock properties. Fundamentally this method and its derivatives are the only that can perform global optimization and offer similar advantages if not more, than the Simulated Annealing method. The problems that the Genetic Algorithms address are similar to the usual workload of Simulated Annealing. According to Rao (1996) often mixed continuous and discrete variables may be searched for during optimization in a discontinuous or

nonconvex search space. The Genetic Algorithms are well adapted to address such problems. The development of the Genetic Algorithms is attributed to Holland (1975) and the main core of the method rests on the Darwinian theory of the survival of the fittest. The majority of the Genetic Algorithms perform the optimization process in the binary system using string lengths representing the design variables and subsequently the whole design vector. The main elements of a Genetic Algorithm are as follows (Rao, 1996):

- The procedure starts from a population of trial vectors, instead of a single point. For an n-variable problem, the usual population size is $2n$ to $4n$. For highly non-linear objective function higher sizes may be required. This is very similar in principle to the Complex method where the Complex shape is composed of k x n vertices ($k \geq 2$).
- There is no gradient or pattern search direction exploitation.
- Each variable resembles to a chromosome in genetics.
- The objective function value is the equivalent of fitness in genetics. In minimization problems a vector corresponding to a very low function value is a strong candidate and may survive in the future.
- The process is based on repeated generations of new population vectors. The trial vectors of these populations are the result of randomized parental selection, crossover and mutation processes. They are essentially the offspring of previous trial vectors.

8.2. Description of the Differential Evolution Algorithm

As stated previously most of the Genetic Algorithms handle the optimization process using the binary system. This may create programming difficulties and inefficiencies in problems of continuous variable optimization where floating point numbers are used. The Evolution Strategies deal exactly with this issue by bypassing the requirement of binary system usage and also makes the algorithm more user-friendly. A type of Evolutionary Strategy called the Differential Evolution (DE) has been proposed by Storn and Price (1997), and Price and Storn (1997). The DE, like Simulated

Annealing, is a stochastic-based direct method. As a heuristic method it is based on the experimental behavior of a function. With the modern computational power and the particularities of numerical-based back-analyses it is more prudent to test for the fitness of a trial independently from pattern directions or gradients whose existence is questionable. The application of the DE in locating earthquake hypocenter has been examined by Růžek and Kvasnička (2001). Insight on the use and implementation of DE algorithms is also given by Reed and Yamaguchi (2004). The use of the DE in estimation of rock fracture sizes is described by Decker and Mauldon (2006).

The Differential Evolution algorithm, uses two arrays to store a population of NP, D-dimensional real parameter vectors (D=number of parameters=n). The two arrays are called the primary, which contains the present vector population and the secondary array which stores sequentially the products for the next generation. The algorithm starts by filling the primary array with NP vectors with parameters randomly generated. The initial random generation should satisfy the constraints on the parameters. The primary array is also called as Trial Vector, since it contains NP vectors that will later be tried for fitness. Each of those individual randomly generated vectors $\mathbf{X}_i$ is considered sequentially for genetic operations. For each of the chosen vectors, three other vectors $\mathbf{X}_A$, $\mathbf{X}_B$, $\mathbf{X}_C$ are randomly chosen from the remaining vectors of the primary array.

A mutation can then be performed by using the following relation:

$$\mathbf{X}_1^m = \mathbf{X}_A + F(\mathbf{X}_B - \mathbf{X}_C) \tag{57}$$

$\mathbf{X}_1^m$ is the new mutant vector and F is a scaling factor in the range $0 < F \le 1.2$. According to Price and Storn (1997)the optimum value of F is in the range 0.4-1.0. A small modification of the main algorithm is applied here. At this stage the mutant vector $\mathbf{X}_1^m$ is checked for constraint violation. Even though the initially generated $\mathbf{X}_A$, $\mathbf{X}_B$, $\mathbf{X}_C$ vectors are feasible, their linear combination may be violating the constraints. If any parameter constraint is violated, then the sampled vectors $\mathbf{X}_A$, $\mathbf{X}_B$, $\mathbf{X}_C$ are discarded and a new sampling is performed until a feasible vector $\mathbf{X}_1^m$ is found. This intervention is seamlessly integrated in the algorithm and also keeps the true heuristic process of the problem intact.

At this stage the crossover takes place. A random integer number *randint(i)* in the range [1,n] is generated. For each parameter *j*=1,..,*n* a random number *randnum(j)* is generated in the space [0,1]. Then a new vector is created from the original $\mathbf{X}_i$ parent and the mutant vector using the crossover criterion:

$$x'_{i,j} = \begin{cases} x^m{}_{i,j} & if \quad randnum \le XR \quad or \quad randint(i) = j \\ x_{i,j} & if \quad randnum > XR \quad and \quad randint(i) \ne j \end{cases} \tag{58}$$

where *XR* is a crossover rate in the range [0,1].

The crossover scheme essentially means that if *randnum*>*XR* the new ith trial vector will receive the *j* parameter from the parent vector, otherwise the parameter will be obtained from the mutant vector $\mathbf{X}_1^m$. In this way if *XR*=1, then every trial vector will be obtained from the mutant vector, or if *XR*=0, then all except for one parameter will be called from the parent trial vector.

The new vector $\mathbf{X}'_{i,j}$ is tested against $\mathbf{X}_i$ for fitness. Thus two function evaluations occur at this stage. For minimization problems, the vector corresponding to the lower value (fittest candidate) is entered in the secondary array. The same procedure is followed until all vectors of the original primary array are processed and an equal size secondary array has been formed. At this stage the secondary array values are transferred and update the primary array while the secondary array is purged. This constitutes the end of one generation. Obviously many generations are required for convergence. The above steps are repeated until a maximum number of generations is reached. When the algorithm converges to the global optimum, then all vectors of the primary array become equal. This is exactly the same again, as the Complex method where the complex vertices collapse to its centroid if an optimum has been found. The flowchart for one generation of the method is shown in Figure 38.

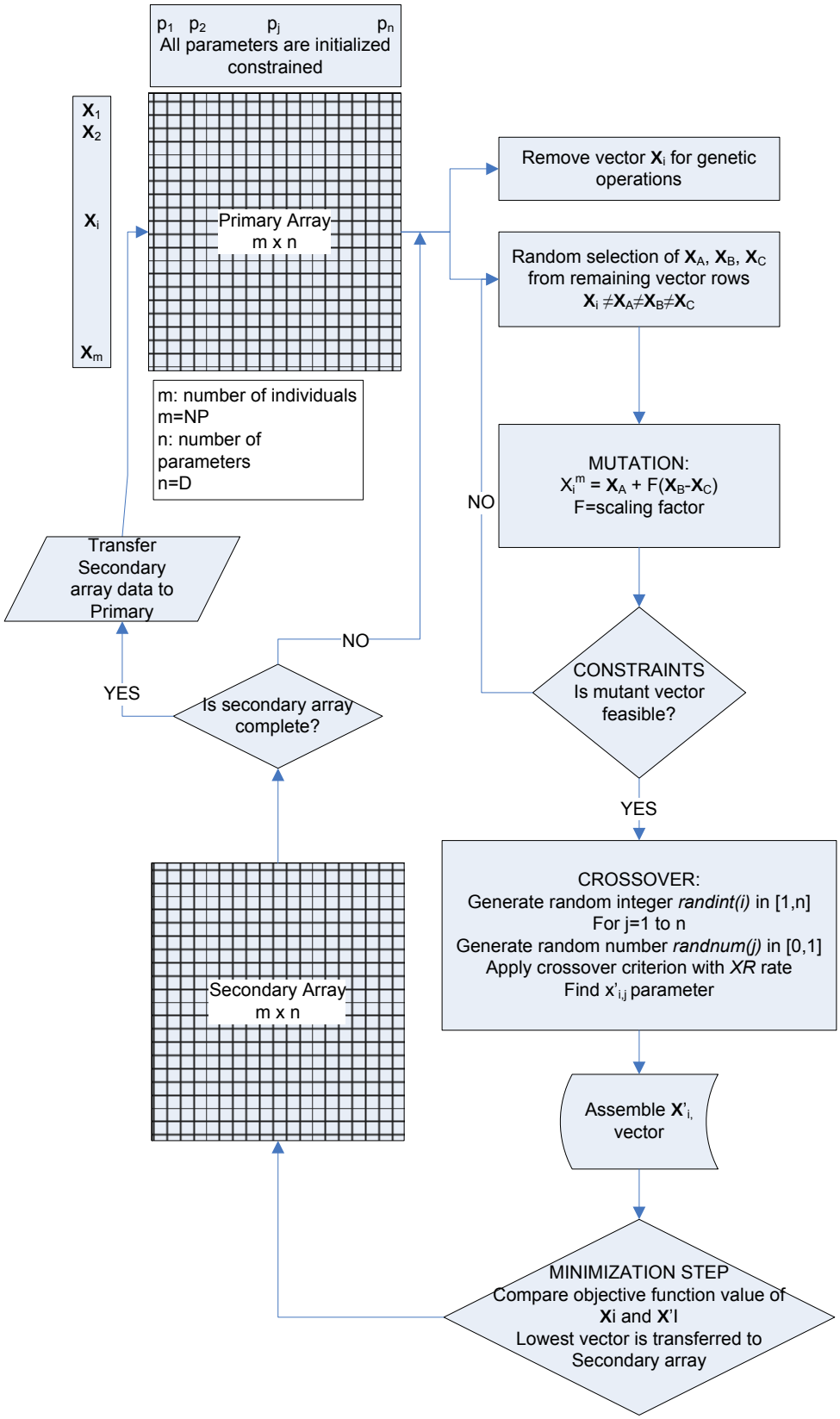

Figure 38: Flowchart for Differential Evolution algorithm

8.3. Case of a deep circular tunnel in plastic ground

The performance of the algorithm was investigated during back-analysis of the deep seated tunnel problem. The exact same model and monitoring data with the model described in section 7.4.1, were used. The Differential Evolution algorithm was programmed in the FISH language of FLAC. In this case n=6 and NP=60. The mutation scaling factor F was taken as F=0.5 and the crossover rate XR=0.7. A total of 70 generations was executed during the back-analysis. The solution shows convergence to the exact theoretical global optimum solution of the problem:

Table 12: Global (true) optimal solution for deep tunnel problem

Analysis # / Parameter	True optimum
E (GPa)	6.0
v	0.25
σ_y (MPa)	14
σ_x (MPa)	6.0
c (MPa)	0.8
ϕ (°)	30

There is some scatter mainly in the elastic modulus but this is probably due to the execution of 70 generations. At a higher number all parameters should converge to a more stable solution, but even at 70 generations the results reveal very good behavior of the code. Given the highly non-linear nature of the problem with multiple local minima, the performance is considered to be outstanding. The primary array results at the end of 70 generations are shown in Table 13. The same analysis was repeated to test the behavior of the code. Five more analyses were executed. In all trials the primary array converged the theoretically true global optimum. The results of three trials will be included herein. From these analyses it is apparent that the specific algorithm is very powerful and may address the difficult problem of having multiple local minima in the objective function. In order to further test the algorithm, the problem of the shallow

tunnel excavation described in section 7.5 was used. The algorithm can by obtained by contacting the author.

Table 13: Results from back-analysis of the deep seated tunnel problem using the Differential Evolution. The primary array of trial 1 at 70 generations is shown

Individual	E (MPa)	v	σ_y (MPa)	σ_x (MPa)	c (MPa)	ϕ (^{o})
1	5.66E+03	2.45E-01	-1.39E+01	-6.10E+00	8.42E-01	2.96E+01
2	5.99E+03	2.49E-01	-1.42E+01	-6.09E+00	8.27E-01	3.00E+01
3	5.92E+03	2.46E-01	-1.37E+01	-5.88E+00	8.35E-01	2.92E+01
4	6.03E+03	2.44E-01	-1.39E+01	-5.99E+00	8.27E-01	2.96E+01
5	6.32E+03	2.49E-01	-1.44E+01	-6.15E+00	7.88E-01	3.03E+01
6	6.11E+03	2.50E-01	-1.43E+01	-6.06E+00	8.04E-01	3.02E+01
7	6.04E+03	2.50E-01	-1.40E+01	-6.00E+00	7.91E-01	3.00E+01
8	6.63E+03	2.49E-01	-1.44E+01	-6.07E+00	7.42E-01	3.06E+01
9	6.43E+03	2.49E-01	-1.49E+01	-6.39E+00	7.97E-01	3.07E+01
10	6.10E+03	2.47E-01	-1.39E+01	-6.00E+00	7.99E-01	2.98E+01
11	5.99E+03	2.47E-01	-1.39E+01	-5.94E+00	8.00E-01	2.99E+01
12	5.16E+03	2.44E-01	-1.27E+01	-5.56E+00	8.59E-01	2.83E+01
13	5.68E+03	2.53E-01	-1.44E+01	-6.25E+00	8.42E-01	3.05E+01
14	5.70E+03	2.45E-01	-1.39E+01	-6.12E+00	8.62E-01	2.96E+01
15	5.74E+03	2.51E-01	-1.44E+01	-6.26E+00	8.31E-01	3.06E+01
16	5.93E+03	2.44E-01	-1.39E+01	-5.99E+00	8.28E-01	2.96E+01
17	5.86E+03	2.49E-01	-1.38E+01	-5.95E+00	8.16E-01	2.98E+01
18	5.78E+03	2.51E-01	-1.42E+01	-6.13E+00	8.23E-01	3.02E+01
19	5.45E+03	2.45E-01	-1.39E+01	-6.23E+00	8.67E-01	2.98E+01
20	5.34E+03	2.51E-01	-1.37E+01	-6.02E+00	8.62E-01	2.96E+01
21	6.16E+03	2.53E-01	-1.41E+01	-5.97E+00	8.10E-01	2.98E+01
22	6.13E+03	2.48E-01	-1.42E+01	-6.10E+00	8.00E-01	3.02E+01
23	6.13E+03	2.50E-01	-1.43E+01	-6.11E+00	7.94E-01	3.04E+01
24	6.39E+03	2.40E-01	-1.41E+01	-6.10E+00	8.01E-01	2.99E+01
25	5.68E+03	2.49E-01	-1.35E+01	-5.86E+00	7.78E-01	2.99E+01
26	6.26E+03	2.46E-01	-1.48E+01	-6.38E+00	8.53E-01	3.02E+01
27	5.39E+03	2.52E-01	-1.34E+01	-5.79E+00	8.45E-01	2.92E+01
28	6.02E+03	2.46E-01	-1.41E+01	-6.04E+00	8.28E-01	2.98E+01
29	6.43E+03	2.51E-01	-1.46E+01	-6.25E+00	7.44E-01	3.10E+01
30	6.07E+03	2.51E-01	-1.43E+01	-6.12E+00	8.08E-01	3.03E+01
31	5.49E+03	2.46E-01	-1.32E+01	-5.71E+00	8.47E-01	2.88E+01
32	5.55E+03	2.49E-01	-1.41E+01	-6.18E+00	8.68E-01	2.98E+01
33	6.16E+03	2.44E-01	-1.42E+01	-6.12E+00	8.47E-01	2.96E+01
34	6.16E+03	2.44E-01	-1.37E+01	-5.89E+00	8.17E-01	2.93E+01
35	5.37E+03	2.48E-01	-1.39E+01	-6.19E+00	8.65E-01	2.98E+01
36	6.14E+03	2.42E-01	-1.40E+01	-6.03E+00	8.35E-01	2.95E+01
37	5.78E+03	2.50E-01	-1.36E+01	-5.88E+00	8.15E-01	2.96E+01
38	5.81E+03	2.49E-01	-1.44E+01	-6.30E+00	8.29E-01	3.05E+01
39	5.49E+03	2.44E-01	-1.32E+01	-5.68E+00	8.17E-01	2.91E+01
40	6.23E+03	2.50E-01	-1.41E+01	-6.05E+00	7.55E-01	3.05E+01

41	6.24E+03	2.48E-01	-1.47E+01	-6.37E+00	8.24E-01	3.05E+01
42	6.14E+03	2.50E-01	-1.36E+01	-5.79E+00	7.89E-01	2.94E+01
43	6.78E+03	2.55E-01	-1.48E+01	-6.18E+00	7.18E-01	3.13E+01
44	5.74E+03	2.56E-01	-1.43E+01	-6.12E+00	8.14E-01	3.05E+01
45	6.32E+03	2.47E-01	-1.46E+01	-6.29E+00	8.14E-01	3.02E+01
46	6.29E+03	2.53E-01	-1.41E+01	-5.98E+00	7.33E-01	3.06E+01
47	6.51E+03	2.45E-01	-1.36E+01	-5.78E+00	8.33E-01	2.86E+01
48	6.36E+03	2.43E-01	-1.42E+01	-6.07E+00	7.84E-01	3.00E+01
49	6.08E+03	2.44E-01	-1.44E+01	-6.23E+00	8.15E-01	3.01E+01
50	6.07E+03	2.53E-01	-1.40E+01	-5.95E+00	8.24E-01	2.98E+01
51	6.34E+03	2.50E-01	-1.43E+01	-6.10E+00	7.47E-01	3.07E+01
52	6.23E+03	2.45E-01	-1.39E+01	-5.96E+00	7.73E-01	3.00E+01
53	5.42E+03	2.47E-01	-1.34E+01	-5.91E+00	8.14E-01	2.96E+01
54	5.94E+03	2.44E-01	-1.38E+01	-5.96E+00	8.18E-01	2.96E+01
55	5.10E+03	2.48E-01	-1.30E+01	-5.62E+00	8.71E-01	2.86E+01
56	6.25E+03	2.55E-01	-1.47E+01	-6.22E+00	8.08E-01	3.07E+01
57	5.23E+03	2.46E-01	-1.33E+01	-5.90E+00	8.40E-01	2.94E+01
58	5.67E+03	2.51E-01	-1.35E+01	-5.82E+00	8.16E-01	2.96E+01
59	5.57E+03	2.43E-01	-1.38E+01	-6.07E+00	8.46E-01	2.95E+01
60	5.81E+03	2.51E-01	-1.40E+01	-6.03E+00	8.08E-01	3.00E+01

Table 14: Results from back-analysis of the deep seated tunnel problem using the Differential Evolution. The primary array of trial 2 at 70 generations is shown

Individual	E (MPa)	v	σ_y (MPa)	σ_x (MPa)	c (MPa)	ϕ (^{o})
1	6.43E+03	2.48E-01	-1.41E+01	-6.03E+00	7.49E-01	3.04E+01
2	6.03E+03	2.46E-01	-1.40E+01	-6.04E+00	8.00E-01	2.99E+01
3	5.33E+03	2.53E-01	-1.35E+01	-5.83E+00	8.29E-01	2.96E+01
4	6.40E+03	2.46E-01	-1.49E+01	-6.42E+00	8.00E-01	3.08E+01
5	6.60E+03	2.42E-01	-1.43E+01	-6.13E+00	7.71E-01	3.02E+01
6	5.91E+03	2.49E-01	-1.35E+01	-5.79E+00	7.72E-01	2.97E+01
7	5.54E+03	2.53E-01	-1.34E+01	-5.73E+00	8.08E-01	2.95E+01
8	5.72E+03	2.51E-01	-1.39E+01	-5.98E+00	8.17E-01	2.99E+01
9	5.81E+03	2.46E-01	-1.37E+01	-5.94E+00	8.07E-01	2.97E+01
10	6.00E+03	2.45E-01	-1.39E+01	-6.00E+00	7.94E-01	2.98E+01
11	6.88E+03	2.42E-01	-1.48E+01	-6.29E+00	7.79E-01	3.04E+01
12	5.66E+03	2.51E-01	-1.35E+01	-5.84E+00	7.85E-01	2.98E+01
13	6.54E+03	2.48E-01	-1.46E+01	-6.25E+00	7.84E-01	3.05E+01
14	6.09E+03	2.47E-01	-1.40E+01	-6.03E+00	7.74E-01	3.03E+01
15	6.39E+03	2.55E-01	-1.44E+01	-6.04E+00	7.43E-01	3.08E+01
16	5.81E+03	2.53E-01	-1.41E+01	-6.03E+00	8.01E-01	3.03E+01
17	5.79E+03	2.50E-01	-1.38E+01	-5.93E+00	8.00E-01	2.99E+01
18	5.14E+03	2.55E-01	-1.28E+01	-5.50E+00	8.26E-01	2.89E+01
19	6.14E+03	2.48E-01	-1.43E+01	-6.15E+00	8.02E-01	3.02E+01
20	6.11E+03	2.51E-01	-1.43E+01	-6.12E+00	7.97E-01	3.03E+01
21	6.37E+03	2.45E-01	-1.44E+01	-6.19E+00	7.98E-01	3.02E+01
22	6.23E+03	2.50E-01	-1.45E+01	-6.20E+00	7.95E-01	3.05E+01
23	6.36E+03	2.50E-01	-1.45E+01	-6.20E+00	7.79E-01	3.06E+01
24	6.34E+03	2.43E-01	-1.45E+01	-6.23E+00	7.96E-01	3.03E+01
25	5.98E+03	2.47E-01	-1.37E+01	-5.88E+00	7.88E-01	2.97E+01
26	6.30E+03	2.44E-01	-1.46E+01	-6.30E+00	8.16E-01	3.03E+01
27	6.29E+03	2.51E-01	-1.44E+01	-6.10E+00	7.62E-01	3.06E+01
28	6.71E+03	2.44E-01	-1.44E+01	-6.12E+00	7.82E-01	3.00E+01
29	5.98E+03	2.47E-01	-1.39E+01	-5.96E+00	7.87E-01	2.99E+01
30	6.03E+03	2.49E-01	-1.43E+01	-6.19E+00	8.20E-01	3.02E+01
31	5.81E+03	2.50E-01	-1.39E+01	-6.00E+00	8.17E-01	2.99E+01
32	6.02E+03	2.54E-01	-1.42E+01	-6.04E+00	7.93E-01	3.02E+01
33	6.11E+03	2.52E-01	-1.43E+01	-6.09E+00	7.80E-01	3.05E+01
34	6.44E+03	2.49E-01	-1.44E+01	-6.10E+00	7.41E-01	3.07E+01
35	6.15E+03	2.46E-01	-1.38E+01	-5.95E+00	7.64E-01	3.00E+01
36	6.07E+03	2.47E-01	-1.44E+01	-6.22E+00	8.20E-01	3.02E+01
37	5.71E+03	2.52E-01	-1.37E+01	-5.89E+00	8.02E-01	2.99E+01
38	6.40E+03	2.48E-01	-1.44E+01	-6.11E+00	7.89E-01	3.02E+01
39	6.19E+03	2.53E-01	-1.43E+01	-6.04E+00	7.80E-01	3.04E+01
40	6.56E+03	2.45E-01	-1.46E+01	-6.25E+00	7.64E-01	3.06E+01
41	5.85E+03	2.53E-01	-1.41E+01	-6.04E+00	7.86E-01	3.04E+01
42	5.99E+03	2.46E-01	-1.42E+01	-6.17E+00	8.24E-01	3.00E+01
43	5.99E+03	2.50E-01	-1.41E+01	-6.03E+00	8.27E-01	2.98E+01
44	6.28E+03	2.53E-01	-1.40E+01	-5.96E+00	7.35E-01	3.05E+01

45	5.97E+03	2.48E-01	-1.43E+01	-6.18E+00	8.23E-01	3.02E+01
46	6.13E+03	2.50E-01	-1.47E+01	-6.33E+00	8.00E-01	3.07E+01
47	6.15E+03	2.48E-01	-1.46E+01	-6.29E+00	8.21E-01	3.04E+01
48	5.83E+03	2.47E-01	-1.42E+01	-6.16E+00	8.31E-01	3.00E+01
49	6.61E+03	2.51E-01	-1.45E+01	-6.15E+00	7.59E-01	3.06E+01
50	6.10E+03	2.46E-01	-1.44E+01	-6.22E+00	8.11E-01	3.02E+01
51	5.56E+03	2.51E-01	-1.33E+01	-5.72E+00	8.17E-01	2.94E+01
52	5.62E+03	2.55E-01	-1.37E+01	-5.86E+00	7.93E-01	3.00E+01
53	6.38E+03	2.45E-01	-1.44E+01	-6.17E+00	7.81E-01	3.03E+01
54	5.58E+03	2.53E-01	-1.38E+01	-5.91E+00	8.08E-01	2.99E+01
55	6.10E+03	2.46E-01	-1.40E+01	-6.04E+00	8.13E-01	2.97E+01
56	6.56E+03	2.46E-01	-1.46E+01	-6.24E+00	7.80E-01	3.05E+01
57	6.08E+03	2.52E-01	-1.38E+01	-5.87E+00	7.51E-01	3.02E+01
58	6.50E+03	2.51E-01	-1.43E+01	-6.05E+00	7.30E-01	3.08E+01
59	5.59E+03	2.49E-01	-1.35E+01	-5.85E+00	8.13E-01	2.96E+01
60	5.98E+03	2.49E-01	-1.41E+01	-6.03E+00	8.05E-01	3.00E+01

Table 15: Results from back-analysis of the deep seated tunnel problem using the Differential Evolution. The primary array of trial 3 at 70 generations is shown.

Individual	E (MPa)	v	σ_y (MPa)	σ_x (MPa)	c (MPa)	ϕ (^{o})
1	5.73E+03	2.54E-01	-1.37E+01	-5.85E+00	7.99E-01	2.99E+01
2	5.83E+03	2.55E-01	-1.36E+01	-5.76E+00	7.84E-01	2.99E+01
3	6.87E+03	2.49E-01	-1.46E+01	-6.17E+00	7.40E-01	3.08E+01
4	6.21E+03	2.56E-01	-1.41E+01	-5.92E+00	7.69E-01	3.03E+01
5	6.05E+03	2.50E-01	-1.40E+01	-5.98E+00	8.14E-01	2.98E+01
6	5.58E+03	2.55E-01	-1.31E+01	-5.58E+00	8.09E-01	2.90E+01
7	6.59E+03	2.53E-01	-1.47E+01	-6.23E+00	7.03E-01	3.14E+01
8	6.44E+03	2.51E-01	-1.48E+01	-6.28E+00	7.96E-01	3.06E+01
9	6.28E+03	2.49E-01	-1.44E+01	-6.16E+00	7.99E-01	3.03E+01
10	5.94E+03	2.52E-01	-1.41E+01	-6.02E+00	8.08E-01	3.00E+01
11	5.90E+03	2.53E-01	-1.39E+01	-5.91E+00	7.86E-01	3.01E+01
12	5.39E+03	2.46E-01	-1.36E+01	-5.95E+00	8.76E-01	2.92E+01
13	6.02E+03	2.52E-01	-1.41E+01	-6.05E+00	8.03E-01	3.01E+01
14	6.46E+03	2.54E-01	-1.45E+01	-6.12E+00	7.51E-01	3.08E+01
15	5.94E+03	2.53E-01	-1.41E+01	-6.03E+00	8.16E-01	3.01E+01
16	6.76E+03	2.37E-01	-1.47E+01	-6.32E+00	8.06E-01	3.01E+01
17	5.67E+03	2.49E-01	-1.39E+01	-6.04E+00	8.17E-01	2.99E+01
18	6.12E+03	2.51E-01	-1.40E+01	-5.99E+00	7.57E-01	3.03E+01
19	6.37E+03	2.46E-01	-1.44E+01	-6.16E+00	7.88E-01	3.03E+01
20	5.64E+03	2.50E-01	-1.35E+01	-5.86E+00	7.89E-01	2.99E+01
21	6.31E+03	2.51E-01	-1.43E+01	-6.08E+00	7.79E-01	3.04E+01
22	6.01E+03	2.53E-01	-1.43E+01	-6.14E+00	7.94E-01	3.04E+01
23	6.19E+03	2.48E-01	-1.37E+01	-5.86E+00	7.77E-01	2.99E+01
24	5.25E+03	2.52E-01	-1.31E+01	-5.66E+00	8.57E-01	2.88E+01
25	5.67E+03	2.52E-01	-1.36E+01	-5.81E+00	8.35E-01	2.94E+01
26	5.29E+03	2.50E-01	-1.36E+01	-5.90E+00	8.49E-01	2.95E+01
27	6.19E+03	2.46E-01	-1.36E+01	-5.78E+00	7.74E-01	2.96E+01
28	6.35E+03	2.51E-01	-1.49E+01	-6.40E+00	7.94E-01	3.09E+01
29	5.80E+03	2.45E-01	-1.36E+01	-5.91E+00	8.38E-01	2.93E+01
30	5.85E+03	2.51E-01	-1.38E+01	-5.92E+00	7.73E-01	3.01E+01
31	5.53E+03	2.45E-01	-1.31E+01	-5.65E+00	8.25E-01	2.88E+01
32	6.17E+03	2.48E-01	-1.45E+01	-6.22E+00	8.21E-01	3.02E+01
33	5.60E+03	2.52E-01	-1.35E+01	-5.80E+00	7.83E-01	2.99E+01
34	6.02E+03	2.52E-01	-1.39E+01	-5.94E+00	8.17E-01	2.97E+01
35	6.08E+03	2.50E-01	-1.41E+01	-6.03E+00	7.72E-01	3.02E+01
36	6.27E+03	2.55E-01	-1.44E+01	-6.11E+00	7.56E-01	3.07E+01
37	5.32E+03	2.52E-01	-1.30E+01	-5.59E+00	8.34E-01	2.90E+01
38	5.16E+03	2.51E-01	-1.32E+01	-5.73E+00	8.46E-01	2.92E+01
39	7.20E+03	2.37E-01	-1.50E+01	-6.41E+00	7.63E-01	3.06E+01
40	6.31E+03	2.51E-01	-1.45E+01	-6.18E+00	7.49E-01	3.09E+01
41	6.11E+03	2.48E-01	-1.45E+01	-6.27E+00	8.20E-01	3.03E+01
42	5.64E+03	2.41E-01	-1.36E+01	-5.95E+00	8.61E-01	2.91E+01
43	5.60E+03	2.45E-01	-1.37E+01	-5.96E+00	8.49E-01	2.93E+01
44	5.39E+03	2.47E-01	-1.30E+01	-5.66E+00	7.93E-01	2.93E+01

45	6.36E+03	2.53E-01	-1.45E+01	-6.13E+00	7.84E-01	3.04E+01
46	5.79E+03	2.46E-01	-1.37E+01	-5.94E+00	8.33E-01	2.95E+01
47	5.57E+03	2.43E-01	-1.35E+01	-5.90E+00	8.45E-01	2.92E+01
48	5.35E+03	2.49E-01	-1.32E+01	-5.72E+00	8.54E-01	2.91E+01
49	5.83E+03	2.44E-01	-1.38E+01	-5.99E+00	8.41E-01	2.94E+01
50	5.43E+03	2.46E-01	-1.30E+01	-5.61E+00	8.14E-01	2.89E+01
51	5.71E+03	2.56E-01	-1.29E+01	-5.46E+00	7.97E-01	2.89E+01
52	6.10E+03	2.51E-01	-1.36E+01	-5.79E+00	7.75E-01	2.96E+01
53	6.37E+03	2.49E-01	-1.46E+01	-6.21E+00	7.82E-01	3.06E+01
54	5.06E+03	2.50E-01	-1.34E+01	-5.83E+00	8.88E-01	2.90E+01
55	6.25E+03	2.47E-01	-1.42E+01	-6.09E+00	7.97E-01	3.01E+01
56	5.92E+03	2.54E-01	-1.35E+01	-5.74E+00	7.85E-01	2.96E+01
57	6.81E+03	2.50E-01	-1.47E+01	-6.19E+00	7.37E-01	3.09E+01
58	5.50E+03	2.49E-01	-1.37E+01	-5.99E+00	8.43E-01	2.96E+01
59	6.29E+03	2.50E-01	-1.49E+01	-6.40E+00	8.08E-01	3.07E+01
60	5.95E+03	2.49E-01	-1.41E+01	-6.07E+00	7.82E-01	3.03E+01

8.4. Case of a shallow circular tunnel in plastic ground

The performance of the Differential Evolution algorithm was investigated by performing back-analysis of the shallow tunnel problem described in section 7.5. Again all conditions are kept equal in order to compare the solutions. In this case the objective function to be minimized is better defined and with fewer local optima since measurements commence prior to the excavation. This is reflected by the excellent converged solution shown in the results of Table 16. All the individuals of the primary array have practically converged to the same optimal vector which is the global minimum solution. This performance along with the ability to perform the back-analysis using a widely available commercial program makes the method ideal for back-analysis purposes.

Table 16: Back-analysis results of shallow tunnel problem using the Differential Evolution algorithm. Results at 70 generations.

Individual	E (kPa)	K_o	c (MPa)	ϕ (°)
1	2.96E+04	5.01E-01	7.41E+00	2.49E+01
2	3.02E+04	5.01E-01	7.74E+00	2.47E+01
3	3.00E+04	5.02E-01	7.48E+00	2.48E+01
4	3.05E+04	4.98E-01	9.24E+00	2.46E+01
5	2.98E+04	5.01E-01	7.73E+00	2.47E+01
6	3.00E+04	4.98E-01	8.02E+00	2.49E+01
7	3.04E+04	5.01E-01	8.35E+00	2.46E+01
8	2.95E+04	4.97E-01	8.11E+00	2.50E+01
9	2.97E+04	5.00E-01	7.30E+00	2.49E+01
10	3.03E+04	5.00E-01	8.07E+00	2.47E+01
11	3.03E+04	5.01E-01	7.89E+00	2.47E+01
12	3.04E+04	5.02E-01	7.76E+00	2.47E+01
13	3.01E+04	5.00E-01	8.06E+00	2.47E+01
14	3.02E+04	4.99E-01	8.42E+00	2.47E+01
15	3.03E+04	4.98E-01	8.71E+00	2.47E+01
16	3.06E+04	5.03E-01	8.24E+00	2.45E+01
17	2.99E+04	4.98E-01	7.72E+00	2.50E+01
18	3.01E+04	5.02E-01	7.68E+00	2.47E+01
19	2.97E+04	4.97E-01	8.01E+00	2.50E+01
20	2.97E+04	5.00E-01	7.39E+00	2.49E+01
21	3.02E+04	5.02E-01	7.32E+00	2.48E+01
22	3.05E+04	5.00E-01	8.63E+00	2.46E+01
23	2.98E+04	4.99E-01	7.53E+00	2.49E+01
24	3.04E+04	5.04E-01	8.10E+00	2.44E+01
25	2.95E+04	5.00E-01	7.15E+00	2.50E+01
26	3.08E+04	5.03E-01	8.28E+00	2.44E+01
27	3.07E+04	5.00E-01	9.24E+00	2.44E+01
28	3.07E+04	4.96E-01	9.90E+00	2.45E+01
29	3.02E+04	4.99E-01	7.68E+00	2.49E+01
30	3.01E+04	5.03E-01	6.90E+00	2.48E+01
31	3.03E+04	5.00E-01	8.26E+00	2.47E+01
32	3.00E+04	5.00E-01	7.66E+00	2.49E+01
33	3.02E+04	5.00E-01	7.95E+00	2.48E+01
34	3.00E+04	5.01E-01	7.74E+00	2.48E+01
35	3.03E+04	5.00E-01	8.08E+00	2.47E+01
36	3.02E+04	5.00E-01	8.10E+00	2.47E+01
37	3.02E+04	5.02E-01	7.65E+00	2.46E+01
38	3.00E+04	5.00E-01	7.74E+00	2.48E+01
39	3.06E+04	5.00E-01	8.57E+00	2.46E+01
40	3.01E+04	5.01E-01	7.75E+00	2.48E+01

8.5. Conclusions

In this chapter the novel use of a Genetic Algorithm type is introduced for back-analysis of tunneling induced displacements. The Differential Evolution algorithm of Storn and Price (1997) is a heuristic type of global optimization algorithm which shows very good convergence properties and efficiency. It is perhaps the only algorithm comparable to the heuristic features of the Simulated Annealing method of global optimization. It has been seen that when plane strain approximations are used in conjunction with relative displacement monitoring, then the objective function to be minimized will by characterized by multiple local minima and therefore the performance of a local search algorithm is questionable. The DE algorithm is more efficient than the standard form of Simulated Annealing and requires less computational effort. The implementation of the method in FLAC via the FISH programming language is also appealing. It was also seen that the method shares some of the population-driven logic of the Simplex and Complex methods. In fact the population used by the DE algorithm is directly comparable to the Complex vertices.

The method has shown, via two different but frequently encountered tunneling problems that it is able to respond well to the challenge. The global search strategy is also very appealing. However due to the population-based nature, the method becomes almost deterministic from a global optimization standpoint. If reasonable crossover and mutation parameters are used it has a high chance of finding the global optimum, provided that there is one. This may cause some implications when there is noise in the monitoring data due to the uncertainties and reliability issues with their performance, installation etc. as discussed in chapter 3. This error theoretically affects the shape of the objective function. Considering the precision tolerance of FLAC or any other finite element or finite difference program, this could mean that if some noise is introduced then the global minimum could also change position. It also possible, that depending on this error, the global minimum could be balancing between a few but strong local minima which could be quite apart in some cases. In that case the Simulated Annealing algorithm posses a significant advantage. The ability to scan these minima with strong regions of attraction and inform the analyst of their existence, based on the scanning history.

CHAPTER 9. Case study of the Heshang highway tunnel in China

9.1. General geology and preliminary data

The Heshang highway tunnel is located in South East China at the Fujian province, about 5km southeast of the Fuzhou city. It will serve as part of the transportation system between the local airport and Fuzhou city. It is a twin tunnel project with and it is approximately 450 m long. The tunnel passes through highly weathered old volcanic material. The tunnel construction was completed on August 30, 2006. Despite the short length, during construction of the twin tunnel, instrumentation was used to assess the performance of the excavation. Due to the poor quality of the surrounding rock mass, and also due to the lateral proximity of the two tunnels, numerous ground stabilization techniques as well as a wide array of instrumentation methods were employed. Towards the Northwest portal the tunnel penetrates through weathered tuff lavas and residual loam. In the central section, the majority of the rock mass is weathered tuff lava while at the Southeast portal the quality drops again, with moderate and highly weathered tuff lava. Figure 39 presents the longitudinal geologic section along the tunnel route.

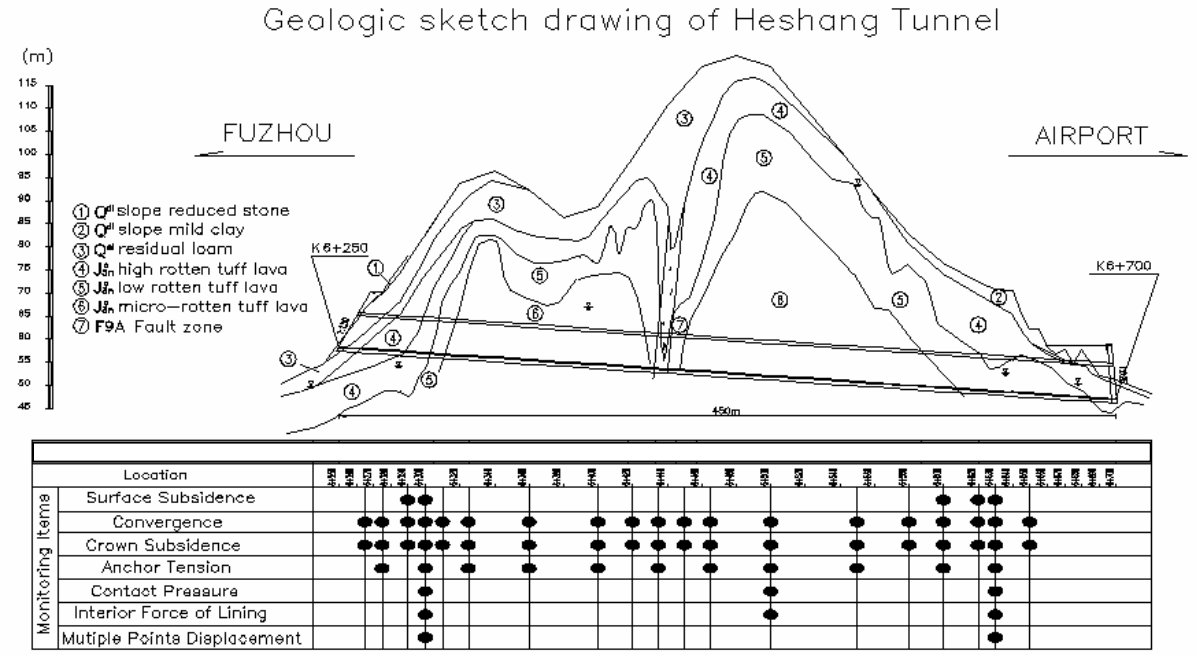

Figure 39: Geologic section of the Heshang tunnel in China.

Typical geotechnical properties of the various rock quality grades of the general geologic region were available from preliminary geological studies and are shown in Table 17. The tunnel passes mostly through rock grades III-VI. At the portal sections the quality is very low and corresponds to grades V-VI.

Table 17: Typical properties per rock grade of the Heshang tunnel.

Rock grade	E (GPa)	μ	γ (kN/m^3)	c (MPa)	φ (º)
I	>33	<0.2	26~28	>2.1	>60
II	20~33	0.2~0.25	25~27	1.5~2.1	50~60
III	6~20	0.25~0.30	23~25	0.7~1.5	39~50
IV	1.3~6	0.3~0.35	20~23	0.2~0.7	27~39
V	1~2	0.35~0.45	17~20	0.05~0.2	20~27
VI	<1	0.4~0. 5	17~17	<0.2	<20

9.2. Tunnel design and monitoring data

9.2.1. Tunnel design

The sequential excavation of the Heshang tunnel was designed in accordance to anticipated ground conditions and excavation sequence varied between the two tunnels. During construction three sections were fully instrumented. Such instrumentation included surface subsidence, convergence measurements, crown subsidence by surveying, anchor tensioning, lining axial and radial pressure, as well as multipoint extensometer measurements. The locations of the three fully instrumented sections are shown in Table 18 along with the corresponding estimates of the rock mass grade. For the back-analysis presented here later, section K6+300 was examined. The goal of the back-analysis is to validate the prior design assumptions and improve prior estimate for forward modeling of subsequent excavations (e.g., experience from the behavior from one portal region can be applied to predictions during excavation of the other portal).

Table 18: Rock mass grade for three instrumented sections.

NO.	Section	Rock grade
1	K6+300	V
2	K6+500	III
3	K6+630	V
		VI

For section K6+300 the sequential excavation pattern is shown in Figure 40. In order to simplify the back-analysis, only monitoring data from the left tunnel are considered since the right tunnel had not yet been advanced to the degree that it will influence the left tunnel. The multi-staged excavation of the left tunnel is a typical sequential type, with two side drifts, a top and a bottom core. The right tunnel is excavated by a top heading, two bench sections and followed by an invert. The tunnels are approximately 11.5 m. high by 15.0 m. wide.

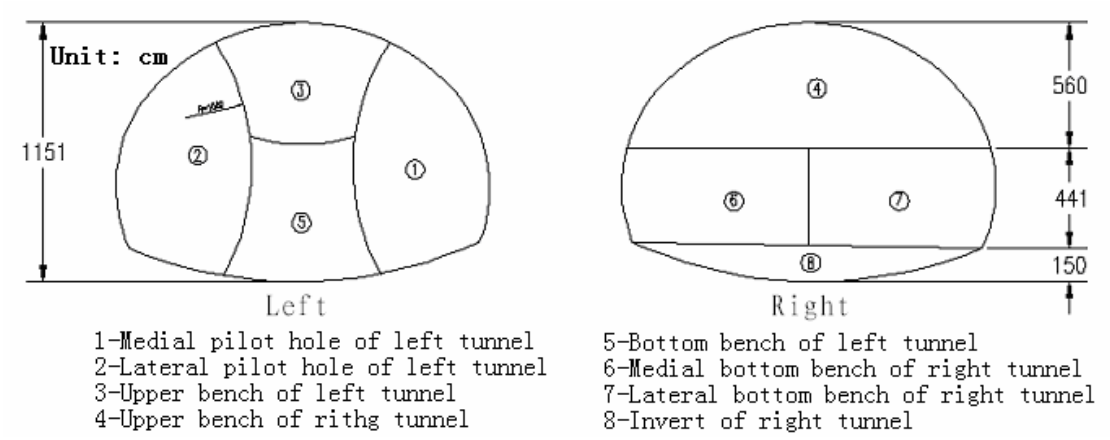

Figure 40: Construction sequence pattern at station K6+300. The rock mass quality corresponds to grade V in both right tunnel and left tunnel.

A variety of primary support systems and ground improvement techniques was used at the Heshang tunnel. More specifically, the ground around the tunnel is reinforced before the excavation using a sequential forepoling umbrella. The reinforcement is composed of 50 mm diameter steel pipes of 5.0 mm thickness and 5.0 m length. These

are installed at two alternating angles of 15° and 40° relative to the tunnel axis. The circular interval of the pipes is 300 mm and the longitudinal spacing is 2.5 m.

Forepoling was also used for the intermediate rock wall between the two tunnels. The details of the forepoling umbrella are shown in the parallel to the tunnel longitudinal cross section of Figure 41 and the perpendicular cross section of Figure 42. The forepoling system included concrete injection through the pile elements.

The primary support system consisted of 270 mm thick shotcrete. The shotcrete was reinforced with a steel mesh of 6 mm diameter bar using a 200 mm x 200 mm grid. U type steel beams were installed at every 0.5 m. The tunnel walls and roof were also reinforced with hollow rock bolts of 25 mm outside diameter and 4.0 m length. The bolts were installed at a 0.8 m x 0.8 m grid. The secondary (final lining) composed of reinforced impermeable concrete lining of 550 mm thickness. Details of the rock bolt arrangement and the steel beam section are given in Figure 43 and Figure 44 respectively.

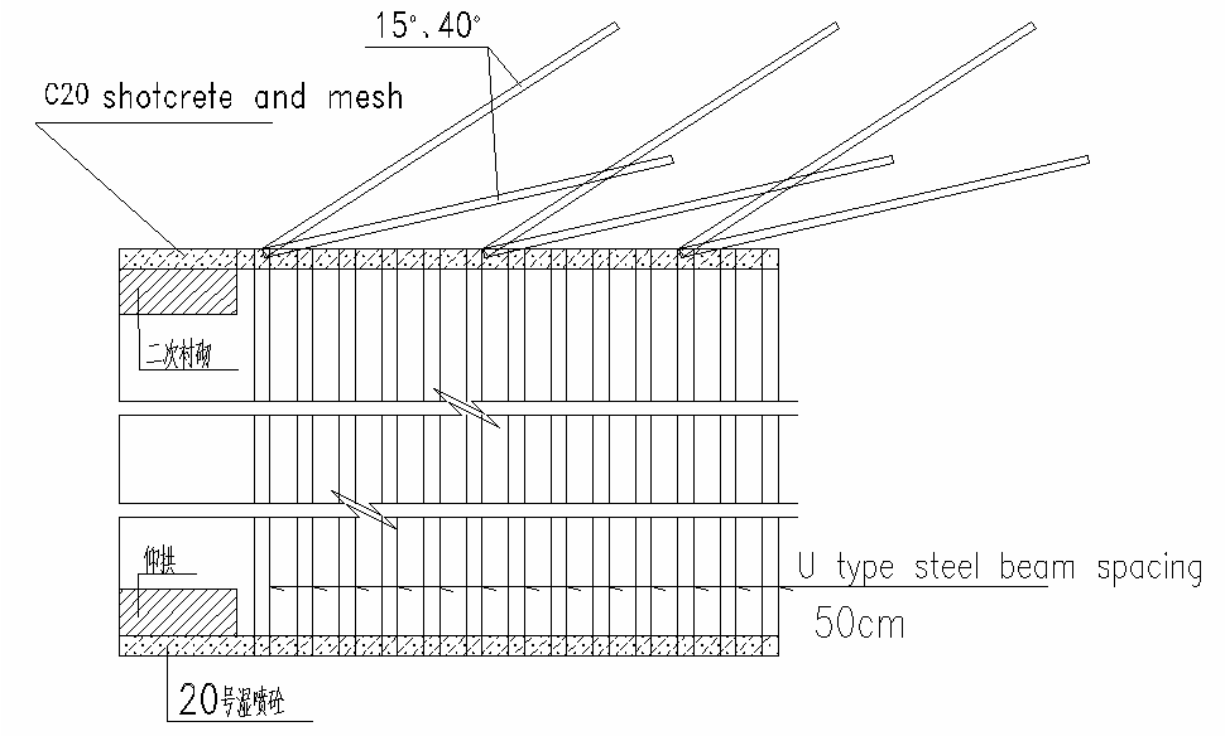

Figure 41: Detailed longitudinal cross section of the forepoling umbrella.

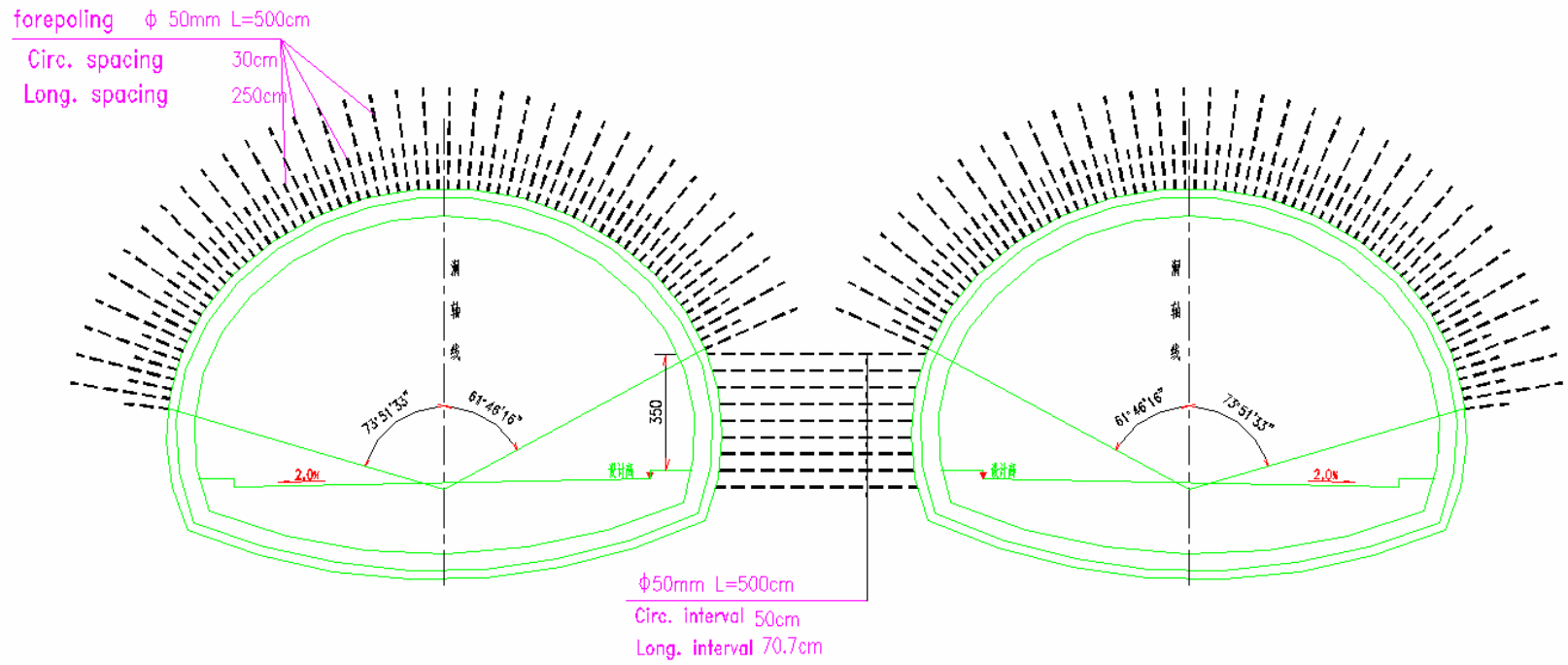

Figure 42: Cross section view of the ground improvement work around the tunnels

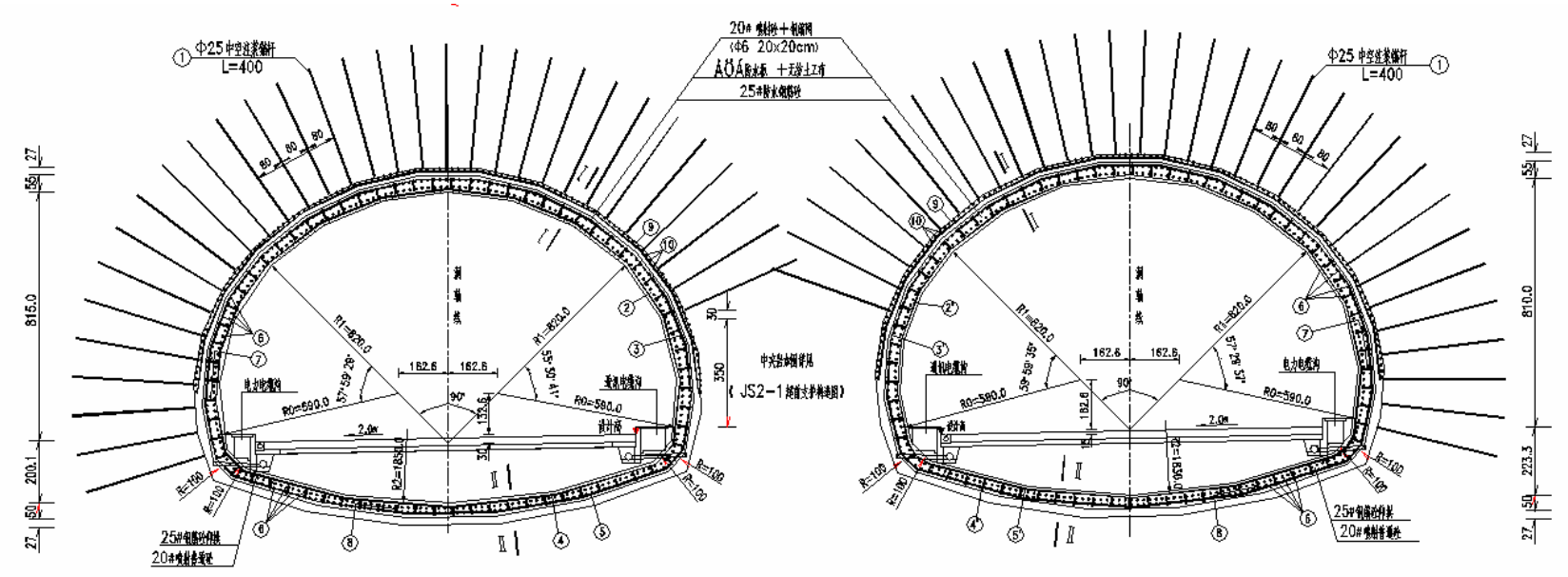

Figure 43: Location of rock bolt reinforcement around the tunnels.

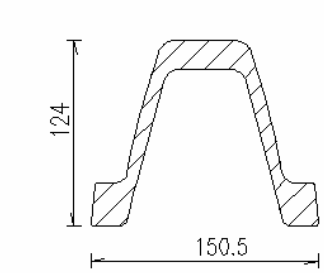

Figure 44: Steel beam cross section dimensions.

9.2.2. Excavation monitoring

The back-analysis for the left tunnel at section K6+300 was performed using deformation data. These included surface subsidence measurements and multipoint extensometer data. Vertical displacements were monitored at points P1-P8 shown in Figure 45. The surface settlement data are shown in Figure 46.

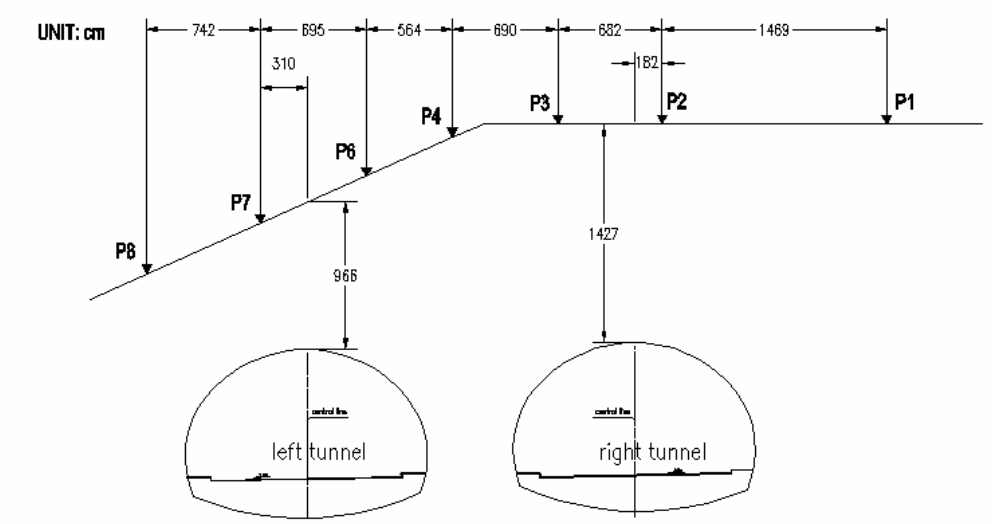

Figure 45: Layout of surface subsidence monitoring points in Heshang tunnel at station K6+300.

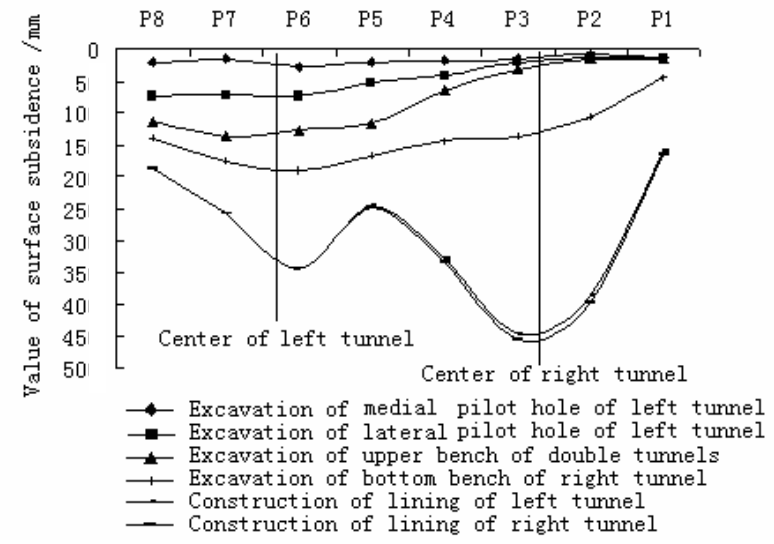

Figure 46: Surface settlement data.

For the left tunnel, data from extensometers KO1 and KO2, were utilized in the back-analysis. The locations of the extensometers are shown in Figure 47. Figures 48 and 49 depict the data from the multipoint extensometers KO1 and KO2. For the back-analysis, data from two different stages of the construction were used. The first set was taken after the end the right drift tunnel was excavated and some additional deformation has occurred because of the advancement of the left drift tunnel. This is represented by point B in Figures 48 and 49 which designates the start of the excavation of the left drift tunnel (some pre-deformation due to this stage has already occurred). The second measurement set was assumed after the excavation and support equilibrium of the top core of the same tunnel. By this time the right tunnel had not reached or influenced the monitored section. This is represented by point D in the above figures. The same construction stages are represented by the second and fourth settlement curves from the top, of Figure 46.

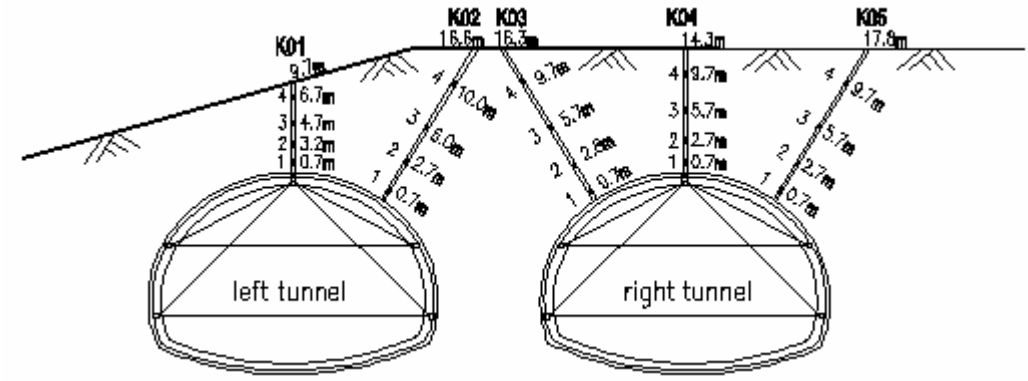

Figure 47: Layout of multiple point extensometers in Heshang tunnel at station K6 + 300.

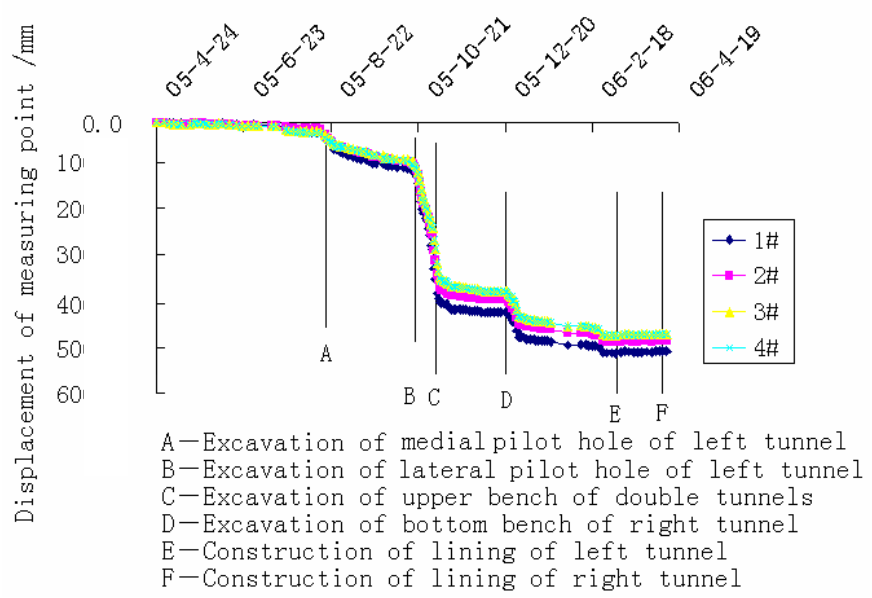

Figure 48: Curves of multiple point extensometer data with time in borehole K01 at station K6 + 300.

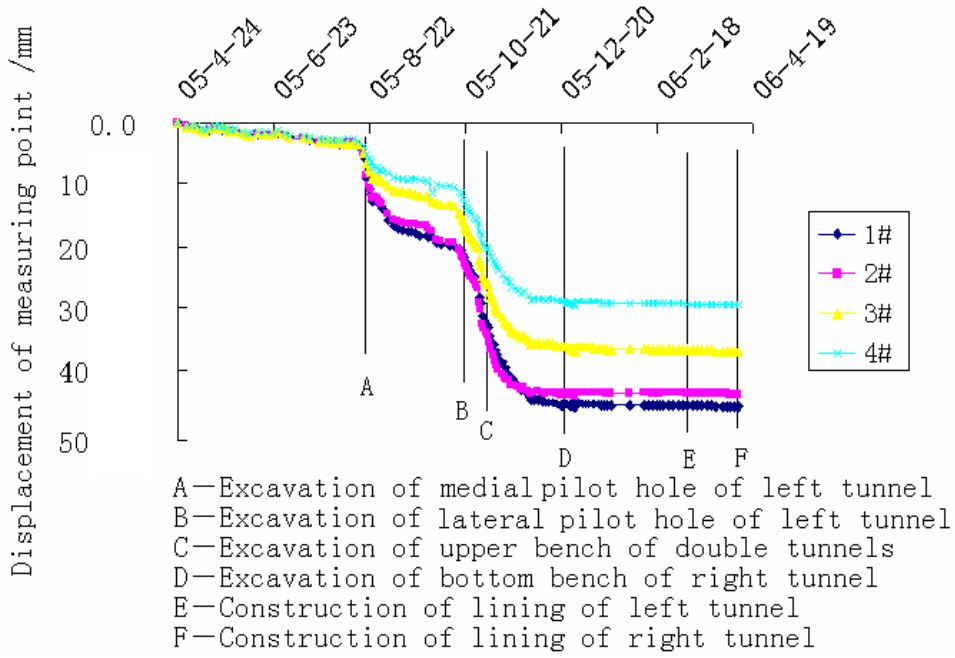

Figure 49: Curves of multiple point extensometer data with time in borehole K02 at station K6 + 300.

9.3. Back-analysis of the Heshang tunnel

9.3.1. Modeling setup

A model extending 80 m. laterally and approximately 40 m high was designed in FLAC. The model is shown in Figure 50. The region around the tunnel is refined in order to better simulate a possible plastic zone. Certain gridpoints where measurements take place were located to conform to the actual monitoring points of the construction. The Mohr-Coulomb failure criterion is assumed for the ground and the forepoling elements. The forepoling umbrella is simulated using finite difference zones, instead of using structural elements. The equivalent forepoling properties are calculated using a simple homogenization scheme described later. The unknowns are the elastic properties, the strength parameters c, ϕ and the average unit weight of the rock. The numerical simulation steps are the following:

1. At the start of every iteration, the model is reset to its initial state. All deformations, velocities and stresses are reset to zero. Any previously installed support elements (liner and cables) are deleted. Any previous null excavation zones or forepoling zones are re-assigned new ground properties as the rest of the model.
2. A calculation is performed to initialize the stresses in the model since a new unit weight is introduced. After the consolidation stage, the displacements and velocities are reset to zero.
3. The right drift tunnel is let to relax by 30% by gradually relaxing the initial gridpoint forces around the tunnel periphery. This is done to simulate some initial pre-deformation which occurs in the rock mass before the forepoling becomes effective. Should the forepoling have longer pile elements, then this step would be avoided due to the greater pre-excavation supporting effect.
4. The forepoling section of the right tunnel drift is installed by assigning new properties to the corresponding finite difference zones.

5. The right drift tunnel is let to relax by 65% (of the initial forces). This slightly high relaxation is assumed in order to compensate the model for volume loss, the gradual shotcrete hardening and the some deformations that occur in the ground, before the steel beams come in contact with the ground.
6. The primary support system is installed.
7. The tunnel is fully let to relax at 100%.
8. The left drift tunnel is relaxed by 30%.
9. The first set of data at the measurement points is taken via a FISH function.
10. The left section of the forepoling is installed by assigning appropriate properties in the forepoling zones.
11. The left drift tunnel is let to relax by 65%.
12. Primary support is installed at the left drift.
13. The left drift tunnel is let to fully relax until ground-support equilibrium is achieved.
14. The top core is let to relax by 30%.
15. Forepoling is installed at the crown section to complete the forepoling umbrella.
16. The top core is let to relax by 70% due to delays in the support which has to be structurally connected with the beam elements from the left and side drift.
17. The left and right supporting beam sidewalls, enveloping the top core are deleted. Primary support is installed at the roof. The roof lining is structurally connected to the left and right drift lining elements.
18. The top core is let to relax fully
19. The second set of measurements is taken via a FISH function.

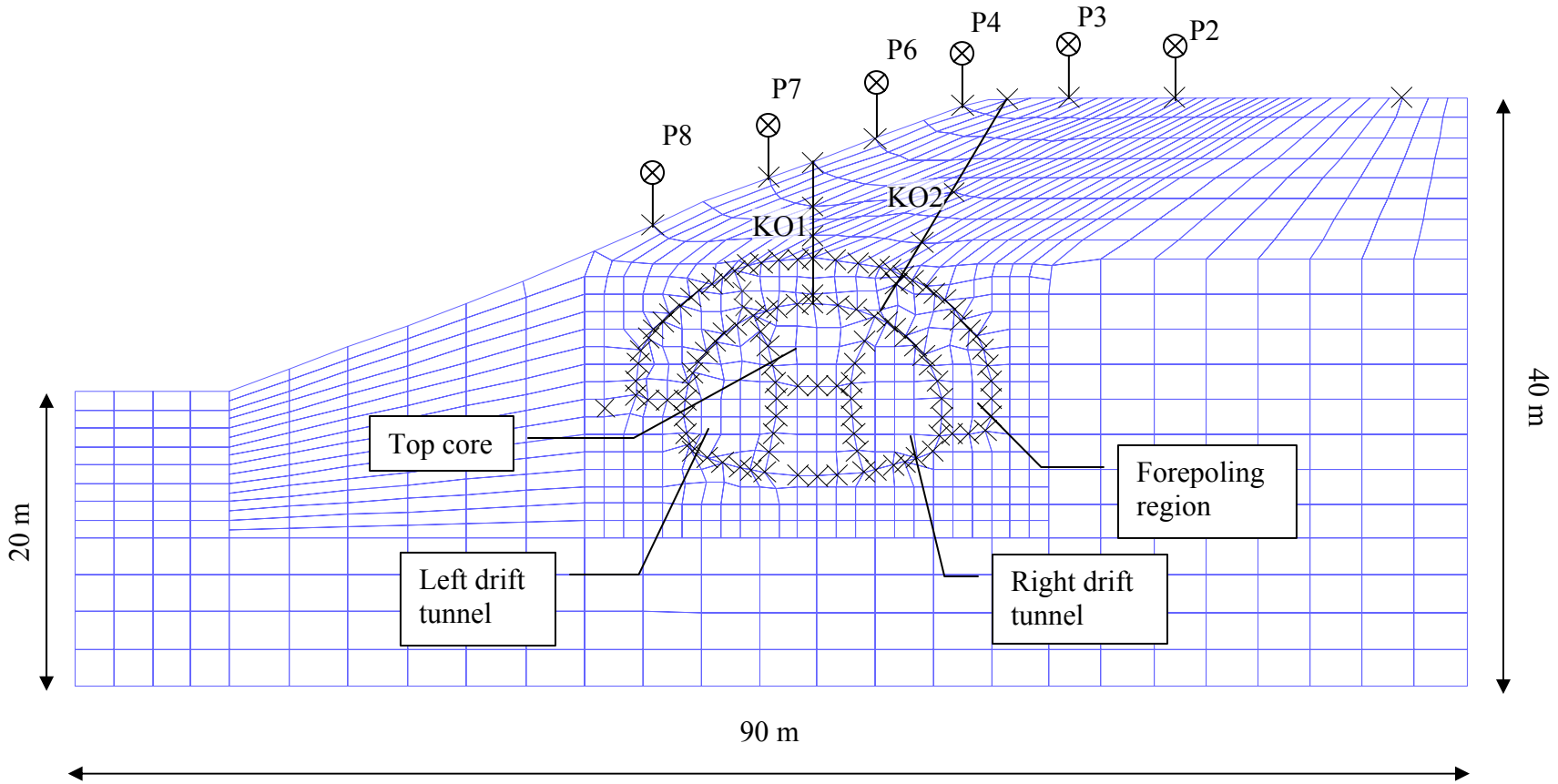

Figure 50: FLAC tunnel model and measurement gridpoint locations.

The above process is assumed to yield a numerical model comparable to the actual construction. Due to the shallow overburden and the poor quality of the rock mass, deformations are expected to be relatively large, which is also evidenced by the monitoring results of Figures 46, 48 and 49.

A simple averaging scheme, suggested by Hoek (2003), was used in order to estimate the properties of the forepoling region. According to this approach, the strength and deformability of the equivalent forepoling material can be estimated using weighted average contributions of the respective hosting rock and reinforcing material quantities, in a unit cross section of the homogenous material. Thus, the uniaxial strength is estimated by summing the products of the strength of each participating material (steel pipe, grout, rock) by their corresponding cross sectional area and by dividing the sum with the total forepoling section area. It was also assumed that the equivalent forepoling properties remain constant during the back-analysis. The later is generally a valid assumption since the reinforced ground has more predictable properties than the native ground. Based on the above, the equivalent forepoling properties, assuming properties for a rock grade V (see Table 17) as the native ground, are estimated as follows:

- γ=24 kN/m^3 (saturated unit weight)
- E=3000 MPa
- v=0.3
- c=4.5 MPa
- ϕ=25°
- Tensile strength = 1.0 MPa

9.3.2. Back-analysis results

Before executing the back-analysis, a preliminary forward analysis was performed, in order to study the performance of the numerical model, using average input properties. The following properties were used:

- γ=18.5 kN/m^3
- E=500 MPa
- v=0.35
- c=0.02 MPa

- ϕ=25°

The main purpose of the preliminary analysis is to overview the performance of the model and to specify constraints for the analysis. By using average properties for the rock mass it is possible to assess to a first degree, how close to the optimum an initial trial based on prior field investigations can be. In the second case, the model's input parameters are perturbed manually, to investigate on the stability of the code under unfavorable parameter combination. This can be used effectively to adjust the parameter constraints, so that even under the most unfavorable combination of stress vs. strength the model will be stable and error free. This ensures a problem-free subsequent execution of the optimization algorithm and generally increases the efficiency of the process.

Figure 51 presents the calculated initial stresses. The stresses are initialized automatically using gravity loading and the boundary conditions. The only parameter essentially affecting this step is the unit weight and the Poisson's ratio (i.e., no lateral deformations) of the rock mass.

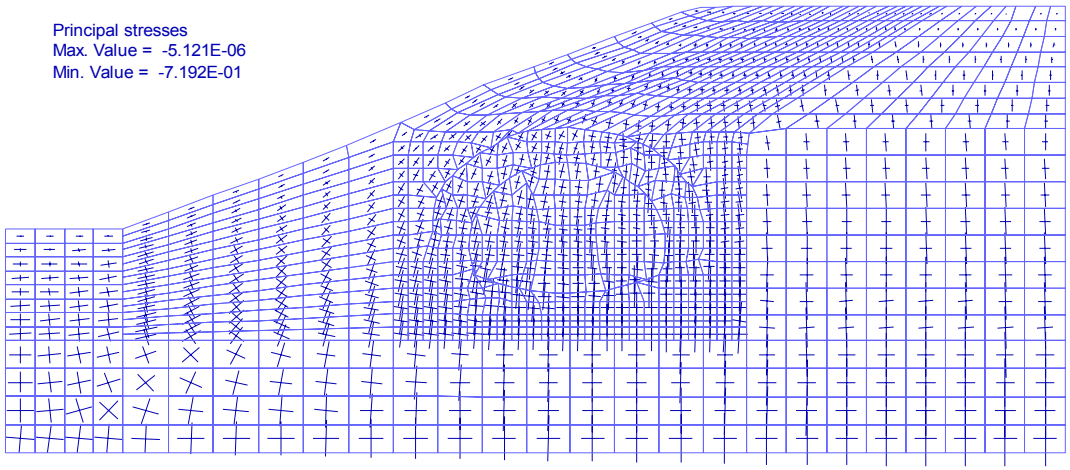

Figure 51: Stress initialization stage for station K6+300 of the Heshang tunnel model.

Figure 52 shows contours the vertical displacements at equilibrium of the right drift tunnel and after 30% relaxation of the left tunnel. The right tunnel drift is supported by its corresponding forepoling region, a continuous closed composite beam and rock bolts. At this time the first set of measurements is taken and stored in memory using a

FISH function in FLAC. Figure 53 shows contours of vertical displacements at full relaxation of the left drift tunnel and after 30% relaxation of the top core. The ground has been improved by the two forepoling regions of the left and right drift and the third region (roof) will be installed at the next step. The left drift is supported by rock bolts and a continuous closed composite beam.

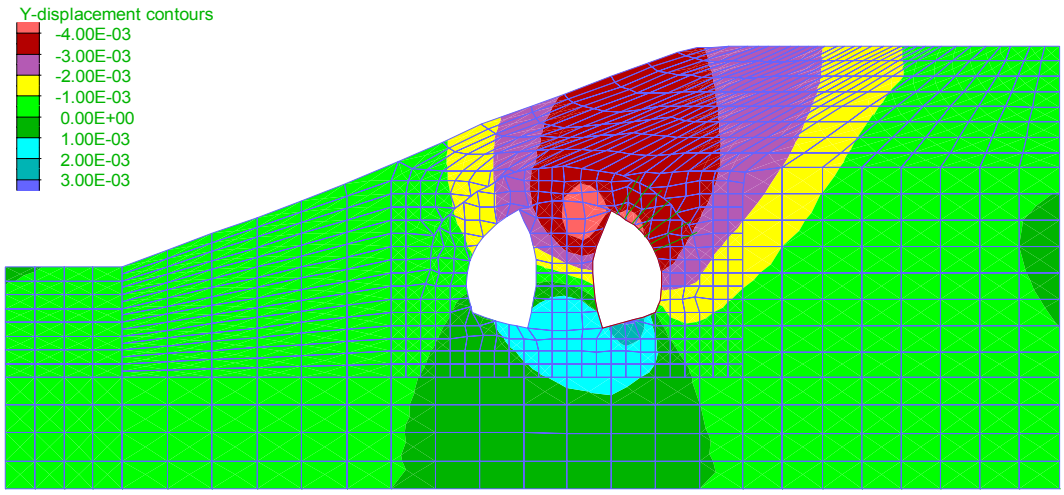

Figure 52: Vertical displacements at equilibrium of right drift tunnel and 30% relaxation of the left tunnel. The first set of measurements is taken at this time.

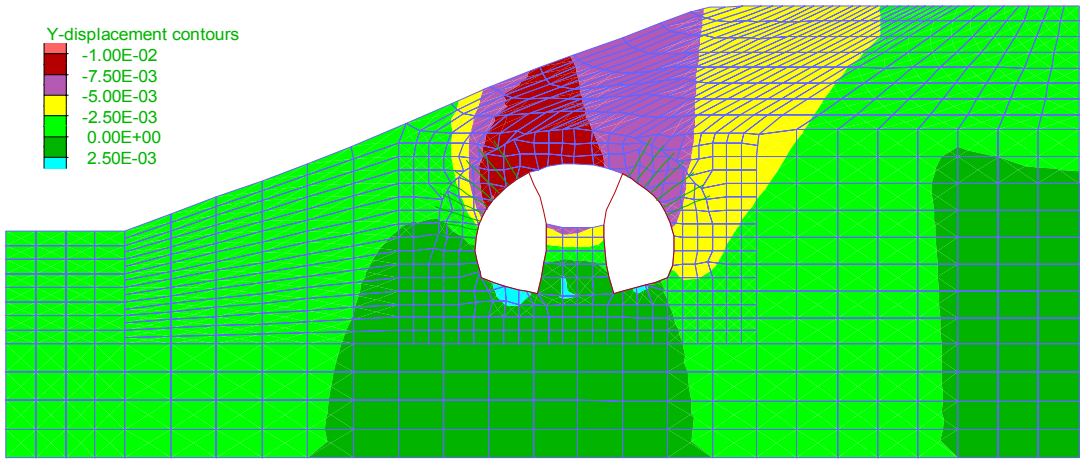

Figure 53: Vertical displacements at full relaxation of the left drift tunnel and after 30% relaxation of the top core.

Figure 54 depicts vertical displacement contours at equilibrium after the top core excavation. The second set of measurements is taken at this stage. The analysis predicts significantly lower displacements than the monitored values. Specifically at the tunnel crown line, the vertical displacement is approximately 16 mm while the measured value is closer to 50 mm. Despite the fact the delays in the support installation and some volume loss have been incorporated in the analysis, the preliminary results are still in disagreement with the measured values. Even though the strength and deformability parameters used are rather conservatively low the above discrepancy suggests that a lower strength material exists in the region of interest. The full scale back-analysis will be employed to investigate this behavior. Due to the higher efficiency of the Differential Evolution relative to the standard Simulated Annealing algorithm, the earlier was chosen for the back-analysis. Two back-analysis trials were performed. In the first trial data from all deformation measurements were taken. The normalized error function of (2) was used. In the second trial, only the extensometer data were used in the analysis.

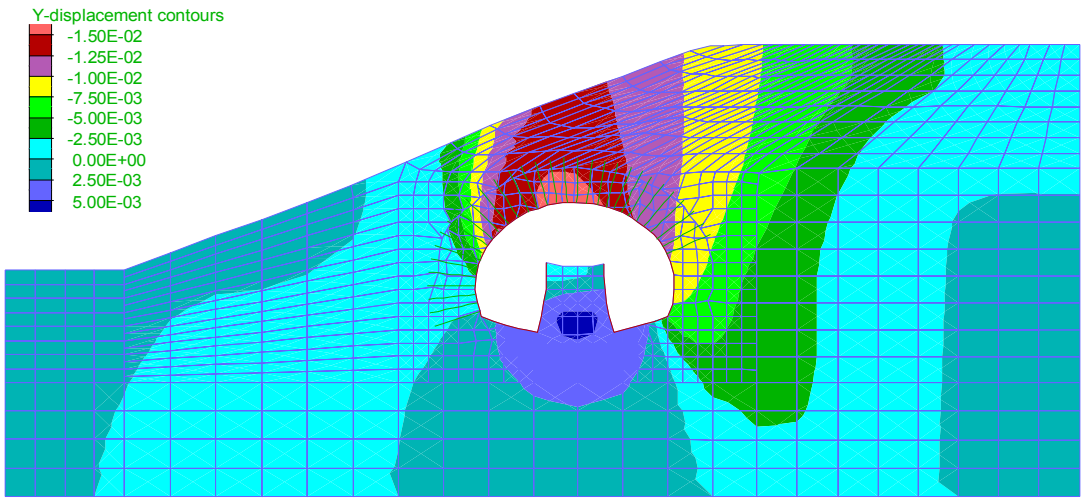

Figure 54: Vertical displacements at full top core relaxation. The supporting sidewalls are removed as the top core advances and the roof lining is closed to form a continuous support.

The first back-analysis performed, took approximately 40 generations to converge and yielded the results shown in Table 19. The comparison plots shown in Figure 56 and Figure 56a,b reveal a relative agreement between predictions and measurements of the surface settlement data but a disagreement in the extensometer data. This behavior most probably designates a problem in the available monitoring data. More specifically, it is evident that the large displacements in the order of 4.5 cm close to the tunnel are practically incompatible with the small displacements at the tunnel surface. This could be due to modeling uncertainties in the model (e.g., varying ground properties with depth). More specifically the measurements suggest low surface displacements and very large deformations very close to the tunnel. The FLAC model on the other hand, predicts a more uniform displacement field, with fairly high surface settlements as well. It is possible that the model cannot predict explicitly the gradual increase in displacements perhaps due to inhomegenity in the ground. Moreover, the surface data may not reliable in relation to the extensometer data. Judging from the results of the first back-analysis, most properties are of reasonable range. However, the predicted Young's modulus E and the unit weight of the surrounding ground may be considered as low, since their values have converged to their lower constraints respectively. Another back-analysis was performed assuming the extensometer data only.

Table 19: Back-analysis results using surface settlement and extensometer data

Parameter	E (MPa)	ν	γ (kN/m^3)	c (MPa)	φ (°)
Constraints	100-1500	0.3-0.45	16-23	0.02-0.1	24-35
Final solution	142.6	0.36	16.2	0.037	23

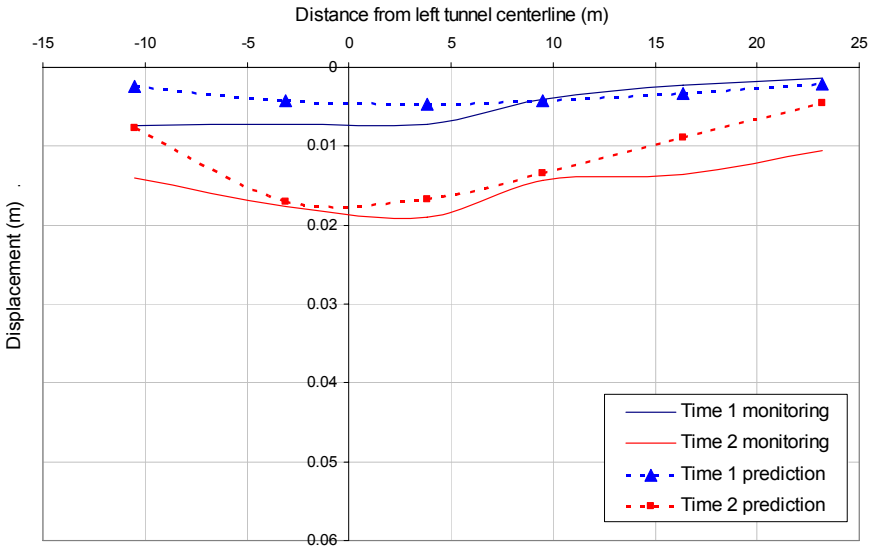

Figure 55: Measured and predicted surface settlement plots from the firth back-analysis trial.

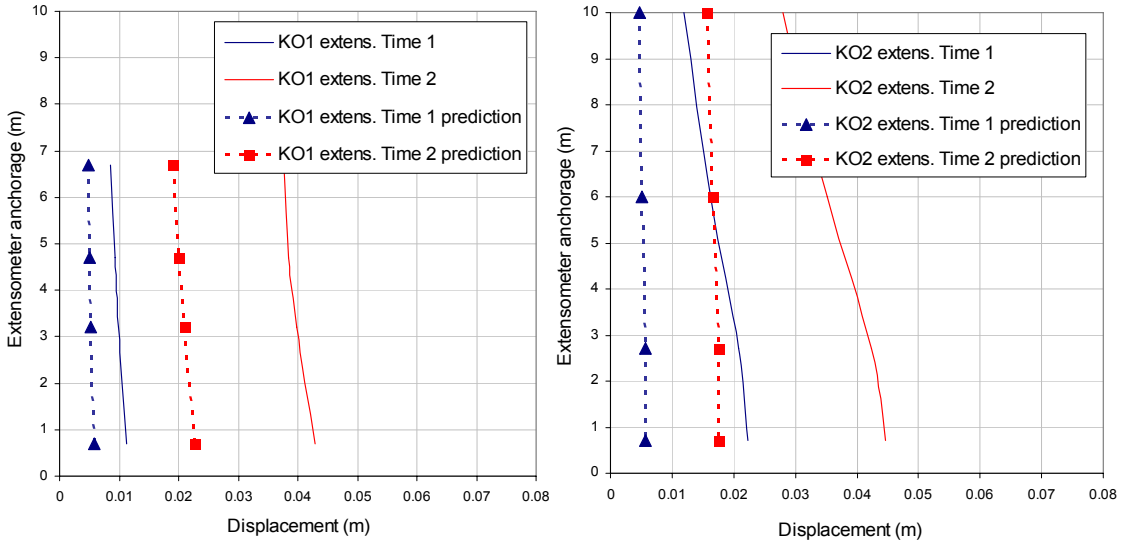

Figure 56: Comparison plots from the first back-analysis of the Heshang tunnel, a) extensometer KO1, b) extensometer KO2.

The results from the second back-analysis are shown in Table 20. The solution vector is very close to the previously obtained, with the exception of the unit weight and cohesion parameters. The unit weight is estimated at 21 kN/m^3 and the cohesion is lower at 0.02 MPa. The unit weight is more compatible with a low quality rock mass and the low strength parameters also suggest the same. A comparison between the measured and predicted extensometer deformations is shown in Figure 57. It is apparent that the extensometer deformation predictions are in better agreement with the measurements. More specifically for extensometer KO1 the predictions almost match the measurements while for extensometer KO2 the predictions even though they do not match exactly, they are in fair agreement with the magnitudes of the measured deformation values. Such differences could be the result of the assumption of a homogenous ground material throughout the model or a

Table 20: Back-analysis results using extensometer data only

Parameter	E (MPa)	ν	γ (kN/m^3)	c (MPa)	φ (°)
Constraints	100-1500	0.3-0.45	16-23	0.02-0.1	24-35
Final solution	200	0.35	21	0.02	24

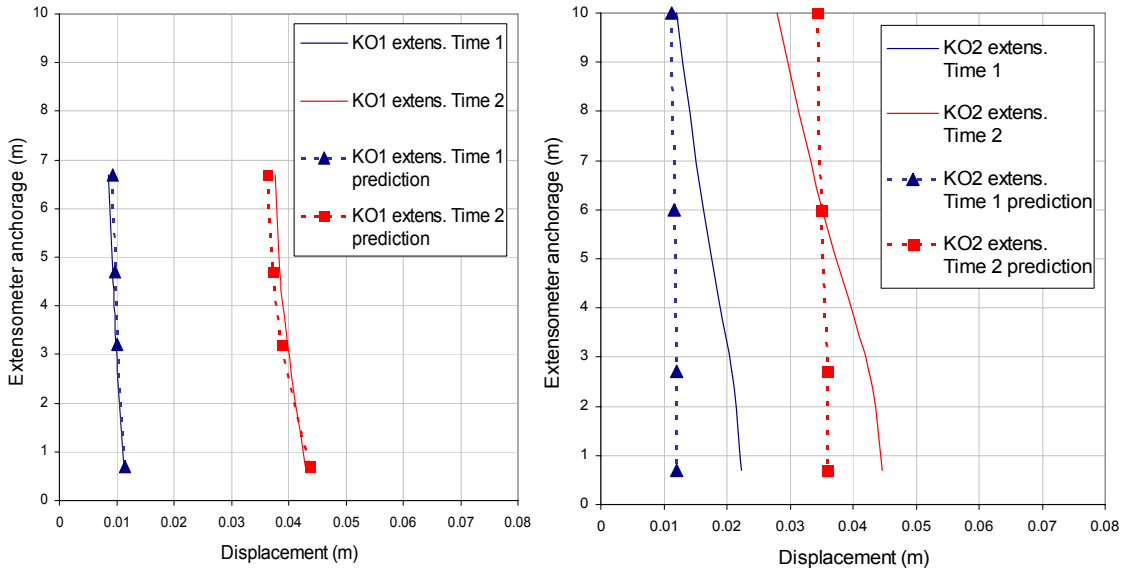

Figure 57: Comparison of measured and predicted extensometer deformations from back-analysis using extensometer displacements.

The previous analysis reveals some important issues when applying optimization-based back-analysis. The solution is highly dependent on the objective function used, which in turn is a function of the type and amount of monitoring data used. Very often various methods of monitoring have different uncertainties associated with them, or reliability issues. The extensometer data may be more appropriate and reliable to use in shallow excavations, when they start recording the tunnel behavior from the beginning of the construction. They also record information inside the ground rather than at a ground boundary. The implementation of various monitoring data in the same back-analysis should be checked for consistency between the data. In the previous example, it was evident that the surface measurements were most probably affected by some error. The inclusion of extensometer data only provided more insight on the validity of the back-analysis results. The finally obtained results yield predictions comparable to the measured extensometer data.

The modeling process is also a factor to consider carefully. The Hashang tunnel example is a fairly difficult case to study using a two-dimensional modeling approach and thus it may deviate from the actual three-dimensional problem to some extent. The relaxation factors used in order to simulate the three-dimensional tunnel closure in FLAC can influence the back-analysis results as well. It is practically impossible to exactly estimate and incorporate all these parameters in a two-dimensional model. On the other hand, three-dimensional back-analysis even though it is possible, it would require an excessive amount of solution time. Therefore a balance between reliability and efficiency using a two-dimensional modeling sequence has to exist. In some cases the assumption of more advanced constitutive models may be more appropriate and require the incorporation of other parameters in the back-analysis (e.g., strain softening material models). It is the responsibility of the modeler and engineer to assess the degree of analogy between the physical and numerical model and based on that, start a back-analysis. A fully satisfying solution, which will closely lead to a match of monitored and predicted performance, is rather difficult to achieve. The various unknowns with respect to the subsurface conditions and the model behavior can make the back-analysis difficult since multiple local optima may exist. The use of global optimization algorithms, even though it is more time consuming than a local optimization algorithm, it is able to cope

with non-linearity of the objective function and provide a good solution estimate. The example of the Heshang tunnel shows the dependency of this method to the assumed model and of course the reliability of the data. Nevertheless, it is the conclusion of this analysis that the proposed method is very promising for a wide range of problem and the algorithms presented can be adapted easily to other numerical simulation software. Both Simulated Annealing and the Differential Evolution method are formidable candidates for problems with large numbers of unknowns. Representative results from the final back-analysis are shown in Figure 58 for the first stage of the measurements and in Figure 59 for the final stage.

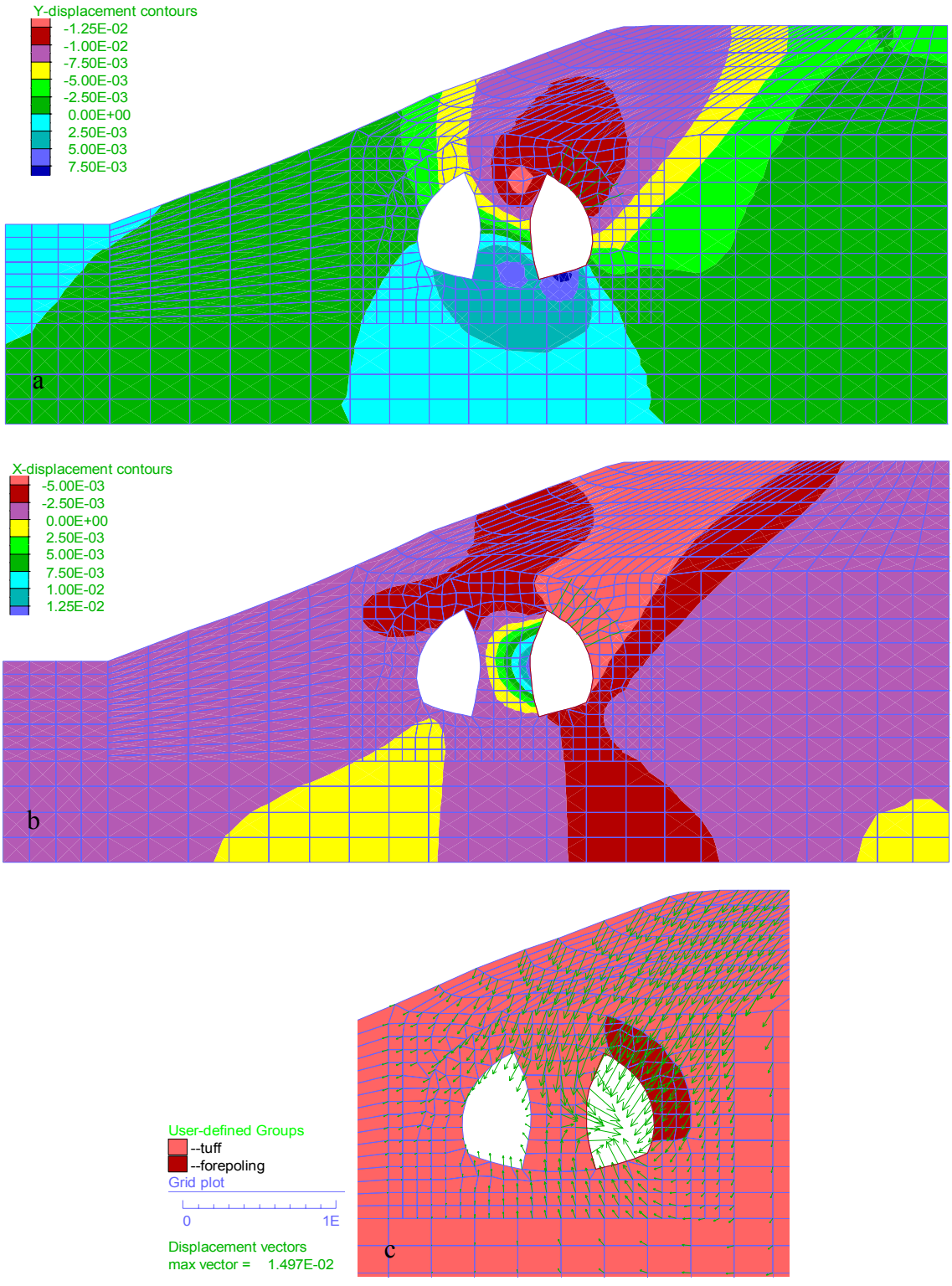

Figure 58: Back-analysis results at the first measurement stage. a) contours of vertical displacements, b) contours of horizontal displacements and c) total displacement vectors.

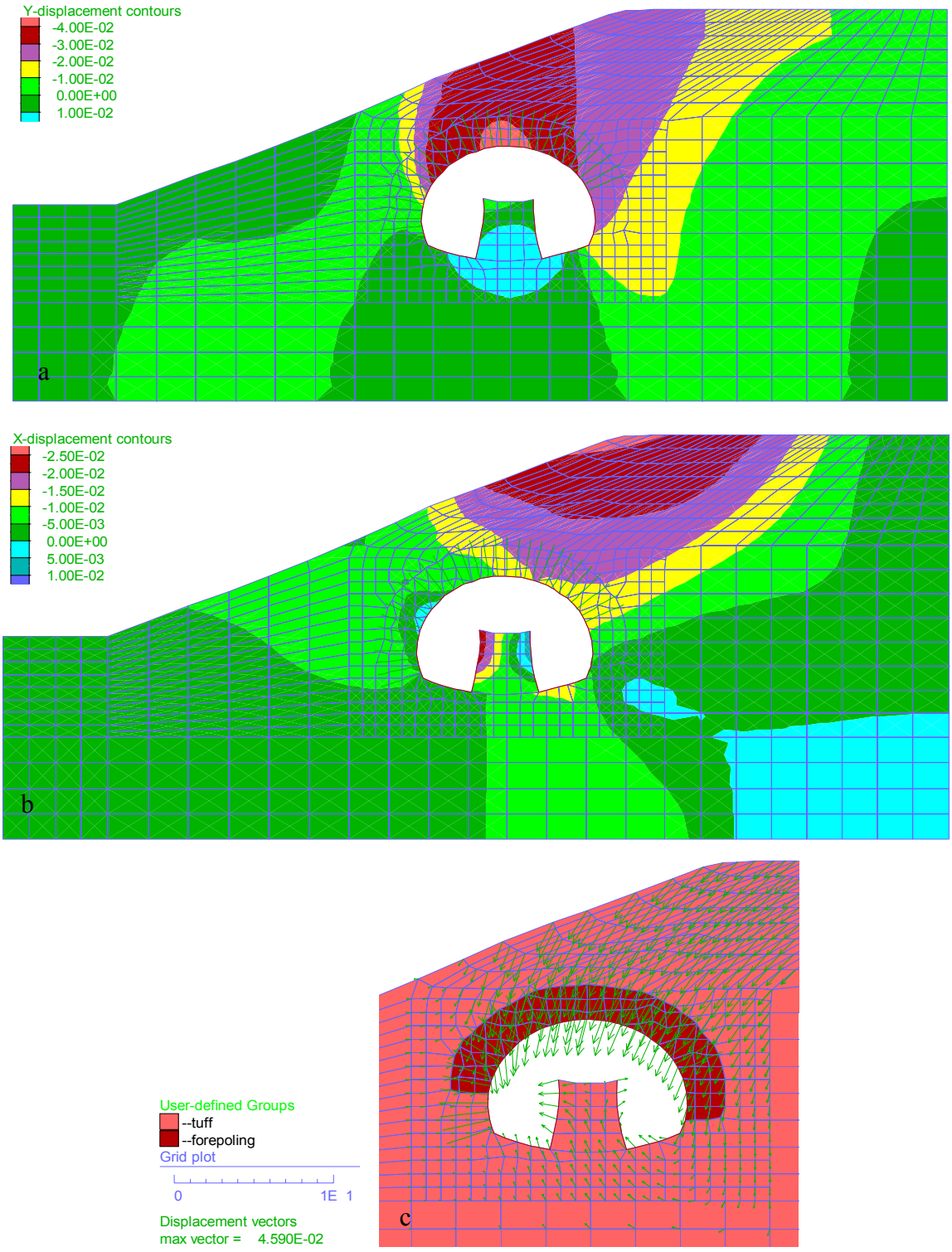

Figure 59: Back-analysis results at the final measurement stage. a) contours of vertical displacements, b) contours of horizontal displacements and c) total displacement vectors.

CHAPTER 10. General research conclusions

This research has focused in the application of parameter identification methods for optimal design of underground construction. Simplified and more elaborate techniques were explored and their use has been demonstrated with insightful examples.

The primary target of this research has been to develop parameter identification methodologies that can be directly applied to actual problems, by using one of the most widely available numerical programs for geotechnical analyses. These methods were implemented in such a way that they can be easily used by engineers and practitioners. Many of the methods suggested can be extended to other types of geotechnical back-analysis, i.e., soil or rock slope stability, retaining wall performance or foundation problems. During application of the method, the back-analysis procedure must be frequently applied to confirm the initial designs or simulations. The consecutive analyses will gradually build a database of design parameters along the direction of the excavation and better forecasting can be made.

The back-analysis methodologies suggested herein are based on principles of Operations Research and as such, they utilize an appropriate optimization algorithm. Other methods such as the Artificial Neural Networks (ANNs) are not included in this research. The use of optimization driven back-analysis allows for more transparent use and interaction with the identification process and it can be applied relatively easily.

The problem of the circular tunnel under isotropic stress conditions in elastoplastic ground has been the benchmark reference in ground-support interaction for a long time and advancements in the application of the convergence confinement method were suggested. The use of longitudinal convergence profiles for simplified back-analysis is more appropriate in order to capture a more overall behavior of the excavation than to use only the ground and support characteristic curves. However, in more irregular tunnel designs under various conditions, a continuum based numerical method is more applicable. New convergence ratio models were presented for unsupported and supported tunnels and compared to previous approximations from the literature. Usually the coefficient and exponential parameters of such relations like equation (20) are obtained from a least squares type of fitting to monitoring convergence data. This formulates a

simplified type of back-analysis but with some shortcomings. It was demonstrated that even the use of very efficient local search algorithms can lead to erroneous results with respect to the identified parameters. The assumed model to describe the behavior of the rock mass (e.g., elastic or elastoplastic) as well as the convergence ratio model used can influence the back-analysis results. The importance of the assumption regarding the ground relaxation at the tunnel face was also examined through parametric analyses and useful relations are suggested. The simplified back-analysis presented herein focuses on a hybrid Monte-Carlo and local search approach which is essentially a variation of the Random Search method. This part of the research demonstrated the need for an algorithm able to deal with uncertainties and the highly non-linear nature of the objective function. The proposed method contains elements of global optimization and heuristic search approaches.

In chapters 6, 7 and 8 the commercially available program FLAC was used to develop and test back-analysis methods. The method involving a local gradient-based minimization algorithm, even though it performs very well in well defined problems, failed to locate a local optimum in more complex problems. This is mainly attributed to the existence of multiple local minima all of which are close to each other. In the fundamental problems that were examined, a known global optimum solution exists since it was initially used to generate measurement data for the back-analysis tests.

When the modified Newton-Raphson method was invoked for back-analysis in plastic ground conditions the algorithm failed to converge. It could either converge to a local optimum or not converge at all. Even if the original trial vector was taken to be sufficiently close to the theoretical optimum, the algorithm deviated greatly and failed to converge. A significant difficulty of gradient based approaches is the need to estimate the derivatives involved. In the Newton-Raphson method, the presence of second order partial derivatives makes the process even more difficult. The choice of the required step size is a significant disadvantage and requires testing for calibration of the back-analysis algorithm. Too small of a step can “confuse” the algorithm and the function perturbations may be undetectable during a finite difference approximation of the derivatives. It should be understood that the numerical precision required by the algorithm may be overshadowed by the precision limits of the finite element or finite difference program.

Thus the chosen step size for any gradient based approach should be such that a reasonable estimate of the finite difference partial derivatives is obtained. Too small of a size can lead to inaccurate derivative estimates and a completely unreliable Hessian matrix. Too large of a step, however, proved to be too rough for the algorithm, in order for it to be able to follow the local characteristics of the objective function. Thus a balance between the two should prevail.

During the application of the Newton-Raphson method, it was also evidenced that the use of a normalized objective function such as equation (2) is preferred by the algorithm over a simple least squares error function like equation (1). In fact this could be problematic in applying a function like equation (34). The normalization helps the algorithm by essentially boosting the sensitivity of the objective function on the governing parameters. When using equation (34) the required precision could become quite high depending on the order of magnitude of squared measurement-prediction error and the order of magnitude of the squared error expressing the deviation from the original estimate. There can be cases where one part can overshadow the importance of the other only due to differences in the order of magnitude. In turn, there could be cases where a small change in one of the parameters could result in minor change of some monitoring points and large change in other measurement points. This can be problematic, as in this way some points become essentially unimportant for the algorithm. The normalization addresses this effectively.

The initial trials of the Newton-Raphson method showed inability to converge if an objective function like equation (1) was used. Other local search methods can also be applied. Gradient based methods should be applied with extreme caution even though they are fast converging algorithms. Direct algorithms such as Powell's algorithm and the Complex method may be more appropriate but can require extended programming depending on the programming language used. Furthermore, the majority of local search algorithms (with the exception of the Nelder-Mead and the Complex algorithms) necessitates the use of a one-dimensional optimization calculation at every new point (e.g., in the Newton method) or after a series of some points (e.g., in Powell's method). Methods like the Golden Section have to be employed. This further slows down the performance, due to more function evaluations required.

For the reasons described above, an alternative approach was investigated for the first time. Two global search strategies are intuitively employed to solve the constrained optimization problem. Both attempt to simulate natural processes and demonstrate excellent characteristics in back-analysis. They are able to adapt to various optimization conditions, and can be programmed easily in the FISH proprietary language of Itasca's codes. Constraints for the governing parameters can be easily implemented in both algorithms without modifications of the objective function, and without interrupting or altering the algorithms' stochastic nature.

It is demonstrated that Simulated Annealing and the Differential Evolution can be successfully applied in back-analysis using two-dimensional plane strain models. A three -dimensional version using the finite element or finite difference methods, would be computationally expensive to run as an iterative back-analysis procedure. Hybrid boundary element-finite element analyses can potentially overcome this. The problems that need to be focused on are the type of monitoring data (e.g., deformations, strains, stresses) and the time when these were taken. When a two-dimensional analysis is performed, the three-dimensional or construction time effect is completely lost unless a controlled relaxation method is followed, which brings again the use of some form of longitudinal profiles into the problem in order to associate the degree of relaxation with the distance from the tunnel face. In modern tunneling it is widely acknowledged that the degree of relaxation before any support is installed plays the most crucial role in optimal design and safety. In addition the fact that most often convergence instead of absolute deformation magnitudes are measured, complicates the mathematical solution of the problem in a two-dimensional approach. There can be much more than one solution for the same given measured convergence values from a tunnel section. For these reasons a probabilistic or global search approach needs to be followed.

Back-analysis is generally a difficult task and in order to be reliable, a large number of iterations needs to be executed. The use of plane strain numerical simulations inevitably limits the back-analysis from using longitudinal deformation or convergence profiles. Thus, only few measurements can be incorporated to the numerical model and these should comply with the actual location and construction time. A simple example is the use of different sets of measurements at different construction times such as after a

top heading and after a bench excavation monitoring. All these can be incorporated in an objective function of the type given in equations (2) or (34). This generally leads to an increase in the number of local optima, especially when a non-linear or a plastic constitutive model is used. The use of advanced optimization algorithms like the Simulated Annealing or the Differential Evolution does not guarantee an ideal solution. If the numerical model does not emulate the physical model adequately then the back-analysis is unreliable. It is the responsibility of the engineer, to apply judgment in the analogy between the numerical and the physical model before execution of the back-analysis. This holds true for any back-analysis method. These reasons are why the global optimization algorithms are suggested for parameter identification. As stated above, the search of an "ideal" solution may be futile, due to modeling uncertainties, accumulation of error in the data, geotechnical uncertainties, etc. However, the above algorithms are very capable of searching for a global or at least a local optimum with a very strong region of attraction in the *n*-dimensional space.

Experience using the Simulated Annealing reveals that the various parameters involved, are problem dependent. A very important factor is the annealing schedule. Some schedules may work for a particular problem while others may not work. The exponential cooling schedule of (52) has shown good results in the problems examined. The parameters of the cooling schedule should also be tested. Similarly for the Genetic Algorithm usage, there is no mathematically fundamental explanation or proof, of convergence to a global optimum or an expected iteration time, until this occurs. Provided that there is ample annealing time in SA or ample generations and individuals in the GAs, there is a high chance of convergence to a global optimum. Simulated Annealing is very good memory-less global evolutionary progress. The implementation presented here is the simplest form of annealing but shows the strengths and potential of the algorithm. Various enhancements can be made in order to make the algorithm more efficient, e.g., by modifying the acceptance criterion so that approximately 50% of the trials are accepted. Such modifications in conjunction with the improvement of computer processing capabilities can promote the use of SA in geotechnical applications. The SA has a advantage over DE, because the areas of strong attraction can become evident by observing the history of the solution path. These are the areas of the strongest local

optimum solutions and very good final candidates. During annealing the best solution should always be recorded simultaneously with the current accepted trial and both could be interpreted as potential results.

The Differential Evolution is a very efficient global optimization approach. It requires less function evaluations for the same problem and like annealing it is not influenced by the continuity of differentiability of the objective function. It is based on the theory of the survival of the fittest and it attempts to find the global optimum by continuously "reshaping" an array of possible trial vectors (primary array of individuals). Towards the end, the array vectors should coincide. This is very similar to the Complex method. The success of the method is based on the size of the array (number of individuals) and the efficiency is controlled by the crossover scheme. Different crossover schemes can be used. In the present algorithm the crossover is based on independent binomial experiment outcomes. The DE was modified in this research, in order to account for parameter constraints while preserving the stochastic nature of the algorithm. The DE should converge to the global optimum possible solution, provided that a reasonably large population is used. According to Price and Storn (1997) this population's size should be $NP \geq 5D - 10D$ $(D = number\ of\ \ parameters = n)$. For the mutation scaling factor they suggest: $F \in (0, 1.2]$ and more often: $F \in [0.4, 1.0]$, while $XR \in [0, 1.0)$.

For any of these methods, precalibration can be computationally expensive but efficient in the long run for the back-analysis algorithm. In this case, the numerical model is set up to approximate the natural process as much as possible. The finite element mesh or finite difference grid has to be modified so that the actual measurement points coincide with existing nodes or gridpoints of the model (for displacement measurements). An initial analysis is performed to generate artificial data at the desired monitoring points. These data are used for a "calibration back-analysis" during which the parameters of the algorithm are chosen so the back-analysis yields comparable results (if not the same) to the original input used. The algorithm parameters are retained from the calibration process, and the back-analysis is repeated using the true data. This ensures more reliable parameter identification, and can also be used to assess any problems in the modeling assumptions before the actual back-analysis is performed.

APPENDIX A

A1. Rock mass classification using a PDA-based field-book

The potential merits of data acquisition using handheld devices are significant in relation to their cost. Current handheld devices such as PDAs are distinguished by low weight, relatively low cost, availability of many types of peripherals, ease of use, and good processing power and data storage capacity. PDAs have strong potential to facilitate and improve field data acquisition and logging involved in rock mass characterization by the use of rock mass classification systems. Geosyntec (2001) developed a database PDA form to perform field drill core logging. Another example of such work has been presented by Rose (2005) who developed a PDA-based database for a proprietary rockfall management system for the Tennessee Department of Transportation.

Two of the most widely accepted and used rock mass classification systems are the Geomechanics Classification System (RMR/SMR) by Bieniawski (1989) and the Q System developed by Barton et al. (1974). Other classification schemes exists and a review of the different systems is given by Bieniawski (1989). Both rock mass classification systems have been developed on an empirical basis based on many case histories of excavations in rocks. There are some key differences between the two systems which will be described below. It should also be recognized that in general there is no general-purpose system since rock mass classification systems are typically developed for specific applications.

The formats of the RMR/SMR and the Q systems allow for good conversion into a portable electronic database system. Combination of these two classification systems with technologies such as Global Positioning System, digital photography, and wireless data transmission to a personal computer, all in a compact form, can be a useful and promising tool for geological field work. Several benefits can accrue from the use of digital field books using PDAs. Digital field acquisition and recording can lead to faster data acquisition and logging as it eliminates the need to transmit and convert paper-based data to digital form. In turn, the readily available data can be analyzed faster and information gained from the analysis can be acted upon in a timelier manner. Faster data acquisition and recording also means more data can be gathered in the field for a given

time. Digital field recording can also provide a more robust and safer storage of data than paper-based system. Digital field books can be programmed to quality-control and pre-edit data in the field and reduce errors associated with the data gathering With GPS and digital camera, supporting materials such GPS coordinates and digital pictures can be gathered and stored together with the other information required in the rock mass classification system. Use of wireless of communication allows real-time field data transmission and seamless integration in databases. Finally, easy-to-use menus and digital forms can help train and familiarize new users in the application of rock mass classification systems.

A2. Software and hardware components

Software component

In order to construct dedicated rock mass classification systems in a PDA digital field book, the Pendragon Forms 4.0® by Pendragon Software Corporation (2004) was used in the programming. This software permits the development of data collection forms in a personal computer environment (PC format). Once developed, the forms are then transmitted for use in a PDA. With this utility, a data entry forms can be conveniently constructed in a PC according to the designer's preferences. The Pendragon Forms also provide a utility to temporarily store data in the PC after a PC-PDA synchronization.

The Pendragon software permits the user to design a form that suits his/her needs and make a unique and purpose-specific interface. The form is basically constructed as a series of related fields where data are inputted. Data from the input fields are stored sequentially (and can be later be modified) in single file each time the form is called by the PDA Pendragon program. Early versions of Pendragon Forms were specifically developed for Palm Pilot® devices, while newer versions are also compatible with PDAs that run under the Pocket PC format. A useful feature of Pendragon Forms is the provision for relational or mathematical subroutines which can be written by the user as a script code. The script code supports a wide variety of commands, some best suited for mathematical calculations and some suited for more general database related actions, i.e., programming of commands for buttons, field value manipulations, etc.

Hardware component

The vast majority of PDA's currently available in the market, either Palm Pilots or Pocket PC's, are compatible with the latest version of the Pendragon Forms. The data acquisition system described in this paper was developed using a Palm Tungsten T2® PDA. However, the system is general enough and can be used in other types and brands of PDAs. The Palm Tungsten T2 PDA includes a 144MHz core processor, 30 MB RAM of memory and a 320x320 pixel color monitor. This PDA has built-in infrared and Bluetooth wireless communication systems, and an SD expansion slot for additional memory or other input devices. The size of the screen allows for good viewing during the pen-based input process even under strong sunlight conditions. The PDA is augmented by an external wireless Bluetooth GPS receiver by DeLorme (Model Earthmate BlueLogger GPS) for coordinate data acquisition. This GPS was chosen for its compatibility with the software and hardware used. It is also one of the few WAAS enabled portable receivers that can obtain Differential GPS data for higher precision post-processing of the obtained coordinates. Using the GPS, a user can select and lock the coordinates by simply clicking a button and the coordinates will automatically be entered and viewed in the database. With the present hardware the connection was performed via Bluetooth and the baud rate was set to 19200 bps, which is fairly fast.

During the development of the digital field book, it was quickly evident that a digital photo accompanying field data would be useful. The Pendragon software allows for direct photographing controls for various PDA models and this provision was taken into account during the development of the forms. Many new models of PDAs offer a built-in small digital camera. However, most of these built-in cameras offer only low resolution images. An alternative is to use a Bluetooth enabled separate pocket digital camera which can wirelessly sent files to the PDA. The user, while using the electronic field book, can select an image file to be stored in the database. This is a more flexible solution since higher quality photos can be taken for the classification purposes. Cost effective Bluetooth enabled cameras are nowadays available from many electronic manufacturers. Otherwise another solution is to obtain photos separately by a digital camera and then share the memory chip with the PDA and store the photos in the

database. Based on the described software and hardware elements, the principles of the rock mass classification field book are depicted in Figure 60.

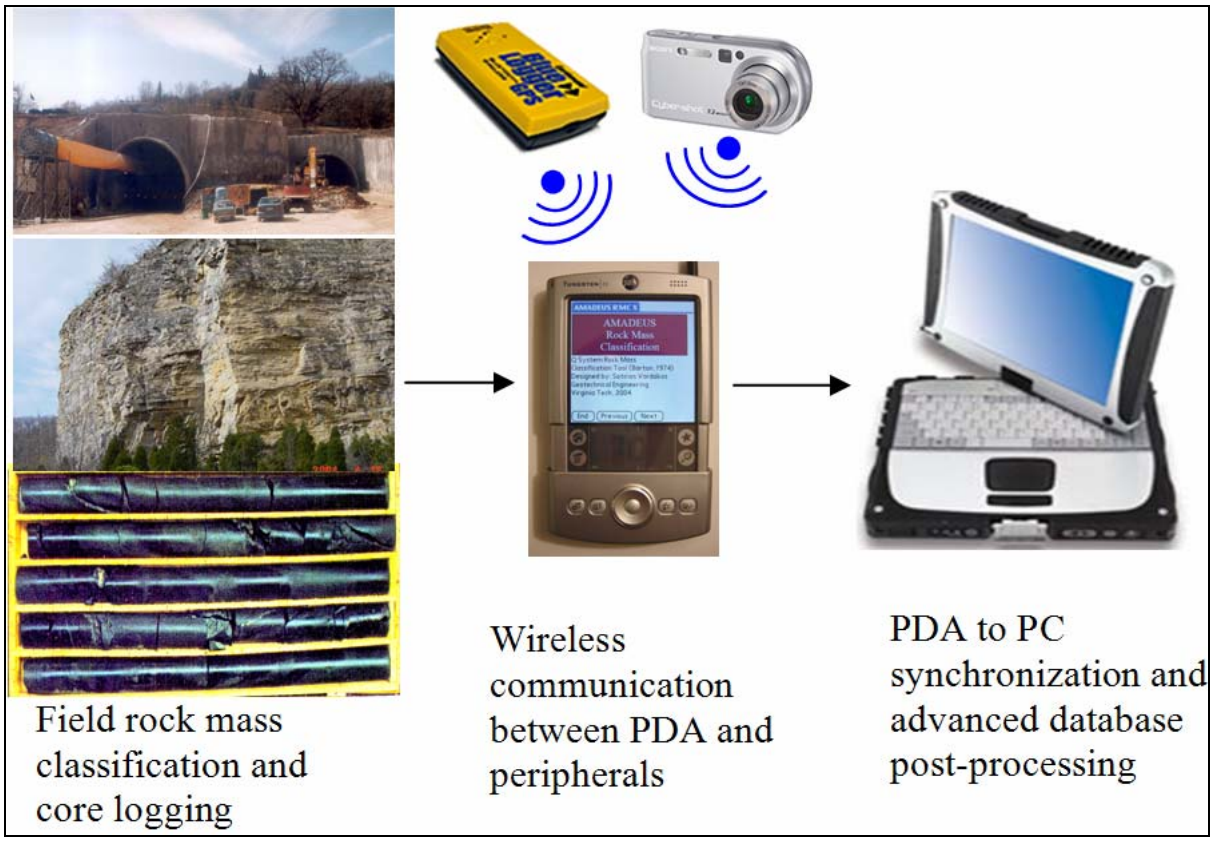

Figure 60: Use of PDA as digital field book for field rock mass classification

A3. Rock mass classification systems used

The RMR/SMR Systems

The Geomechanics classification was developed by Bieniawski (1973). By 1989, around 350 case histories have been used as the basis of the system. As also recognized by Bieniawski (1989), the system benefited from extensions and modifications by various researchers, and such developments allowed the system to adapt it to various engineering applications. The parameters used by the Geomechanics classification are: 1) The uniaxial compressive strength *UCS* or the point load strength of the intact rock material, 2) The rock quality designation RQD, 3) The spacing of the discontinuities, 4) The

condition of the discontinuities (persistence, aperture, roughness, filling, and weathering), 5) The groundwater conditions, 6) The orientation of the discontinuities, and 7) The intended type of project.

For each parameter, the rating is often provided in a tabulated format, where an average rating is given for a representative range of the governing parameter. For the case of the intact rock strength parameter, the RQD and the discontinuity spacing parameter, Bieniawski (1972, 1973) presented curves of the rating versus actual parameter value. These curves were directly programmed into the digital field book. The user needs only to enter the observed parameter value (i.e., spacing of each joint set) and the rating is calculated automatically. The calculation is done by internal execution of three polynomial equations that approximate the Bieniawski curves. Alternatively the user can enter a rating manually. The approximation equations are given as follows:

Intact rock: $Rating = -0.0002 \cdot UCS^2 + 0.1065 \cdot UCS + 0.8693$ (59)

RQD: $Rating = 0.0006 \cdot RQD^2 + 0.1148 \cdot RQD + 2.7808$ (60)

Joint spacing: $Rating = 1.3 \cdot 10^{-9} \cdot S^3 - 5.579 \cdot 10^{-6} \cdot S^2 + 0.0135 \cdot S + 5.31$ (61)

In the above equations, *UCS* is in MPa and *S* is the spacing in mm ($S \leq 2000$ mm). With respect to joint orientation, spacing, persistence, separation, roughness, infilling and alteration, the form was designed so that the user can collect information for up to four joint sets independently. This allows for better conclusions to be drawn during post-processing.

For the case of rock mass classification for slopes, Romana (1985) presented a set of four correction factors to adjust the RMR rating. This extension of the RMR also known as Slope Mass Rating (SMR) is a very useful tool for preliminary assessments of slope stability and more details are described by Romana (1993). Romana has summarized frequently observed slope failure modes, which are: planar failures, wedge type failures, toppling failures, soil like failure modes. The SMR rating is obtained from the basic RMR rating value using the following relation:

$$SMR = RMR + (F_1 \cdot F_2 \cdot F_3) + F_4 \quad (62)$$

where $F_{1,2,3,4}$ are correction factors.

The Q System

Classification using the Q system of Barton et al. (1974) can be used for core logging and field mapping results that are quantified and represented statistically. Initially introduced in 1974, the Q system received gradual refinements and verifications, the last being in 1993-1994 as described by Barton and Grimstad (1993, (1994). According to the Q system, the rock mass quality is designated by the index Q which is a function of the form:

$$Q = \frac{RQD}{J_n} \cdot \frac{J_r}{J_a} \cdot \frac{J_w}{SRF} \tag{63}$$

The parameters involved in the Q system are: *RQD*: the rock quality designation (%), J_n: the number of joint sets, J_r: the joint roughness, J_a: the alteration of the joints; J_w: seepage and water effects in the joints, and *SRF*: parameter considering the effects of stress, squeezing or fault induced instability phenomena. The Q index varies from 0.001 for exceptionally poor rock masses to 1000 for exceptionally good qualities.

Barton (1974) notes that the parameters J_r/J_a must be made with respect to the weakest or most influencing discontinuity set in a given classified zone of rock mass. Full guidelines in using the Q system are not the scope of the present paper and can be found in Barton and Grimstad (1993) and Barton (2002). The second step in the application of the Q index system is the quantitative estimation of the type of support to be used depending on the ground conditions and the size of the excavation. An updated reference chart by Barton and Grimstad (1994) is used to assist in the permanent support estimation in accordance to the Norwegian Method of Tunneling described by Barton and Grimstad (1994).

A4. Data acquisition using the RMR system

The digital field book for the Geomechanics Classification is composed of a series of fields were the user enters the information, depending on the type of the field, either by typing information (text or numeric format) or by selecting choices from dropdown menus. This form was design so that each record will handle the observations of the user for a specific location. This design is mostly helpful not only for experienced but also

novice users. The user may also jump to a section of interest in the form, back and forth to make changes as needed.

Initial information are recorded for the location or jobsite, the structural region were classification will take place, the name of the field geologist or engineer, etc. Time and date are recorded automatically. For the case were the classification is done underground, the user can enter a range of chainage stations between which the observations were made. In case the data are obtained in open field, coordinate data can be logged manually or automatically via a GPS device. Digital pictures or snapshots can also be obtained and stored. Next the rock mass classification parameters are entered. Figure 61 presents the RMR form fields for the previously described data entries.

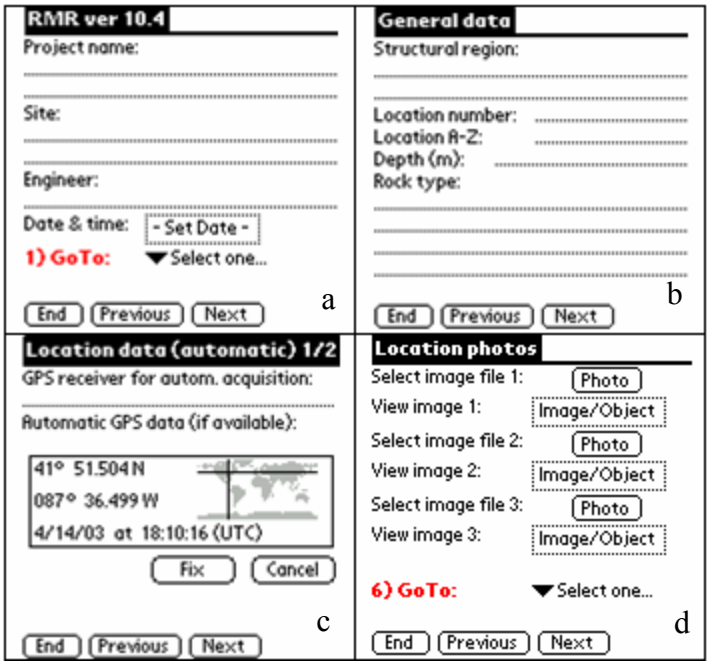

Figure 61: General data, GPS coordinates and digital image fields for the rock mass classification using the PDA.

The uniaxial compressive strength in MPa is entered and the rating is calculated automatically using equation (59). For RQD, a convenient field in a slider form varying from 0 to 100% is provided which is depicted in Figure 62a. Following the RQD, the user is asked to select up to four joint sets that exist in the observed rock mass. The user is also asked to choose between a simplified or detailed method of joint orientation data logging. In the former, an equivalent number of fields will unfold and the user will enter information regarding mean orientation, discontinuity spacing (mm), persistence, aperture, roughness, infilling type and weathering. If the detailed method is selected, then the user is automatically guided to a new subform. This subform allows for detailed field recording of joint orientation data of any planar or linear geologic feature. The user can choose either a strike/dip or a dip/dip direction format. When the entry of data in the subform is completed, the user is redirected to the parent form. This setup is very useful since the subform can be also used independently. It is important to note, however, that when the user enters the subform from a parent form record, then the subform was designed to store identification properties of the parent form so that the parent record is specifically linked to the multiple subform record entries. This feature is desirable for geo-locating of the obtained data. The remaining parameters are entered similarly by dropdown lists interactively and the ratings are calculated automatically by the tool. Examples of these database entries are shown in Figure 62.

The user can also specify stress-related conditions in subsequent fields. Such fields record an estimate of the magnitude and level of in situ stresses (σ_1 and σ_3), depth of excavation and any observations of squeezing conditions. The existence of faulting in the observed location can be recorded in a separate page or otherwise in the previously described subform. Fields for the general description of the fault, the fill material and numerical fields to record the orientation of the fault have been incorporated. Finally, corrections of the RMR rating can be made by choosing a work type such as tunnel, rock foundation or rock slope. In the later case, the SMR correction factors are used. Again, all the necessary corrections are made in a user-friendly manner by using dropdown menus. At the end of the input process, the form calculates the basic RMR rating as well as the adjusted RMR from the optional corrections along with the corresponding rock mass class number (1 to 5). The user may also quickly observe a overall average of the RMR

rating from the existing records in the form, a feature available by the Pendragon database. For the case of slopes and tunnels, the form subsequently leads the user to some empirical estimates of required support according to literature references. The primary result output is shown in Figure 63.

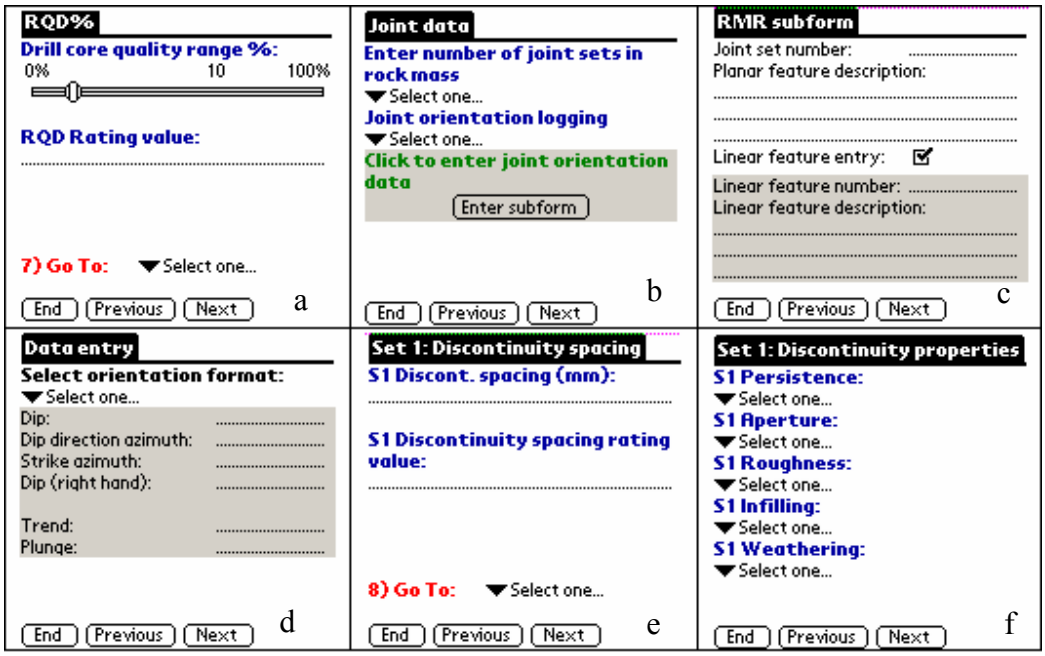

Figure 62 a) Slider field for the RQD in the RMR classification form; b,c,d) Detailed joint orientation fields in RMR subform; e) Joint set spacing parameter and d) Joint condition parameters in RMR form.

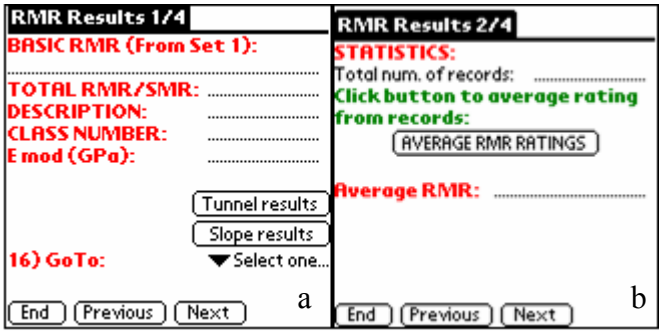

Figure 63 a) Final results in terms of basic RMR (based on properties of joint set 1 and adjusted RMR/SMR; b) Averaging of results while working in an open record of the RMR form.

When the user completes the acquisition and synchronizes the PDA with a personal computer, the "parent" and "child" databases are updated in the PC and the data become available for post-processing. In the current version of the digital field book, the user can specify using Pendragon Forms to directly export the data to Microsoft Excel®. For this reason, a proprietary post-processing spreadsheet was developed to assist in data analysis. Other numerical, database and geo-referencing applications can similarly be used.

A5. Data acquisition using the Q system

Barton (2002) suggested a convenient way to record and to evaluate trends of the Q parameters by constructing histograms of the different parameter. Based on this logging chart, it is possible to quickly estimate a typical range of the Q-values, as well as a mean value of the rating. This is the framework typically used for storing, handling and visualizing results from rock mass classification when working in the field, in a tunnel or simply by examining boxes of core materials. A similar technique was adapted for the development of the digital field book for field mapping using the Q system.

There are two possible ways to implement the Q-logging described above. The first approach is to use an interactive type of form which will collect many records independently like the previously described database for the Geomechanics RMR/SMR System. Since the main purpose of the form is data collection, this type of form can assist the user by providing reference lookup lists and dedicated help menus when needed for each parameter. In the second approach, the user can manually enter directly a number of observations in specified fields, for each possible value of a parameter (e.g., 15 observed instances of the RQD being in the range 70-80%). This necessitates that a single record in the form will handle many observations at the same time. However, due to restrictions in PDA visual capabilities in terms of what can be viewed on the screen, an inexperienced user may find it cumbersome to use such a scheme of data collection. On the other hand, experienced users can use this scheme immediately. Both the above proposed collection formats were implemented and two distinct form designs were developed with the Pendragon software. In the following sections, the use of the forms is briefly explained and examples are also given.

Independent record form

This form was developed similarly with the previously described RMR/SMR form. The user initially enters all the general data regarding the project, its location, and any electronic image files for attachment to the record. The multitude of the different cases for the parameters in the Q-system required the use of cascading lookup references. This means that when the user selects a general description of the parameter (e.g.,. thin mineral fillings in the J_a parameter) then the next field will depend on the previous selection. This is useful as an interface since the database stores not only the value of a specific rating but also its general description.

When it comes to entering information for the rock mass jointing via the J_n parameter, the user can also enter information in a separate subform. The subform has the same design as in the RMR system, and each parent Q logging record can be linked to multiple joint orientation entries. Example snapshots of the Q system independent record form are shown in Figure 64. In this figure the final result screen is also shown. Once the data collection is completed, post-processing in a spreadsheet allows for quick data evaluation. The spreadsheet can calculate typical minimum, maximum, mean and most frequent values of the Q rating. The Q minimum involves estimation of the minimum values of RQD, J_r and J_w and maximum ratings of the J_n, J_a and *SRF* parameters. Maximum values of the individual parameters are used to calculate Q maximum. The weighted average is calculated for each of the six parameters p from the corresponding number of observations according to.

$$\overline{p} = \frac{\sum_{i=1}^{k} r_{p_i} * n_i}{\sum_{i=1}^{k} n_i} \qquad (6)$$

where k is the number of distinct rating classes (or ranges) for each parameter p as suggested by the Q system reference tables, r is the rating value for each parameter class, and n is the number of observations per class of parameter. For example, the RQD parameter i distinguished into k=11 ranges for ease of use: 10, 10-20, 20-30, 30-40,…, 90-100, 100 with mean rating in each range as: r_{ai}=10, 15, 25, 35, …, 95, 100. If n=4 observations were made at a location for the range RQD=70-80, 5 observations for

RQD=80-90, 12 observations for RQD=90-100 and 4 observations for RQD=100, then for that location the mean RQD calculated by the PDA is:

$$\overline{RQD} = \frac{4\times 5 + 5\times 85 + 12\times 95 + 4\times 100}{4+5+12+4} = 90.6$$

In some cases there are parameters of the Q system that have the same rating under different conditions. For example, the parameter J_r has the same value of 1.5 for slickensided undulating surfaces and for rough or irregular and planar rock joint surfaces. This information is ultimately lost during the overall statistical classification process although it still exists in the database records. An example of typical results from data processing using the Q system is shown in Figure 65 . The plots present frequency plots of the different ratings after processing. Such plots can be made for a specific location in a tunnel section or for a series of sequential sections. Additionally the data can be processed and clustered.

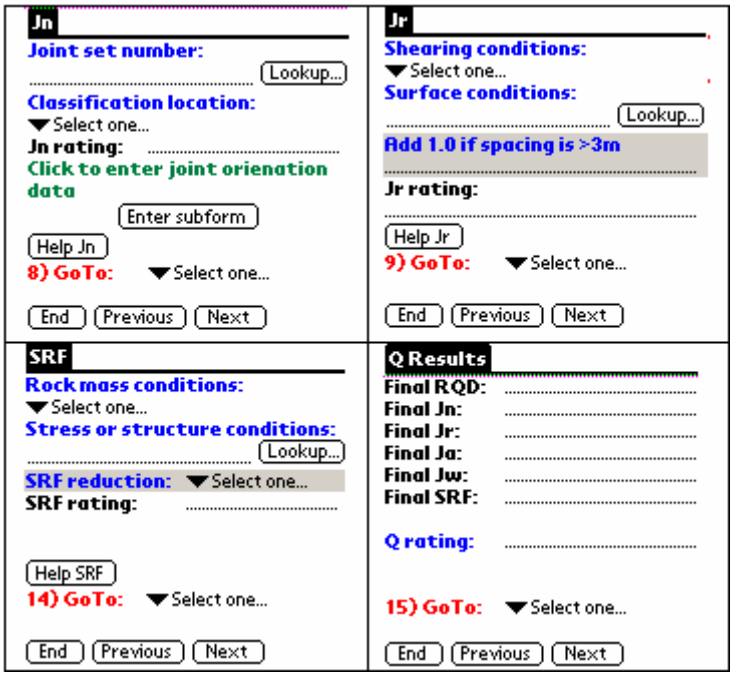

Figure 64: Screenshots of the Q system independent record form for the Jn, Jr and SRF parameters. The final results screen is also depicted.

Post-processing using a spreadsheet allows for plotting of the results in the NMT support chart developed by Barton Barton (2002). After specification of an excavation span or height and the Excavation Support Ratio (*ESR*), the minimum, maximum, mean and weighted average results are plotted on top of the design chart. Figure 66 displays how the calculated range of Q-values can be used to estimate a support system for the excavation.

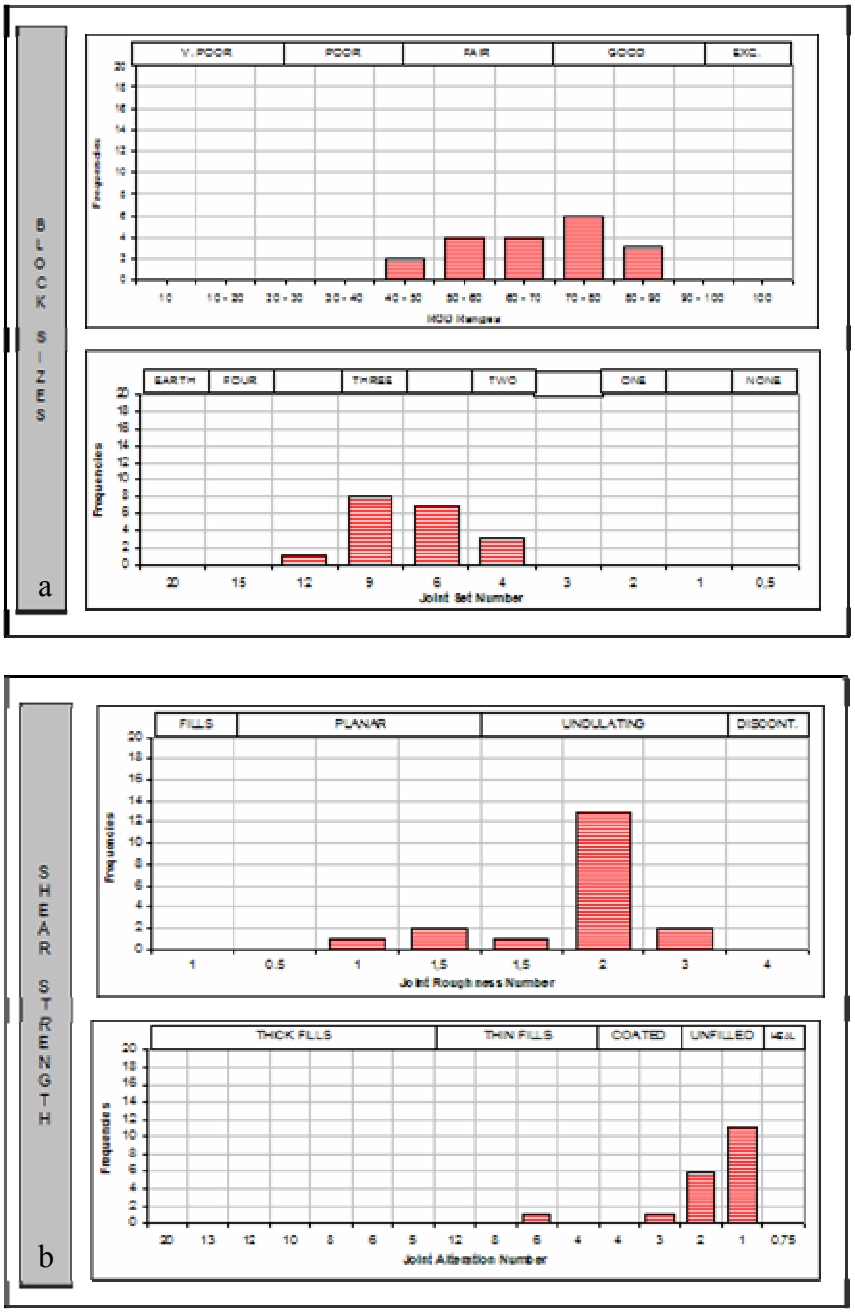

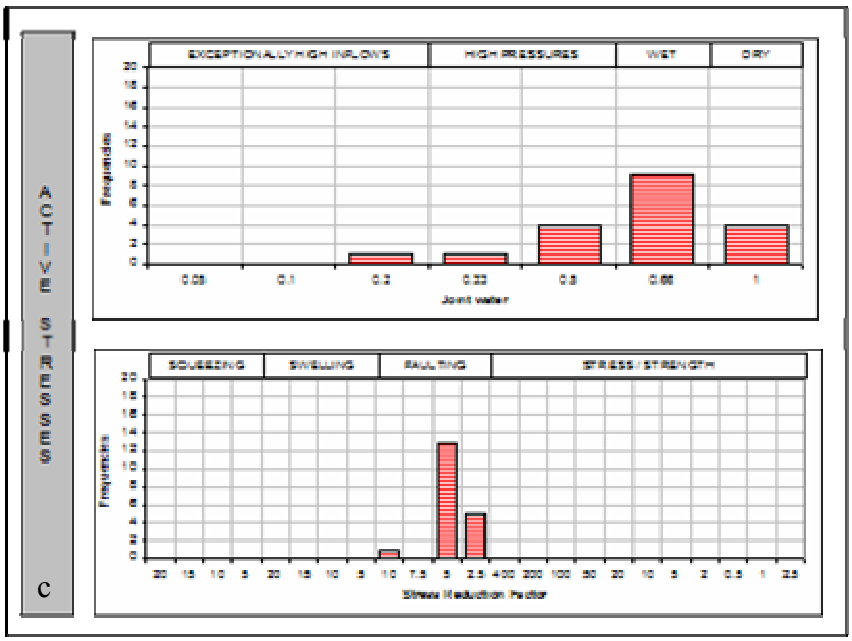

Figure 65 a,b,c: Statistical post-processing of the results (after Barton, 2002)

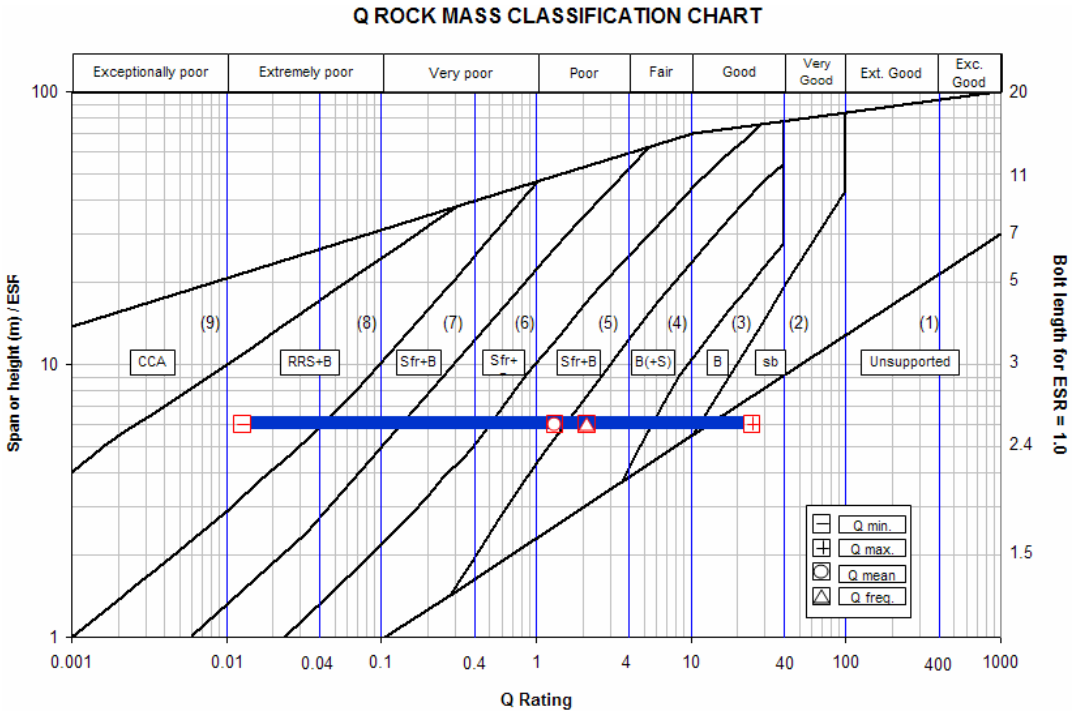

Figure 66: Post-processed database records plotted in the reference design chart of the Q-NMT system (Barton and Grimstad, 1994) leading to estimates of a range of recommended supports.

Cumulative record form

The previously described data acquisition approach offers user friendliness but may be cumbersome to use when the records or numbers of observations are too numerous. Instead, it might be useful to compress and summarize data from several independent records into a single record. Each record can include multiple observations for each of the six Q parameters. This type of data recording uses typical value ranges for the parameters in accordance to the suggestions by Barton (2002) and the user inputs the number of observations for each of these range of values. For example, for the RQD range from 60-70 the input is how many observations of this range were encountered on a specific section of the site. This format can is more convenient for an experienced user. Example screenshots of the data entry are shown in Figure 67. Statistical processing of the accumulated data can be performed by a spreadsheet in a similar fashion to the previous cases.

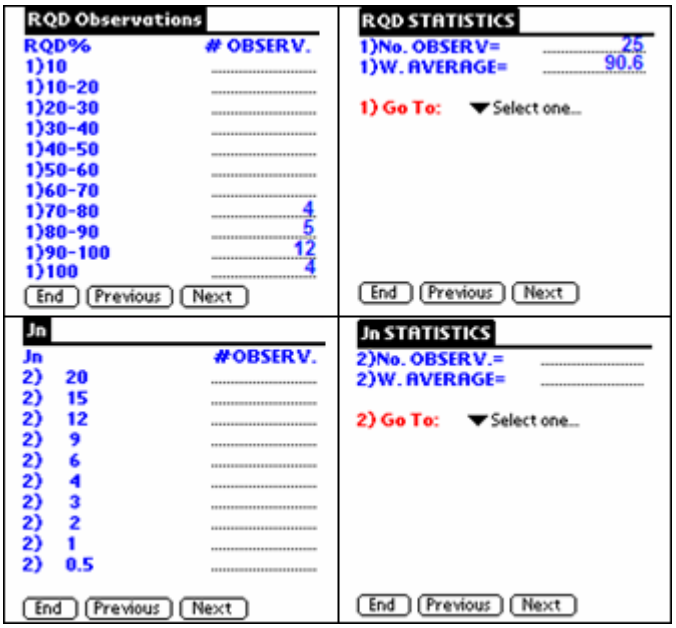

Figure 67: Example of occurrence entries for the RQD and Jn fields in the cumulative for for the Q System

A6. Conclusions

The PDA-based digital field book for rock mass classification presented here is intended to be used by civil, mining engineers, geologists and anyone performing rock mass classification in the field. The main function of the digital field book is to provide a user friendly interface for the systematic paper-free recording of data, and transmission and quick processing of collected data in a desktop/laptop computer. The digital field book can provide immediate initial estimates of rock mass quality whenever a record is completed. Optional geo-referencing by using a wireless GPS receiver makes field data easily incorporated into larger organizational project or worksite databases and GIS utilities. The Geomechanics RMR/SMR and Q systems are currently implemented in the digital field book. However, the same procedures used for these two system can be employed to program other rock mass classification systems such as the Geological Strength Index rock mass classification suggested by Hoek et al. (2000) and Marinos and Hoek (2000).

Bibliographic references

Alonso, E. E., Alejano, L. R., Varas, F., Fdez-Manin, G., Carranza-Torres, C., 2003. Ground response curves for rock masses exibiting strain-softening behavior. International Journal for Numerical and Analytical Methods in Geomechanics 27, 1153-1185.

Asef, M. R., Reddish, D. J., Lloyd, P. W., 2000. Rock support interaction analysis based on numerical modelling Geotechnical and Geological Engineering 18, 23-37.

Baldick, R., 2006. Applied optimization - Formulation and algorithms for engineering systems, edn. Cambridge University Press, New York, 768.

Barton, N., 2002. Some new Q-value correlations to assist in site characterization and tunnel design International Journal of Rock Mechanics and Mining Sciences 39, 185-216.

Barton, N., Grimstad, E., 1993. Updating of the Q system for NMT. Proceedings, International Symposium on sprayed concrete-Modern use of wet mix sprayed concrete for underground support, Fagernes, Oslo, Norway, pp. 46-66.

Barton, N., Grimstad, E., 1994. The Q system following twenty years of application in NMT support selection. Felsbau 12 (6), 428-436.

Barton, N., Lien, R., Lunde, J., 1974. Engineering classification of rock masses for the design of tunnel support. Rock Mechanics 6, 189-236.

Bernaud, D., Rousset, G., 1992. La nouvelle méthode implicite pour l'étude du dimensionnement des tunnels. Revue Française de Géotechnique 60, 5-26.

Bernaud, D., Rousset, G., 1996. The New Implicit Method for tunnel analysis. International Journal for Numerical and Analytical Methods in Geomechanics 20, 673-690.

Beveridge, G. S. G., Schechter, R. S., 1970. Optimization: Theory and Practice, edn. McGraw-Hill, New York, 773.

Bieniawski, Z. T., 1973. Engineering classification of rock masses. Transactions of the South African Institution of Civil Engineers 15 (12), 335-344.

Bieniawski, Z. T., 1989. Engineering rock mass classifications, edn. John Willey and Sons, Pennsylvania, USA, 29-95.

Box, M. J., 1965. A new method of constrained optimization and a comparison with other methods. Computer Journal 8 (1), 42-52.

Brown, E. T., Bray, J. W., 1982. Rock support interaction calculations for pressure shafts and tunnels. Proceedings, Symposium of the International Sociatey of Rock Mechanics, Aachen, Germany, 26-28 / 5 / 1982, pp. 555-565.

Brown, E. T., Bray, J. W., Ladanyi, B., Hoek, E., 1983. Ground response curves for rock tunnels. ASCE, Journal of Soil Mechanics and Geotechnical Engineering 109 (1), 15-39.

Carranza-Torres, C., Fairhust, C., 1999. The elasto-plastic response of underground excavations in rock masses that satisfy the Hoek-Brown failure criterion. International Journal of Rock Mechanics and Mining Sciences 36, 777-809.

Carranza-Torres, C., Fairhust, C., 2000. Application of the Convergence-Confinement method of tunnel design to rock masses that satisfy the Hoek-Brown failure criterion Tunelling and Underground Space Technology 15, 187-213.

Chern, J. C., Shiao, F. Y., Yu, C. W., 1998. An empirical safety criterion for tunnel construction. Proceedings, Regional Symposium on Sedimentary Rock Engineering, Nov. 20-22, Taipei, Taiwan, pp. 325-330.

Chi, S.-Y., Chern, J.-C., Lin, C.-C., 2001. Optimized back-analysis for tunneling-induced ground movement using equivalent ground loss model. Tunneling and Underground Space Technology 16, 159-165.

Cho, K.-H., Choi, M.-K., Nam, S.-W., Lee, I.-M., 2006. Geotechnical parameter estimation in tunneling using relative convergence measurement. International Journal for Numerical and Analytical Methods in Geomechanics 30, 137-155.

Chua, C. G., Goh, A. T. C., 2005. Estimating wall deflections in deep excavations using Bayesian neural networks. Tunnelling and Underground Space Technology 20, 400-409.

Cividini, A., Jurina, G., Gioda, G., 1981. Some aspects of characterization problems in geomechanics. International Journal of Rock Mechanics and Mining Sciences 18, 487-503.

Cividini, A., Maier, G., Nappi, A., 1983. Parameter estimation of a static geotechnical model using a Bayes' rule approach. International Journal of Rock Mechanics and Mining Sciences 20, 215-226.

Corana, A., Marchesi, M., Martini, C., Ridella, S., 1987. Minimizing multimodal functions of continuous variables with the "Simulated Annealing" algorithm. Association for Computing Machinery - Transactions on Mathematical Software 13 (3), 262-280.

Corbetta, F., Bernaud, D., Nguyen Minh, D., 1991. Contribution á la methode convergence-confinement par le principe de la similitude. Revue Française de Geotechnique 54, 5-12.

de Mello Franco, J. A., Armelin, J. L., Santiago, J. A. F., Telles, J. C. F., Mansur, W. J., 2002. Determination of the natural stress state in a Brazilian rock mass by back analysing excavation measurements: a case study. International Journal of Rock Mechanics and Mining Sciences 39, 1005-1032.

Decker, J., Mauldon, M., 2006. Determining size and shape of fractures from trace data using a differential evolution algorithm. Proceedings, 41st U.S Symposium on Rock Mechanics, pp. .

Deng, D., Nguyen Minh, D., 2003. Identification of rock mass properties in elasto-plasticity. Computers and Geotechnics 30, 27-40.

Deng, J. H., Lee, C. F., 2001. Displacement back analysis for a steep slope at the Three Gorges Project site. International Journal of Rock Mechanics and Mining Sciences 38, 259-268.

Duncan Fama , M., 1993. Numerical modeling of yield zones in weak rock. In: J. A. Hudson, T. Brown, C. Fairhurst and E. Hoek (Eds.) Comprehensive Rock Engineering, (2) Pergamon Press, Oxford, pp. 49-75.

Dunnincliff, J., 1988. Geotechnical instrumentation for monitoring field performance, 1 edn. John Wiley and Sons, New York, 75-78, 199-295, 453-466.

Dutro, H. B., 1989. Instrumentation. In: R. S. Sinha (Eds.) Underground structures, design and instrumentation, (1) Elsevier, Amsterdam, pp. 372-405.

Eykhoff, P., 1974. System identification - Parameter and state estimation, edn. John Wiley and Sons, Great Britain, 147-151, 519-526.

Feng, X.-T., An, H., 2004. Hybrid intelligent method optimization of a soft rock replacement scheme for a large cavern excavated in alternate hard and soft rock strata. International Journal of Rock Mechanics & Mining Sciences 41, 655–667.

Feng, X.-T., Zhang, Z., Sheng, Q., 2000. Estimating mechanical rock mass parameters relating to the Three Gorges Project permanent shiplock using an intelligent displacement back analysis method. International Journal of Rock Mechanics 37, 1039-1054.

Fenner, R., 1938. Untersuchungen zur Erkenntnis des gebirgsdruckes. Glückauf 74, 681-695.

Finno, R. J., Calvello, M., 2005. Supported excavations: the Observational Method and inverse modeling. Journal of geotechnical and geoenvironmental engineering 131 (7), 826-836.

Fletcher, R., Reeves, C. M., 1964. Function minimization by conjugate gradients. Computer Journal 7 (2), 149-154.

Gaudin, B., Polacci, J., Panet, M., Salva, L., 1981. Soutenement d'une galerie dans les marnes du Cenomanien. Proceedings, 10th International Conference on Soil Mechanics and Foundation Engineering, Stockholm, Sweden, pp. 293-296.

Gens, A., Ledesma, A., Alonso, E. E., 1996. Estimation of parameters in geotechnical backanalysis - II. Application to a tunnel excavation problem. Computers and Geotechnics 18 (1), 29-46.

Geokon. (2005), www.geokon.com..

Geosyntec. (2001), "Geotechnical data acquisition using PDA," http://www.geosyntec.com/news_story10.asp..

Gioda, G., 1985. Some remarks on back analysis and characterization problems. Proceedings, 5th International Conference on Numerical Methods in Geomechanics, Nagoya, Japan, 1-5 April, 1985, pp. 47-61.

Gioda, G., Sakurai, S., 1987. Back analysis procedures for the interpretation of field measurements in geomechanics. International Journal for Numerical and Analytical Methods in Geomechanics 11, 555-583.

Guenot, A., Panet, M., Sulem, J., 1985. New aspects in tunnel closure interpretation. Proceedings, 26th US Symposium on Rock Mechanics: Research and Engineering Applications in Rock Masses, Rapid City, Utah, 26-28 June 1985, pp. 455-460.

Hajek, B., 1988. Cooling schedules for optimal annealing. Mathematics of operations research 13 (2), 311-329.

Himmelblau, D. M., 1972. Applied nonlinear programming, edn. McGraw-Hill, New York, .

Hochmair, H., 1998. Konvergenzmessungen in der NÖT - Graphische darstellungsformen und der bezug zur tunnelmechanic. Thesis, Technischen Universität Wien, Wien, Austria, 101.

Hoek, E., (2003), "Numerical modelling for shallow tunnels in weak rock," Rocscience, .

Hoek, E., Kaiser, P. K., Bawden, W. F., 2000. Support of underground excavations in hard rock, edn. Balkema, Rotterdam, 232.

Holland, J. H., 1975. Adaptation in natural and artificial systems, edn. University of Michigan Press, Ann Arbor, Michigan, .

Horst, R., Pardalos, P. M., (1994), "Handbook of Global Optimization (Nonconvex Optimization and Its Applications)," Springer, 900.

Hoshiya, M., Yoshida, I., 1996. Identification of conditional stochastic field. ASCE, Engineering Mechanics 122 (2), 101-108.

Itasca Consulting Group. 2005. FLAC 5.0 Manuals, edn. Minneapolis, Minnesota, USA, .

Jeon, Y. S., Yang, H. S., 2004. Development of a back analysis algorithm using FLAC. International Journal of Rock Mechanics and Mining Sciences 41 (3), .

John, M., 1977. Adjustment of programs of measurements based on the results of current evaluation. Proceedings, International Symposium of Field Measurements in Rock Mechanics, Zurich, Switzerland, pp. 639-656.

Kirkpatrick, S., Gelatt, C. D., Vecchi, M. P., 1983. Optimization by simulated annealing. Science 220 (4598), 671-680.

Kolymbas, D., 2005. Tunnelling and tunnel mechanics, A rational approach to tunnelling, edn. Springer-Verlag, Berlin, Germany, 437.

Kovari, K., Amstad, C., 1993. Decision making in tunneling based on field measurements. In: J. A. Hudson, T. Brown, C. Fairhurst and E. Hoek (Eds.) Comprehensive Rock Engineering, Pergamon Press, pp. 571-606.

Kuester, J. L., Mize, J. H., 1973. Optimization techniques with Fortran, edn. McGraw-Hill, New York, 500.

Lecampion, B., Constantinescu, A., Nguyen Minh, D., 2002. Parameter identification for lined tunnels in a viscoplastic medium. International Journal for Numerical and Analytical Methods in Geomechanics 26, 1191–1211.

Ledesma, A., Gens, A., Alonso, E. E., 1996. Estimation of Parameters in Geotechnical Backanalysis - I. Maximum Likelihood Approach. Computers and Geotechnics 18 (1), 1-27.

Lee, J., Akutagawa, S., Yokota, Y., Kitagawa, T., Isogai, A., Matsunaga, T., 2006. Estimation of model parameters and ground movement in shallow NATM tunnel by means of neural network. Tunnelling and Underground Space Technology 21, 242.

Londe, P., 1977. Field measurements in tunnels. Proceedings, International Symposium on Field Measurements in Geomechanics, Zurich, Switzerland, pp. 619-638.

Long, J. C. S., 1993. Construction of equivalent discontinuum models for fracture hydrology. In: J. A. Hudson, T. Brown, C. Fairhurst and E. Hoek (Eds.) Comprehensive rock engineering, (4) Pergamon Press, pp. 241-295.

Marinos, P., Hoek, E., 2000. GSI: A geologically friendly tool for rock mass strength estimation. Proceedings, GeoEng 2000, Melbourne, Australia, pp. 1422-1442.

Mauldon, A. D., Karasaki, K., Martel, S., Long, J. C. S., Landsfeld, M., Mensch, A., Vomvoris, S., 1993. An inverse technique for developing models for fluid flow in fracture systems using simulated annealing. Water Resources Research 29 (11), 3775-3789.

Metropolis, N., Rosenbluth, A., Rosenbluth, M., Telle, A., Teller, E., 1953. Equations of state calculations by fast computing machines. Chemical Physics 21, 1087-1092.

Müller, G., Müller, L., 1970. Monitoring of dams with measuring instruments. Proceedings, 10th ICOLD Congress, International Commision on Large Dams, Montreal, Quebec, pp. 1033-1046.

Nelder, J. A., Mead, R., 1965. A simplex method for function minimization. Computer Journal 7, 308.

Neumaier, A., (2007), "Global Optimization," http://www.mat.univie.ac.at/~neum/glopt.html..

Nguyen-Minh, G., Corbetta, F., 1991. New calculation methods for lined tunnels including the effect of the front face. Proceedings, International Congress on Rock Mechanics, Aachen, Germany, 1991, pp. 1335-1338.

Nguyen Minh, D., Guo, C., 1993. A ground support interaction principle for constant rate advancing tunnels. Proceedings, Eurock '93, Lisbon, Portugal, pp. 171-177.

Oreste, P., 2003. Analysis of structural interaction in tunnels using the convergence-confinement approach. Tunnelling and Underground Space Technology 18, 347-363.

Oreste, P., 2005. Back-analysis techniques for the improvement of the understanding of rock in underground constructions. Tunnelling and Underground Space Technology 20, 7-21.

Oreste, P., Peilla, D., 1996. Radial passive rockbolting in tunneling design with a new convergence-confinement model. International Journal of Rock Mechanics Mining Sciences and Geomechanics Abstracts 33 (5), 443-454.

Otten, R. H. J. M., Ginneken, L. P. P. P., 1989. The annealing algorithm, edn. Kluwer, Boston, 201.

Pacher, F., 1963. Deformationsmessungen in Versuchsstollen als Mittel zur Enforschung des Gebirgsverhaltens und zur Bemessung des Ausbaues. Proceedings, 14 Symposium of the Austrian Regional Group of the ISRM, Salzburg, September, 1963, Salzburg, Austria, 1964, pp. 149-161.

Panet, M., 1993. Understanding deformations in tunnels. In: J. A. Hudson, T. Brown, C. Fairhurst and E. Hoek (Eds.) Comprehensive Rock Engineering, (1) Pergamon Press, New York, pp. 663-690.

Panet, M., 1995. Le calcul des tunnels par la méthode convergence-confinement, edn. Presses de l'Ecole Nationale des Ponts et Chaussées, Paris, France, 177.

Panet, M., 2001. Recommendations on the convergence-confinement method. Association Française des Travaux en Souterrain (AFTES), Paris, France..

Panet, M., Guenot, A., 1982. Analysis of convergence behind the face of a tunnel. Proceedings, Conference on Tunnelling, Brighton, United Kingdom,1982, pp. 197-204.

Pardalos, P. M., Romeijn, H. E., (2002), "Handbook of Global Optimization Volume 2 (Nonconvex Optimization and Its Applications)," Springer, 580.

Peck, R. B., 1969. Deep excavation and tunneling in soft ground. Proceedings, 7th International Conference on Soil Mechanics and Foundation Engineering, Mexico City, pp. 225-290.

Peila, D., Oreste, P. P., 1995. Axisymmetric analysis of ground reinforcement in tunnel design. Computers and Geotechnics 17, 253-274.

Pendragon Software Corporation. 2004. Pendragon Forms 4.0 Software Manual, edn. Pendragon, 484.

Pichler, B., Lackner, R., Mang, H. A., 2003. Back analysis of model parameters in geotechnical engineering by means of soft computing. International Journal for numerical Methods in Engineering 57, 1943-1978.

Powell, M. J. D., 1962. An iterative method for finding stationary values of a function of several variables. Computer Journal 5, 147-151.

Powell, M. J. D., 1964. An efficient method for finding the minimum of a function of several variables without calculating derivatives. Computer Journal 7 (4), 303-307.

Press, W. H., Teukolsky, S. A., Vetterling, W. T., Flannery, B. P., 1999. Numerical recipes in C, The art of scientific computing, edn. Cambridge University Press, Cambridge, United Kingdom, .

Price, K., Storn, R., 1997. Differential evolution - a simple evolution strategy for fast optimization. Dr. Dobb's Journal April 1997, 18-24,78.

Rao, S. S., 1996. Engineering Optimization, Theory and Practice, Third edn. John Wiley and Sons, New York, ch.3,5,6,7.

Reed, P. M., Yamaguchi, S., 2004. Simplifying the parameterization of real-coded Evolutionary Algorithms. Proceedings, World Water and Environmental Resources Congress 2004, Salt Lake City, Utah, USA, pp. 1-9.

Richardson, J. A., Kuester, J. L., 1973. The Complex method for constrained optimization. Communications of the Association for Computing Machinery 16 (8), 487-489.

Romana, M. R., 1985. New adjustment ratings for application of Bieniawski's classification to slopes. Proceedings, ISRM Symposium on Rock Mechanics: The role of rock mechanics in excavations for mining and civil works, Zacatecas, Mexico, pp. 49-53.

Romana, M. R., 1993. A geomechanical classification for slopes: Slope Mass Rating. In: J. A. Hudson, T. Brown, C. Fairhurst and E. Hoek (Eds.) Comprehensive Rock Engineering, Principles-Practice and Projects, Pergamon Press, pp. 575-600.

Rose, B. T., 2005. Tennessee Rockfall Management System. Ph.D. Thesis, Virginia Tech, Blacksburg, 107.

Rosenbrock, H. H., 1960. An automatic method for finding the greatest or least value of a function. Computer Journal 3 (3), 175-184.

Růžek, B., Kvasnička, M., 2001. Differential evolution algorithm in the earthquake hypocenter location. Pure and applied geophysics 158, 667-693.

Saguy, I., 1982. Utilization of the "Complex Method" to optimize a fermentation process. Biotechnology and Bioengineering XXIV, 1519-1525.

Sakurai, S., 1978. Approximate time-dependent analysis of tunnel support structure considering progress of tunnel face. International Journal for Numerical and Analytical Methods in Geomechanics 2, 159-175.

Sakurai, S., 1993. Back analysis in rock engineering. In: J. A. Hudson, T. Brown, C. Fairhurst and E. Hoek (Eds.) Comprehensive Rock Engineering, (4) Pergamon Press, pp. 543-569.

Sakurai, S., 1998. Lessons learned from field measurements in tunneling. Tunnelling and Underground Space Technology 12 (4), 453-460.

Sakurai, S., Abe, S., 1981. Direct strain evaluation technique in construction of underground opening. Proceedings, 22nd U.S Symposium on Rock Mechanics: Rock Mechanics from Research to Application, MIT, Cambridge, Massachusetts, pp. 278-282.

Sakurai, S., Akutagawa, S., Takeuchi, K., Shinji, M., Shimizu, N., 2003. Back analysis for tunnel engineering as a modern observational method. Tunnelling and Underground Space Technology 18, 185-196.

Sakurai, S., Shimizu, N., Matsumuro, K., 1985. Evaluation of plastic zone around underground openings by means of displacement measurements. Proceedings, 5th

International Conference on Numerical Methods in Geomechanics, Nagoya, Japan, 1-5 April, 1985, pp. 111-118.

Sakurai, S., Takeuchi, K., 1983. Back analysis of measured displacements of tunnels. Rock Mechanics and Rock Engineering 16 (3), 173-180.

Scherbaum, F., Palme, C., Langer, H., 1994. Model parameter optimization for site-dependent simulation of ground motion by simulated annealing: re-evaluation of the Ashigara Valley prediction experiment. Natural Hazards 10 (3), 275-296.

Simpson, A. R., Priest, S. D., 1993. Application of genetic algorithms to optimisation problems in geotechnics. Computers and geotechnics 15 (1), 1-19.

Spendley, W., Hext, G. R., Himsworth, F. R., 1962. Sequential application of simplex designs in optimization and evolutionary operation. Technometrics 4, 441.

Storn, R., Price, K., 1997. Differential Evolution - A simple yet efficient heuristic for global optimization over continuous spaces Journal of Global Optimization 11, 341-359.

Sulem, J., Panet, M., Guenot, A., 1987. Closure analysis in deep tunnels. International Journal of Rock Mechanics Mining Sciences and Geomechanics Abstracts 24 (3), 145-154.

Swoboda, G., Ichikawa, Y., Dong, Q., Zaki, M., 1999. Back analysis of large geotechnical problems. International Journal of Numerical and Analytical Methods in Geomechanics 23, 1455-1472.

Vardakos, S., Gutierrez, M., 2006. Simplified parameter identification for circular tunnels. Tunelling and Underground Space Technology 21 (3-4), 372.

Venkataraman, P., 2002. Applied optimization with MATLAB programming, edn. John Wiley and Sons, New York, ch. 4, 6, 7.

von Rabcewicz, L., 1963. Die Neue Ostereichische Bauweise und ihr Einfluβ auf Gebirgsdruckwirkungen und Dimensionierung. ISRM: Felsmechanik und ingenieurgeologie. Eds: Muller.L., Fairhust, C. 1, 224-244.

Wang, C., Ma, G. W., Zhao, J., Soh, C. K., 2004. Identification of dynamic rock properties using a genetic algorithm. International Journal of Rock Mechanics and Mining Sciences 41 (3), 490-495.

Xiang, Z., G., S., Cen, Z., 2002. Identification of damage parameters for jointed rock. Computers and Structures 80, 1429-1440.

Xiang, Z., Swoboda, G., Cen, Z., 2003a. Optimal layout of displacement measurements for parameter identification process in geomechanics. International Journal of Geomechanics 3 (2), 205-216.

Xiang, Z., Swoboda, G., Cen, Z., 2003b. Parameter identification and its application in tunneling. In: G. Beer (Eds.) Numerical simulation in tunneling, Springer Verlag, Vienna, Austria, pp. 161-200.

Zhang, L. Q., Yue, Z. Q., Yang, Z. F., Qi, J. X., Liu, F. C., 2006. A displacement-based back-analysis method for rock mass modulus and horizontal in situ stress in

tunneling – Illustrated with a case study. Tunelling and Underground Space Technology 21, 636-649.

Zhifa, Y., Lee, C. F., Sijing, W., 2000. Three-dimensional back-analysis of displacements in exploration adits - principles and application. International Journal of Rock Mechanics and Mining Sciences 37, 525-533.

VITAE

Sotirios Vardakos was born in Athens, Greece in November 21st, 1978 and he is the only child of Dr. Spyridon Vardakos and Helen Vardakou. He grew in a traditional classic environment of downtown Athens close to the Ancient monument of the Parthenon in the area of the Acropolis. Even though the family background was mainly inclined towards studies in Social and Political sciences as also towards Financial studies, he soon showed interest towards applied physics and mechanics. He was accepted at the First Experimental High School of Athens where he attended six years of education.

The aspiration to become a geotechnical engineer and his interest in underground engineering, came during his undergraduate studies at the Department of Mining Engineering and Metallurgy, at the National Technical University of Athens were he was accepted in 1997. During these years he had the chance to gain training by Mining Engineering industries, to gain experience from the tunneling practices but significant experience was also gained during his involvement in private geotechnical engineering consulting. After the five year education he graduated as Valedictorian in his class in 2002 with highest academic distinction. He was also honored with a U.S governmental scholarship by the Fulbright Foundation, to study in the United States of America. He was accepted at Virginia Polytechnic Institute and State University where he studied towards his Master of Science Degree and later his Ph. D.

Under the supervision of Dr. Marte Gutierrez, Sotirios Vardakos worked on research regarding numerical analysis for tunneling applications by the use of the distinct element and the finite difference method and it was concluded that the present research in execution and verification of numerical simulations, would be an academically challenging project. In 2003 Sotirios earned his Master of Science Degree and continued toward a Doctoral degree.